HIGH HYDROSTATIC PRESSURE COMBINED WITH HYDROPHOBIC MODIFICATION TO ENHANCE STABILITY AND ACTIVITY OF GLUCOSE OXIDASE AND XANTHINE OXIDASE

by

ALI HALALIPOUR

(Under the Direction of José I. Reyes-De-Corcuera)

ABSTRACT

High hydrostatic pressure (HHP) stabilized glucose oxidase (GOx) from *Aspergillus niger* and xanthine oxidase (XOx) from bovine milk against thermal inactivation. Stability increased 50 times for native GOx at 240 MPa and 74.5 °C and 9.5 times for native XOx at 300 MPa and 70.0 °C compared to the controlled atmospheric pressure at the same temperature. The stabilizing effect of HHP was highest at 74.5 or 70.0 °C where the activation volume ($\Delta V^{\neq}$) of inactivation was 57.0 ± 12.0 cm^3 mol^{-1} or 28.9 ± 2.9 cm^3 mol^{-1} for GOx or XOx respectively. Positive $\Delta V^{\neq}$ for all the treatment confirmed that HHP favored GOx and XOx stabilization.

A second approach to increase GOx and XOx stability involved crosslinking aniline or benzoate. At atmospheric pressure, the thermal stability of GOx was 1.1 times higher after aniline modification (13.4 ± 0.8 min^{-1}), while it was 0.9 times lower upon modification with benzoate (16.2 ± 1.0 min^{-1}) compared to the native GOx (15.3 ± 0.4 min^{-1}) at 80.0 °C. At HHP, the thermal stability of the aniline- and benzoate-modified GOx was higher than the native GOx and it increased 3.7-fold after aniline modification and 2.8-fold after benzoate modification compared to the native GOx at 240 MPa at 80.0 °C. However, the thermal stability of XOx

remained unaffected after 8 ± 1 modifications of carboxyl side groups per XOx monomer with aniline, or 12 ± 5 modifications of amino side groups per XOx monomer with benzoate using DSC analysis.

At HHP and in the presence of substrates, the catalytic activity of the aniline-modified GOx resulted in the fastest reaction followed by the benzoate-modified and native GOx at all the studied temperatures. At 180 MPa and 69.1 °C, the aniline-modified GOx catalyzed the oxidation of glucose 11-fold faster compared to the reaction of the same enzyme at atmospheric pressure and 25 °C. Negative $\Delta V^{\neq}$ were assessed for all the studied temperatures which confirmed HPP favored activation of the enzymes. The highest activation energy was 34.7 ± 2.7, 42.3 ± 3.7, or 39.4 ± 2.4 kJ mol^{-1} at 180 MPa for native, aniline-, or benzoate-modified GOx respectively.

INDEX WORDS: Glucose oxidase, Xanthine oxidase, High hydrostatic pressure, Hydrophobic modification, Stabilization, Activation

HIGH HYDROSTATIC PRESSURE COMBINED WITH HYDROPHOBIC MODIFICATION TO ENHANCE STABILITY AND ACTIVITY OF GLUCOSE OXIDASE AND XANTHINE OXIDASE

by

ALI HALALIPOUR

B.S., Arak University, Iran, 2009

M.S., Sharif University of Technology, Iran, 2012

A Dissertation Submitted to the Graduate Faculty of The University of Georgia in Partial Fulfillment of the Requirements for the Degree

DOCTOR OF PHILOSOPHY

ATHENS, GEORGIA

2016

HIGH HYDROSTATIC PRESSURE COMBINED WITH HYDROPHOBIC MODIFICATION TO ENHANCE STABILITY AND ACTIVITY OF GLUCOSE OXIDASE AND XANTHINE OXIDASE

by

ALI HALALIPOUR

Major Professor:	José I. Reyes-De-Corcuera
Committee:	William L. Kerr
	Fanbin Kong
	Ramaraja Ramasamy

Electronic Version Approved:

Suzanne Barbour
Dean of the Graduate School
The University of Georgia
December 2016

DEDICATION

To my first teachers father and mother for their unconditional love and support. To all my family and friends who encouraged me along the way of my pursuit of a higher education.

ACKNOWLEDGEMENTS

I would like to thank my major advisor Dr. Reyes for his guidance and knowledge throughout my academic career at the University of Georgia. Dr. Reyes energy and enthusiasm encourage his students to accomplish high quality research works. I acknowledge all the assistance and funding provided to me from Dr. Reyes, the Food Science and Technology department, and the USDA-NIFA-AFRI grant. Special thanks to my advisory committee members Dr. Kerr, Dr. Kong, and Dr. Ramasamy for their guidance, direction, mentorship and consideration throughout my studies. I would also like to thank my lab group and friends Dr. Garcia, Daoyuan, Xuan, Victoria, George, Martina, Tristin, Luke, Hanna, Samet, and Anuj for helping a peer and providing cheer throughout academic career. I cannot thank Omid, Duc and Doayuan enough for their continual support and pure friendship. Without whom I could not have made it through this point and achieved my goals.

TABLE OF CONTENTS

LIST OF TABLES

Page

LIST OF FIGURES

Page

CHAPTER 1

INTRODUCTION AND LITERATURE REVIEW

Background

Enzymes are useful biocatalysts for many industry-relevant applications. Global demand for industrial enzyme was $4.5 billion in 2012, $4.8 billion in 2013, and expected to be $7.1 billion in 2018 with an annual growth rate of 8.2% from 2013 to 2018. Four major categories of enzymes based on their industrial applications included detergent enzymes, food enzymes, technical enzymes, and feed enzymes (Sarmiento et al., 2015). Novozymes, DuPont, and DSM are the biggest industrial enzyme producers (Dewan, 2014) and amylase, lipase, protease, ligase, phytase, cellulase, and xylanase constitute the major market of the industrial enzymes (Sarrouh et al., 2012). The global market for detergent enzymes was worth $1.1 billion in 2013 and is expected to grow the fastest at a rate of 11.3% from 2013 to 2018 to reach $1.8 billion global market (Sarmiento et al., 2015).

In 2007, the global market for food enzymes was $830 million (Iyer and Ananthanarayan, 2008). Food enzymes are expected to reach $1.7 billion global market by 2018 with a growth rate of 5.1% from 2013 to 2018. The growth rate in Europe is predicted to be the fastest (Sarmiento et al., 2015). The use of thermostable enzyme increased the number of the processes in the food industry using enzymes by providing the new possibilities for the industrial applications (Haki and Rakshit, 2003). Food enzymes are used to improve the quality of bread

using amylases in the baking industry, to produce cheese using rennet and prepare lactose-free milk using lactase in the dairy industry, and to improve wine color and maintain apple juice clarity using pectinases in the beverages industry (Sarmiento et al., 2015). However, the relatively low stability of enzymes compared to chemical catalysis under industrial conditions limited economically viable utilization of enzymes (Iyer and Ananthanarayan, 2008). The increasing number of publications on enzyme stability in the last 30 years (Figure 1.1) is consistent with the need in the enzyme industry. However, the total number of publications reporting stabilization of enzyme are only 37% of the total number of publications on stability of enzyme obtained in the past 10 years from Science Direct database. Improving enzyme stability using stabilization techniques can increase the practical applications of industrial enzymes.

Glucose oxidase

Glucose oxidase (GOx, EC 1.1.3.4) is a homodimeric glycoprotein with a molecular mass of ~160 kDa that consists of two tightly bound flavin adenine dinucleotide (FAD) molecules per dimer (O'Malley and Weaver, 1972). The enzyme is widely produced using fungi, mainly *Aspergillus niger* (Nakamatsu et al., 1975; Pluschkell et al., 1996). Less commonly, *Penicillium* (Eryomin et al., 2004), and *Saccharomyces* (Earnshaw et al., 1995) are used to produce the enzyme. Table 1.1 summarizes the optimum conditions of temperature and pH for maximal catalytic activity of GOx from *Aspergillus* and *Penicillium*. Among the reported species, the greatest thermostability of GOx is from *Aspergillus niger* (Kalisz et al., 1990). Thermal inactivation of GOx was fitted to a first-order model at atmospheric pressure (Gouda et al., 2003; Katano et al., 2011; Nakamura et al., 1976; Sattari et al., 2013). Inactivation of GOx from *Aspergillus niger* followed a first-order model in the presence or absence of K_2SO_4, NaCl, or

lysozyme in the temperature range of 56-67 °C (Gouda et al., 2003). A first-order model was also reported for the inactivation of GOx from *Aspergillus niger* in the presence of guanidine hydrochloride (denaturant) or ε-poly-L-lysine (stabilizer) at temperatures between 60 and 78 °C (Katano et al., 2011). Thermal inactivation of the native and periodate-oxidized GOx from *Aspergillus niger* between 50 and 72 °C also followed a first-order model (Nakamura et al., 1976). Table 1.2 summarizes the first-order rate constant of the inactivation (k_{inact}) of GOx reported in other studies.

Activity of GOx is commonly determined using continuous spectrophotometric rate evaluation by monitoring the formation of oxidized o-Dianisidine acid in the presence of peroxidase (POx) at 500 nm (Bergmeyer et al., 1974a):

$$\beta\text{-D-Glucose} + O_2 + H_2O \xrightarrow{GOx} \text{D-Glucono-1,5-Lactone} + H_2O_2$$

$$H_2O_2 + \text{o-Dianisidine}_{(reduced)} \xrightarrow{POx} \text{o-Dianisidine}_{(oxidized)} + H_2O$$

Glucose oxidase has found large-scale practical applications since the early 1950s (Fiedurek and Gromada, 1997). Yellow Springs Instrument (YSI) developed the first commercially successful whole blood glucose analyzer in 1975 based on GOx (Wilson and Turner, 1992). Furthermore, GOx is used for several technological applications in food industries including in food packaging as an enzymatic oxygen scavenger in combination with catalase (Ge et al., 2012) and in wine processing for reduced-alcohol wine (Gómez et al., 1995; Pickering et al., 1998). Other processing purposes include bread making (Tang et al., 2014), mayonnaise and potato chip processing (Isaksen and Adler-Nissen, 1997; Jiang and Ooraikul, 1989), as well as

apple and pear purée processing (Parpinello et al., 2002). Further it has seen an increasing number of other potential applications including enhancement of toothpaste and mouth rinse therapeutic effects on recurrent aphthous ulcers (Adler et al., 1993; Fridh and Koch, 1999) and textile bleaching in the textile industry (Tzanov et al., 2002). In addition, the catalytic reaction of GOx has been applied for glucose removal in the processing of liquid egg (Sisak et al., 2006). The enzymatic reaction of GOx is also important for the production of gluconic acid which has important food applications, such as cheese curd formation and prevention of milkstone in dairy industry, and formulation of donuts. Moreover, gluconic acid has been used for pharmaceutical applications such as prevention of the deficiency of iron and calcium (Ramachandran et al., 2006). Gluconic acid is mainly produced by microbial fermentation (Singh et al., 2005). However, the slow production of gluconic acid and presence of unwanted by-products during microbial fermentation (Wong et al., 2008) proposed bioreactor using GOx as a viable substitute for gluconic acid production (Godjevargova et al., 2004; Nakao et al., 1997).

Xanthine oxidase

Xanthine oxidase (XOx, EC 1.17.3.2) from bovine was reported in 1902 as the enzyme responsible for decolorizing of methylene blue in milk samples in the presence of formaldehyde (Massey and Harris, 1997). The enzyme consists of one molecule of FAD, one atom of molybdenum, and four atoms of iron per enzyme subunit (Olson et al., 1974). Xanthine oxidase mainly catalyzes the oxidation of xanthine to uric acid by producing hydrogen peroxide in the presence of oxygen. The oxidation occurs using the molybdopterin center, the pair of iron-sulfur clusters, and the bounded FAD (Bray et al., 1961; Olson et al., 1974). Table 1.3 summarizes the optimum conditions of temperature and pH for maximal catalytic activity of XOx from bovine

milk and *Arthrobacter*. Thermal inactivation of XOx was also reported to follow a first-order kinetics model at ambient pressure: the inactivation of XOx from rat liver in the presence or absence of pyridine at 35 to 65 °C (Amini et al., 2011); and the inactivation of XOx from *Arthrobacter* M3 in the presence or absence of cosolute and osmolyte at 50 °C (Zhang et al., 2014). The reported first-order k_{inact} of XOx are listed in Table 1.2.

Activity of XOx is commonly determined using continuous spectrophotometric rate evaluation by monitoring the formation of uric acid at 295 nm (Bergmeyer et al., 1974b):

$$\text{Xanthine} + O_2 + H_2O \xrightarrow{\text{XOx}} \text{Uric Acid} + H_2O_2$$

Xanthine oxidase ability to catalyze different substrates has been used to fabricate biosensors to evaluate the freshness of fish by detection of hypoxanthine after the death of a fish which imparts the bitter spoiled taste (Dervisevic et al., 2015; Devi et al., 2011; Nakatani et al., 2005), and to detect the caffeine (1,3,7-trimethylxanthine) for evaluation of the quality of commercial instant tea and coffee (Babu et al., 2007). In addition, XOx also used as biosensor to detect theophylline (1,3-dimethylxanthine) content which is one of the most common medications for chronic asthma (Mao et al., 2001; Stredansky et al., 2000). Moreover, the catalytic activity of XOx is important for the conversion of drugs and prodrugs into their active forms in the human body such as pyrazinamide for treatment of infectious diseases (Shih et al., 2013; Yamamoto et al., 1993), and azathioprine for treatment of abnormal immune responses (Sandborn, 2001).

Enzyme enhancement

Enzymes enhancement aims at improving their stability and activity, hence to produce reusable, selective, and competitive industrial biocatalysts. Immobilization, protein engineering, chemical modification, or the use of soluble additives are the most common methods for enzyme enhancement.

Immobilization strategies, in particular attachment to a solid matrix, typically beads, are most commonly used to allow enzyme reusage and decrease the process cost (Garcia-Galan et al., 2011; Katchalski-Katzir, 1993). Immobilization techniques include crosslinking, covalent binding, adsorption, and entrapment (Katchalski-Katzir and Kraemer, 2000). Agarose aldehyde gels was used to immobilize α-chymotrypsin by multipoint covalent attachment (Guisán et al., 1991). The immobilized α-chymotrypsin was 60,000 times more stable compared to the free enzyme. The stabilization was expressed as the ratio of the half-life of the immobilized enzyme to the free enzyme after inactivation at 65 °C. However, immobilization reduced the enzyme activity by 35% compared to the native soluble enzyme.

Glucose oxidase from *Aspergillus niger* was immobilized using cellulose acetate–polymethylmethacrylate membrane (Rauf et al., 2006). The immobilized GOx thermostability increased 46% compared to the native soluble enzyme measured by the retaining activity at 505 nm after incubation at 70 °C. However, immobilization increased the K_m of the enzyme by 2.4 times. Using immobilization on the glass beads maximized the retained activity of GOx from *Aspergillus niger* to 250% compared to the free enzyme after incubation at 70 °C (Sarath Babu et al., 2004). Covalent bonding and entrapment were used to immobilize GOx onto poly(2-hydroxyethyl methacrylate) membranes (Arica and Hasirci, 1993). The entrapment was more efficient (93.7%) in the immobilization compared to the covalent bonding efficiency of 17.4%.

However, the entrapment increased the K_m of the enzyme 2.1 times, whereas the covalent bonding increased the K_m 1.5 times compared to the free enzyme. In another study, the stability of immobilized GOx from *Aspergillus niger* with lysozyme increased using additives and modification of the enzyme. The transition temperature, T_m, increased 9 °C and half-life at 70 °C increased 22 times for the modified GOx with *N*-ethylmaleimide in the presence of K_2SO_4 (Gulla et al., 2004).

Xanthine oxidase was immobilized on beads using polyvinyl alcohol-glutaraldehyde network (Araujo et al., 1997). The activity of XOx retained up to 72.3% compared to the free enzyme. The K_m of the immobilized XOx increased 1.5 times compared to the free native enzyme. Immobilization of XOx onto polymeric support of Enzacryl-TIO increased the half-life of immobilized enzyme to ~100 h compared to the half-life of 3 h at 30°C for the free enzyme (Johnson and Coughlan, 1978). Immobilization of XOx on magnetic polysiloxane-polyvinyl alcohol particles using glutaraldehyde increased the retained activity 3 times compared to the free enzyme incubated at 65 °C (Neri et al., 2011).

Protein engineering (Chen et al., 2002), and medium engineering (Kalisz et al., 1997) are among the stabilization methods that have been used for GOx enhancement. XOx stabilization has also been studied by application of organic media (Amini et al., 2011; Rashidi et al., 2009), and utilization of cosolute (trehalose) and osmolyte (betaine) additives (Zhang et al., 2014). However, stabilization effect of high hydrostatic pressure (HHP) at elevated temperatures on GOx and XOx has not been explored yet.

A large portion of the high pressure literature has reported the inactivating effect of pressure on microorganisms (Earnshaw et al., 1995; Guerrero-Beltrán et al., 2005), and enzymes with deleterious impacts on food quality (Chakraborty et al., 2014; Hendrickx et al., 1998;

Katsaros et al., 2009; Ludikhuyze et al., 2003; Riahi and Ramaswamy, 2004; Sulaiman et al., 2015; Yi et al., 2015). Stabilization or catalytic activity enhancement of several enzymes at HHP have been documented (Eisenmenger and Reyes-De-Corcuera, 2009b). Recent reports include the stabilization effect of pressure on β-glucosidase (Terefe et al., 2013; Vila-Real et al., 2010), pectinases (Tomlin et al., 2013), polyphenoloxidase (Huang et al., 2014), and inulin fructotransferase (Li et al., 2015).

Currently, high capital cost of HHP equipment limited the HHP applications to high value-added product (Balasubramaniam et al., 2015). However, as HHP applications have grew and technology has progressed, the installed high pressure systems exceeded 265 equipment worldwide by 2014 and the capital cost of HHP equipment has decreased up to three fold in the last decade (Balda et al., 2012).

Covalently attaching hydrophobic molecules also reported to stabilize enzymes (Gupta, 1991; Mogharrab et al., 2007; Mozhaev et al., 1990; Stepankova et al., 2013). Surface modification of α-chymotrypsin and *Candida rugosa* lipase using chemoenzymatic glycosylation to increase hydrophilic characteristics, and polyethylene glycol to increase hydrophobic characteristics was studied (Longo and Combes, 1997). Hydrophilic modification decreased the half-life time of α-chymotrypsin by 90% and *Candida rugosa* lipase by 79%, whereas hydrophobic modifications increased the half-life time of α-chymotrypsin by 382% and *Candida rugosa* lipase by 344% at 50 °C. Changes in the properties of the surface residue of the enzyme after crosslinking can increase the enzyme stability. As aromatic residues can engage in π -π stacking, cation-π and anion-quadrupole types of interactions as well as hydrogen bonds, there are many options for interaction with nearby residues, as well as with solvent (Koide and Sidhu, 2009; Philip et al., 2011). Aromatic groups possess a quadrupole moment, leading to their

ability to interact with cations on the ring face (Dougherty, 1996; Gallivan and Dougherty, 1999) or anions on their ring edge (Jackson et al., 2007; Philip et al., 2011). Therefore, presence of phenyl groups can enhance the hydrophobicity of the enzyme, hence potentially increasing the enzyme thermal stability.

Moreover, recent reports documented the activation effect of pressure on polyphenol oxidase from strawberry puree and apple juice (Buckow et al., 2009; Terefe et al., 2010), *Candida antarctica* lipase B (Eisenmenger and Reyes-De-Corcuera, 2010), pectinase formulation from *Aspergillus niger* (Tomlin et al., 2014), protease from *Bacillus* species (Senyay-Oncel et al., 2014), and α-chymotrypsin from bovine pancreas (Levin et al., 2016). Increase in thermal stability of enzymes potentially enable enzymatic reaction at higher temperatures. Consequently, higher reaction rates would be feasible at higher temperatures than it is possible under atmospheric pressure due to thermal inactivation.

Identification of gap of knowledge

To the best of our knowledge: effect of HHP on GOx and XOx stability have not been reported; effects of hydrophobic modification on GOx and XOx stability have not been reported; effect of HHP on the catalytic activity of native and modified GOx and XOx have not been reported.

Research hypotheses

We hypothesized that HHP treatments can stabilize GOx and XOx. Also hydrophobic modification of the enzymes can stabilize GOx and XOx. Moreover, HHP can be used to increase the catalytic activity of GOx and XOx.

Specific objectives

1. To stabilize GOx under HHP and determine the pressure range that results in the greatest stability of the enzyme.
2. To stabilize phenyl-modified GOx under HHP and determine the pressure range that results in greatest stability of the enzyme.
3. To stabilize XOx under HHP and determine the pressure range that results in greatest stability of the enzyme.
4. To increase the catalytic activity of the native and modified GOx under HHP and determine the pressure range that produces the greatest activity of the enzyme.

Table 1.1.

Optimal catalytic activity conditions of GOx from *Aspergillus* and *Penicillium* species.

Species	Optimal temperature (°C)	Optimal pH	Reference
A. niger	40-60	5.5-6.0	(Kalisz et al., 1990)
A. niger	40	5.5	(Bhatti et al., 2006)
A. niger	30	4.0-5.0	(Altikatoglu et al., 2010)
P. purpurogenum	35	5.0	(Nakamatsu et al., 1975)
P. sp. CBS 120262	25	7.0	(Simpson et al., 2007)
P. amagasakiense	25	6.0	(Witt et al., 2000)

Table 1.2.

The first-order rate constant of the inactivation of GOx and XOx at different temperatures.

Enzyme	Temperature (°C)	k_{inact} ($\times 10^{-4}$, s^{-1})	Reference
GOx	60	0.9	(Katano et al., 2011)
	65	2.2	
	70	6.6	
	74	15.0	
	78	34.0	
	56	1.34	(Gouda et al., 2003)
	60	9.6	
	63	16	
	67	24.9	
XOx	35	1.1	(Amini et al., 2011)
	45	1.3	
	55	1.5	

Table 1.3.

Optimal catalytic activity conditions of XOx from *Arthrobacter* and bovine milk.

Species	Optimal temperature (°C)	Optimal pH	Reference
Arthrobacter M3	50	7.0–7.5	(Zhang et al., 2014)
Arthrobacter	50	7.0	(Xin et al., 2012)
bovine milk	37	8.0	(Rashidi et al., 2009)
bovine milk	37	8.5	(Mohamadin and Abdel-Naim, 2003)

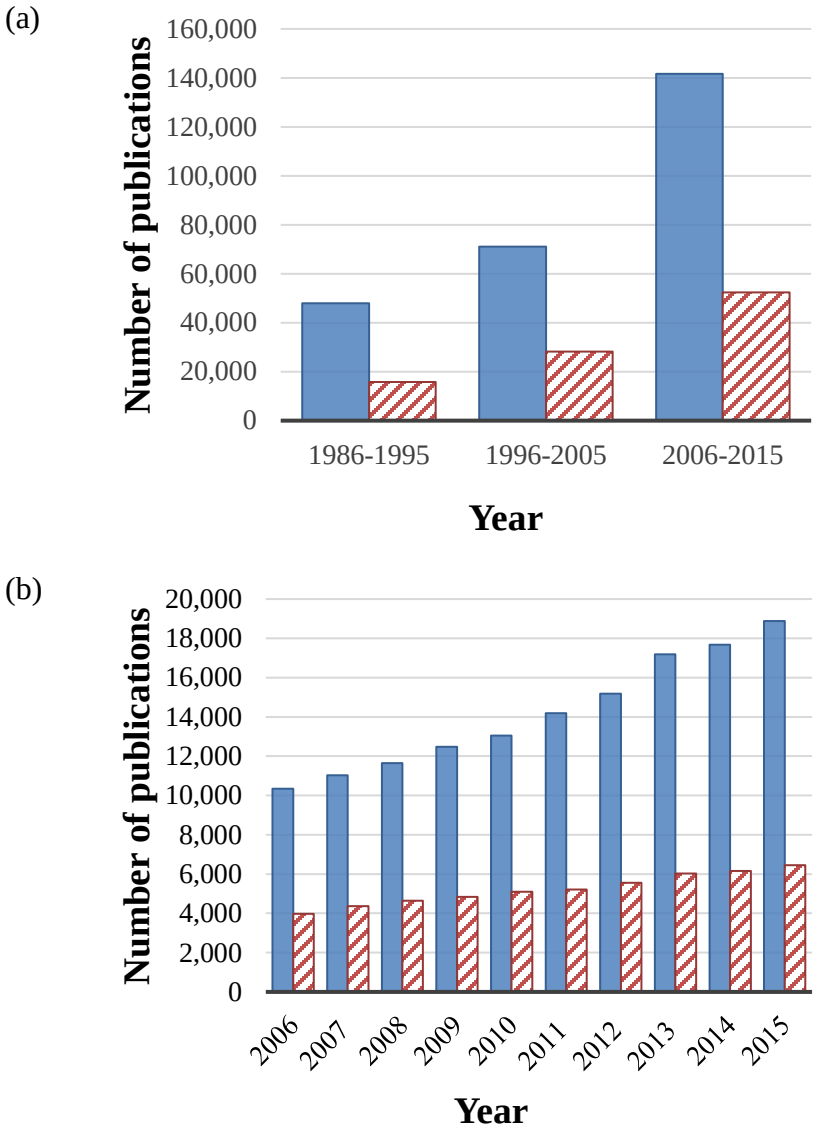

Figure 1.1. Number of publications in Science Direct database using enzyme stability (solid fill) and enzyme stabilization (pattern fill) keywords (a) from 1986 to 2015 for every 10 years and (b) in the past 10 years.

CHAPTER 2

GLUCOSE OXIDASE STABILIZATION AGAINST THERMAL INACTIVATION USING HIGH HYDROSTATIC PRESSURE AND HYDROPHOBIC MODIFICATION [1]

[1] A. Halalipour, M.R. Duff, E.E. Howell, J.I. Reyes-De-Corcuera. Accepted by *Biotechnology and Bioengineering*. Reprinted here with permission of the publisher.

Abstract

High hydrostatic pressure (HHP) stabilized glucose oxidase (GOx) against thermal inactivation. The apparent first-order kinetics of inactivation of GOx were investigated at 0.1-300 MPa and 58.8-80.0 °C. At 240 MPa and 74.5 °C, GOx inactivated at a rate 50 times slower than at atmospheric pressure at the same temperature. The apparent activation energy of inactivation at 300 MPa was 281.0 ± 17.4 kJ mol^{-1} or 1.3 fold smaller than for the inactivation at atmospheric pressure (378.1 ± 25.6 kJ mol^{-1}). The stabilizing effect of HHP was greatest at 74.5 °C where the activation volume of 57.0 ± 12.0 cm^3 mol^{-1} was highest compared to all other studied temperatures. Positive apparent activation volumes for all the treatment temperatures confirmed that HHP favors GOx stabilization. A second approach to increase GOx stability involved crosslinking with N-(3-dimethylaminopropyl)-N'-ethylcarbodiimide hydrochloride (EDC) and either aniline or benzoate. The modified enzyme remained fully active with only slight increases in K_M (1.3 to 1.9 fold increases for aniline and benzoate modification, respectively). The thermal stability of GOx increased by 8 °C with aniline modification, while it decreased by 0.9 °C upon modification with benzoate.

Introduction

Glucose oxidase (EC 1.1.3.4) is a dimeric flavoprotein that consists of two identical polypeptide chains covalently linked by disulfide bonds (Rando et al., 1997). Glucose oxidase (GOx) catalyzes β-D-glucose oxidation to gluconic acid and hydrogen peroxide in the presence of oxygen as the electron acceptor (Kalisz et al., 1991). This enzyme is commonly extracted and purified from fungi, with GOx from *Aspergillus niger* reported to have the greatest thermostability (Kalisz et al., 1990). Glucose oxidase has been used in biosensor fabrication and clinical analysis (Atanasov and Wilkins, 1994; Rando et al., 1997; Zhu et al., 2002), textile bleaching (Tzanov et al., 2002), processing of reduced-alcohol wine (Gómez et al., 1995; Pickering et al., 1998), as oxygen scavenger in food packaging (Ge et al., 2012), and in several other applications. The most successful commercial application is the GOx-based biosensor used to measure blood glucose of individuals suffering from diabetes. However, the short operational life due to the lack of stability of the enzyme is a major limitation that has reduced the availability of commercial GOx biosensors (Altikatoglu et al., 2010) and other enzyme biosensor for continuous measurement of analytes. Environmental factors play important roles in enhancing the thermal stability of enzymes including pH (Caves et al., 2011), and the presence of metal ions (Li et al., 2013), polyelectrolytes (Chaudhary et al., 2009; Srivastava et al., 2005), and small organic molecules that are involved in maintaining osmotic pressure in the cell (Timson et al., 2013; Zancan and Sola-Penna, 2005). Glucose oxidase stability has been improved by using several techniques including immobilization (Bouin and Hultin, 1982; Rauf et al., 2006), protein engineering (Chen et al., 2002), and reaction medium engineering (Kalisz et al., 1997). Also, several studies have reported the activating and stabilizing effects of high hydrostatic pressure (HHP) on enzymes (Duong and Balaban, 2014; Eisenmenger and Reyes-De-Corcuera, 2009b;

Kirsch et al., 2013; Ly-Nguyen et al., 2003; Mozhaev et al., 1996; Terefe et al., 2013; Vila-Real et al., 2010). However, the stabilization effect of HHP is not retained after depressurization. Therefore, HHP alone would not lead to the production of stable biosensors for use at atmospheric pressure. Finally, covalently attaching hydrophobic molecules can stabilize enzymes (Gupta, 1991; Mogharrab et al., 2007; Mozhaev et al., 1990; Stepankova et al., 2013). Cross-linking may contribute to enzyme stability by altering the properties of the enzyme surface. As aromatic residues can engage in π -π stacking, cation-π and anion-quadrupole types of interactions as well as hydrogen bonds (for tyrosine and tryptophan), there are many options for interaction with nearby residues, as well as with solvent (Koide and Sidhu, 2009; Philip et al., 2011).

Based on the above mentioned stabilizing effects of HHP and hydrophobic modification of other enzymes, our findings with lipase (Eisenmenger and Reyes-De-Corcuera, 2009a, 2010) and pectinases (Tomlin et al., 2013; Tomlin et al., 2014), and our obtained preliminary results on GOx, we hypothesized that HHP and derivatization with hydrophobic groups would stabilize GOx against thermal inactivation. Therefore, the objective of this research was to stabilize GOx by applying HHP or by derivatizing surface residues on the protein with phenyl groups.

Materials and methods

Materials

Glucose oxidase from *Aspergillus niger* (EC 1.1.3.4, Type X-S, Product No. G7141), horseradish peroxidase (POx, EC 1.11.1.7, Product No. P8250), glucose, o-dianisidine dihydrochloride, N-(3-dimethylaminopropyl)-N'-ethylcarbodiimide hydrochloride (EDC), N-

hydroxysulfosuccinimide, aniline, sodium benzoate and tri-nitrobenzenesulfonic acid (TNBS) were purchased from Sigma-Aldrich (St. Louis, MO, USA). Econopac desalting columns were purchased from BioRad (Hercules, CA, USA).

The high pressure system consisted of a piston pump (model MP5), two high pressure reactors (model U111) and a controller unit from Unipress Equipment (Warsaw, Poland). The schematic of the HHP system was reported previously (Eisenmenger and Reyes-De-Corcuera, 2009a). Silicone oil was used as the pressure medium and the temperature of the reactors was controlled by connecting the reactor jackets to one of two Isotemp water baths (model 3016D) from Fisher Scientific (Pittsburg, PA, USA). Switching between water baths was performed using an array of two 3-way solenoid pinch valves. All the machineries, pressures, temperatures, and times were controlled and monitored automatically using a computer program written in LabVIEW 2014 and a data acquisition board model NI cDAQ-9174 using NI 9211, NI 9215, NI 9263, and NI 9481 modules all from National Instruments (Austin, TX, USA). Absorbance measurements were done with a USB 2.0 Fiber Optic Spectrometer (Model USB2000+) with UV−vis−NIR light source (model DH-2000-BAL) utilizing deuterium and halogen lamps and OceanView 1.5.0 spectroscopy software, all from Ocean Optics (Dunedin, FL, USA).

Methods

Sample preparation and treatment conditions

Glucose oxidase was diluted in 50 mM sodium acetate buffer pH 5.1 to ~0.6 units mL^{-1} and placed on ice before use. Aliquots of 100 µL of the untreated GOx were transferred into 15×15 mm polyethylene plastic resin pouches, heat sealed, immediately immersed in high pressure reactor fluid initially kept at 10 °C, and the pressure cell closed. The temperature of the

cold water bath was kept at 10 ± 0.1 °C to minimize losing enzyme activity before starting the desired treatments. Atmospheric pressure (0.1 MPa) was used as a control and 60-300 MPa in 60-MPa increments were applied as high pressure treatments. Five incubation times were selected for each temperature (58.8 °C, 63.8 °C, 69.1 °C, 74.5 °C, or 80.0 °C) to evaluate the kinetics of inactivation. Temperatures were selected to provide even increments of the reciprocal of the absolute temperature (1/T). After reaching the pressure set point, the temperature was raised to the incubation set point and when 95% of the desired temperature was reached, the processing time was started. After the processing time was completed, the reactor was cooled back to 15 °C and then depressurized to ambient pressure while temperature continued to decrease to approximately 11 ± 1 °C. Below 15 °C enzyme inactivation was negligible within the time frame needed to carry out residual activity measurements. The shortest temperature come-up time was 66 ± 2 s for 58.8 °C. The shortest temperature come-down time was 42 ± 2 s for 58.8 °C. The longest temperature come-up was 102 ± 2 s for 80.0 °C. The longest temperature come-down time was 64 ± 2 s for 80.0 °C. The order of pressure and temperature sequences was selected to minimize the thermal inactivation of the enzyme during the heating/cooling transient periods (Eisenmenger and Reyes-De-Corcuera, 2009a). If depressurization is done before cooling with the water bath, the adiabatic cooling of depressurization is not sufficient to decrease the temperature to a level below which the enzyme does not inactivate rapidly. Figure 2.1 represents an example of pressure and temperature history and the sequences of the treatments for a sample processed at 300 MPa, 63.8 °C, for 0 or 40 min incubation.

Samples were duplicated and assayed in a randomized block design, blocked by temperature while pressure and processing time were applied in random order. Statistical analysis of treatment was conducted using SAS statistical software (Cary, NC, USA) utilizing

analysis of variance (ANOVA), general linear model (GLM) regression, and Fisher's least significant difference (LSD) pairwise comparison test at individual error rate of α=0.05.

Kinetics of thermal inactivation

Residual enzyme activity after treatment was determined as the ratio of the activity after treatment over the activity after a process time of 0 min (Eq. 1). As shown in Figure 2.1, to obtain treated samples with a process time of 0 min, samples were cooled and then depressurized immediately after reaching the desired pressure and 95% of the desired temperature.

$$Acty_{res} = \left(\frac{Acty}{Acty_0}\right) \times 100 \quad (1)$$

where *Acty* is GOx activity after treatment for a specific process time and $Acty_0$ is GOx activity after the same treatment conditions for a process time of 0 min.

The processed enzyme activity was determined immediately after each treatment at ambient conditions. Enzyme activity was measured as the rate of production of oxidized o-dianisidine. This chromogenic product was measured spectrophotometrically at 500 nm utilizing a miniaturized procedure with 10 times less sample volume (Bergmeyer et al., 1974a):

$$\beta\text{-D-Glucose} + O_2 + H_2O \xrightarrow{GOx} \text{D-Glucono-1,5-Lactone} + H_2O_2$$

$$H_2O_2 + \text{o-Dianisidine}_{(reduced)} \xrightarrow{POx} \text{o-Dianisidine}_{(oxidized)} + H_2O$$

The reaction order (zero, first, or second) was analyzed for GOx inactivation at all processing pressures and temperatures (Table 2.1). Overall, a first-order reaction showed the best fit. Therefore, the rate constant of inactivation was calculated from the relationship between the natural logarithm of residual activity and the incubation time. The standard error of the linear

regression was used as an estimate of the experimental error of the determination of the rate constant of inactivation of GOx.

Effects of temperature and pressure on the rate of inactivation

To quantify the temperature effect on the kinetics of inactivation of GOx at each selected HHP, the activation energy of inactivation was calculated using the Arrhenius equation (Eq. 2).

$$\ln(k_{inact}) = \left(-\frac{E_a}{R}\times\frac{1}{T}\right) + \ln(k_{inact,\,T_o}) \quad (2)$$

where k_{inact} is the rate constant of inactivation of GOx at a constant pressure, E_a the activation energy, R the ideal gas constant of 8.3145 J mol^{-1} K^{-1}, T the absolute temperature, and $k_{inact,\,T_0}$ the rate constant of inactivation of GOx at a reference temperature T_0.

To determine the pressure effect on the kinetics of inactivation at each temperature, the activation volume of inactivation was calculated using the Eyring equation (Eq. 3).

$$\ln(k_{inact}) = \left(-\frac{\Delta V^{\neq}}{RT}\times P\right) + \ln(k_{inact,\,P_o}) \quad (3)$$

where $\Delta V^{\neq}$ is the activation volume, P the pressure, and $k_{inact,\,P_0}$ the rate of GOx inactivation at the reference pressure P_0. The errors in the estimates of the activation energies and volumes were reported as the standard error of the linear regression of Arrhenius or Eyring plots respectively.

Modification of glucose oxidase

Glucose oxidase was chemically modified using EDC and sodium benzoate or aniline. The modification forms an amide bond between benzoate and lysines or aniline with glutamate and aspartate residues. The modification reaction contained 1 mL of a 10 mg/mL solution of glucose oxidase in 150 mM HEPES, pH 7.5 buffer, which was mixed with 500 mM of either sodium benzoate or aniline. The solution was allowed to equilibrate for five minutes on ice. The

modification reaction was initiated by adding 10 mg/mL EDC and N-hydroxysulfosuccinamide. Excess reactants were removed by passing the solution through the desalting column equilibrated in 50 mM Na_2HPO_4, pH 7.1. Modified enzymes were stored at -20 °C prior to further studies.

The number of modifications per monomer of GOx were determined by two methods. The labelling of primary amines (lysines and the N-terminus) by benzoate was measured through a trinitrobenzene sulfonic acid (TNBS) assay. Samples were diluted into 100 mM $NaHCO_3$, pH 8.5 buffer and the absorbance measured. To 500 μL of protein solution 250 μL of 0.01% (w/v) of TNBS was added and the reaction allowed to proceed at 37 °C for two hours. The reaction was quenched by the addition of 125 μL of 1 M HCl and 250 μL of 10% SDS. Sample absorbances at 325 nm were measured on a Shimadzu UV160U UVvis spectrometer. A calibration curve using either glycine or tryptophan was used to quantify the number of amines in the protein.

The number of modifications were also estimated by MALDI-TOF. Samples were prepared according to previous procedures and measured on a Bruker MicroFlex MALDI-TOF instrument (Duff et al., 2016). The difference in the molecular weight of the modified GOx minus the unmodified enzyme was divided by the molecular weight of benzoate, or aniline, minus 18 (for the loss of water upon modification).

Quantifying the effects of modification

Thermal stability of unmodified and modified GOx was performed on a MicroCal VP differential scanning calorimeter (DSC). Scans were performed on 8-12 μM GOx in 50 mM Na_2HPO_4, pH 7.1 from 20 to 90 °C at a scan rate of 1.5 °C min^{-1}. The instrument was controlled by and the data fit using the Origin 7.0 software supplied by MicroCal. Scans were repeated twice to obtain errors.

Michaelis-Menten kinetics were performed in 50 mM sodium acetate, pH 5.1 buffer as a coupled assay with horseradish peroxidase (POx, 150 nM) and o-dianisidine (110 μM). The change in absorbance at 500 nm (ε_{500} = 7500 M^{-1} cm^{-1}) (Bergmeyer et al., 1974a) was monitored on a Perkin-Elmer λ35 UV-vis spectrometer at 35 °C with concentrations of glucose between 5 and 400 mM. Glucose, POx and o-dianisidine were incubated in a cuvette for two minutes and the reaction was initiated by addition of either unmodified, or modified enzyme. The initial rate of reaction was obtained and the data fit to the Michaelis-Menten equation.

Results and discussion

Kinetics of thermal inactivation

The residual activity of GOx decreased with processing time at all processing temperatures and pressures. The reduction of residual activity at two selected temperatures of 63.8 or 69.1 °C at 0.1 or 300 MPa is shown in Figure 2.2. Processing at the high pressure of 300 MPa protected the activity of the enzyme against thermal inactivation compared to ambient pressure. In other words, GOx was stabilized by HHP.

Zero, first, and second-order models were used to characterize the relationship between GOx residual activity and treatment time. Average R^2 values of 0.91, 0.96, or 0.93 for all processing pressures and temperatures were obtained when zero, first, or second-order models were applied respectively (Table 2.1A). Therefore, a first-order reaction was overall the best fit for all the studied pressures among the other order models. Of the studied orders, first and second fitted best the experimental data. Although first order is the most commonly used model to describe the decrease in activity of single enzyme during thermal treatment, at lower temperatures second order model fitted the data slightly better (Table 2.1). This is likely because

in addition to temperature, pressure becomes also a denaturant at lower temperatures. Although determining the exact fractional order may provide a better fit, it would not allow comparison to other reports in the literature. The rate constant of inactivation was calculated from the first-order model and the relationship between the natural logarithm of residual activity and the incubation time. Figure 2.3 illustrates the apparent first-order rate of inactivation of GOx at 74.5 ºC at all studied pressures. Samples treated at high pressures were inactivated at slower rates as indicated by smaller slopes associated with the plots of the natural logarithm of the residual activity *vs*. treatment time compared to the inactivation at ambient pressure. Similar behavior was observed for all other processing temperatures. The effect of pressure treatment on the rate constant of inactivation of GOx was significant for all the studied temperatures ($p < 0.0001$). Calculated apparent first-order rate constants of inactivation of GOx for all pressure and temperature combinations are presented in Table 2.2.

An increase in pressure from 180 MPa for most of the samples resulted in a decrease in R^2 of the first-order model (Table 2.2). The deviation from first-order inactivation kinetics was highest at 58.8 and 63.8 °C. At these temperatures, the average R^2 of the second-order model was higher than that of the first-order model for samples treated at 180, 240 and 300 MPa (Table 2.1B). Better fitting by a second-order process is consistent with a combined inactivation of GOx by temperature and pressure. In other words, inactivation at higher pressures and lower temperatures were closer to second-order inactivation kinetics due to combined inactivation effects of pressure and temperature. However, a first-order model was used to calculate the rate constant for all the treatments for the purpose of comparing our results with those in the literature.

Our results at ambient pressure are consistent with other studies which have also reported that GOx follows an apparent first-order inactivation kinetics at atmospheric pressure: GOx from *Aspergillus niger* inactivation in the presence or absence of additives in the temperature range of 56-67 °C at ambient pressure (Gouda et al., 2003); GOx from *Aspergillus niger* inactivation in the presence of denaturant or stabilizer at temperatures between 60 and 78 °C at ambient pressure (Katano et al., 2011); thermal inactivation of native and periodate-oxidized GOx from *Aspergillus niger* between 50 and 72 °C at ambient pressure (Nakamura et al., 1976); and inactivation of GOx from unknown source between 40 and 70 °C (Sattari et al., 2013). However, none of these studies reported a comparison of other kinetic orders of inactivation.

At each pressure, increasing temperature raised the rate constant of GOx inactivation, k_{inact}. The rate constant of GOx inactivation decreased with an increase in pressure from 0.1 MPa up to at least 180 MPa. There were no significant differences ($p < 0.05$) in the mean of k_{inact} for all treatments at 180, 240, and 300 MPa. The lowest k_{inact} was at pressures of 180 to 300 MPa for all reported temperatures with the exception of 58.8 °C where the lowest k_{inact} was at 180 to 240 MPa. Therefore, maximal HHP stabilization of GOx was in the range of 180 to 300 MPa for each processing temperature with the exception of 58.8 °C where the maximal HHP stabilization was in the range of 180 to 240 MPa (Table 2.2). At pressures where k_{inact} was minimal, the rate of inactivation was 5, 8, 23, 50, or 22 times smaller than at 0.1 MPa at 58.8 °C, 63.8 °C, 69.1 °C, 74.5 °C, or 80.0 °C respectively.

Previously, GOx activity reported at atmospheric pressure and in the range of 20-80 °C showed a great decrease in the enzyme activity remaining after 50 °C treatment to complete inactivation at 80 °C (Altikatoglu et al., 2010). The reported rate constants of inactivation of GOx at atmospheric pressure and at 56 and 63 °C were 0.008 and 0.096 min^{-1} respectively

(Gouda et al., 2003), which are similar to our observed rates at 58.8 and 63.8 °C. In another study, Katano et al. (2011) reported inactivation of GOx from *Aspergillus niger* (Type-II) by means of a bioelectrocatalysis method at atmospheric pressure with k_{inact} values of 0.005, 0.040, and 0.090 min^{-1} at 60, 70, and 74 °C respectively. These values are smaller than our observed k_{inact} values of 0.006, 0.427, and 5.17 min^{-1} at 58.8, 69.1, and 74.5 °C respectively (Table 2.2). The variation in rate constant of inactivation can be attributed to differences in the native enzyme activity, and type of the enzyme and the differences in purification procedures.

Several studies described the pressure inactivation of multiple food enzymes such as lipoxygenase above 300 MPa (Terefe et al., 2014), polyphenoloxidase above 200 MPa (Wang et al., 2012), and *Bacillus amyloliquefaciens* α-amylase above 400 MPa (Grauwet et al., 2010). In contrast, other studies like ours have documented the increase in thermostability of food enzymes at moderate pressures including inulin fructotransferase below 200 MPa (Li et al., 2015), β-glucosidase below 100 MPa (Terefe et al., 2013), carrot pectin methylesterase below 300 MPa (Ly-Nguyen et al., 2003), lipoxyganse below 300 MPa (Heinisch et al., 1995), and polyphenoloxidase below 300 MPa (Huang et al., 2014). This suggests that HHP stabilized enzymes at lower pressure ranges as opposed to destabilizing at higher pressure ranges (Eisenmenger and Reyes-De-Corcuera, 2009b; Smeller, 2002).

Protein stability under pressure has been generally discussed from strengthening molecular interactions that produce states with smaller specific volumes (Royer, 2005). Wilton et al. (2008), measured hydrogen bond lengths in the GB1 domain of protein G by nuclear magnetic resonance (NMR) shorten on average by 0.022 Å up to 200 MPa. This suggests that HHP stabilized hydrogen bonds and hence the protein structure at this pressure range. Mei et al. (1999), measured free energies of unfolding in wild-type and mutant azurins under pressure up to

240 MPa using steady state and dynamic fluorescence techniques. Their results indicated a positive correlation between pressure stabilization and hydrophobicity of protein at this range of pressure. Cioni and Strambini (1996), observed the tightening of alcohol dehydrogenase and alkaline phosphatase dimeric structures by correlating the decreased rate of tryptophan phosphorescence decay at up to 150 MPa with protein rigidity. They observed the opposite phenomenon at 150-300 MPa. The reported increase of protein rigidity may in part explain pressure induced stabilization. Roche et al. (2012), reported that penetration of water molecules inside the structure cavities was the main cause for unfolding of staphylococcal nuclease at pressures up to 300 MPa in the presence of denaturant detected by high pressure NMR spectroscopy. Based on these different reports, one can hypothesize that at moderate high pressures water penetration is impeded by the formation of a more rigid structure because of strengthening hydrophobic interactions and hydrogen bonds resulting in stabilized proteins. At higher pressures water is forced into the protein cavities causing unfolding and loss of activity. However, the extent to which each of these phenomena occur is dependent on the enzyme structure and its environment, the pressure induced stabilization appears to be a common phenomenon observed in several enzymes that are structurally very different (Eisenmenger and Reyes-De-Corcuera, 2009b). However, the mechanisms of pressure stabilization have yet to be fully understood (Royer, 2015; Terefe et al., 2013).

Activation energy

The effect of temperature on the rate constant of inactivation of GOx at each of the selected pressures was calculated as the activation energy (E_a) using the Arrhenius equation. Figure 2.4 illustrates that the Arrhenius plot was linear for each processing pressure (R^2 of 0.98

to 1.00). Table 2.2 shows that the apparent E_a at 300 MPa was 281.0 ± 17.4 kJ mol^{-1} or 1.3 fold smaller than for the inactivation at atmospheric pressure (378.1 ± 25.6 kJ mol^{-1}). In other words, high pressure decreased the dependence of the rate constant of inactivation on temperature which led to higher enzyme stability under HHP. Table 2.2 also shows that the apparent E_a for GOx inactivation significantly decreased with increasing pressure. This observation is in agreement with the trend of a commercial pectinase formulation studied at 0.1-400 MPa and 55.0–85.0 °C (Tomlin et al., 2013). No significant differences were found between the activation energy at low pressure and 400 MPa for stabilization of lipase from *Candida antarctica* in hexane at 40-80 °C (Eisenmenger and Reyes-De-Corcuera, 2009a). This is different from our results where activation energy significantly changed with increasing pressure, suggesting that the HHP effect on stabilization of enzymes is different for different enzymes, and may be dependent on the reaction media as well. Nakamura et al. (1976) reported an activation energy of 368 kJ mol^{-1} (88 kcal mol^{-1}) for GOx thermal denaturation at atmospheric pressure at 50-72 °C which is similar to our calculated activation energy. At 52-65 °C and 0.1 MPa, the activation energy of GOx thermal denaturation from *Aspergillus niger* was 280 kJ mol^{-1} (Zoldák et al., 2004). This value was smaller than ours (378.1 kJ mol^{-1}) or Nakamura et al. (1976) because it was derived from measurements at lower temperatures, different reaction media and pH.

Activation volume

The pressure effects on the rate constant of inactivation of GOx were quantified by calculating the apparent activation volume ($\Delta V^{\neq}$) from Eyring's equation. The differences between calculated $\Delta V^{\neq}$ were significant ($p < 0.05$) at all studied temperatures (Table 2.2). The rate constant of inactivation decreased with pressure up to 180 MPa, following a similar trend for

all temperatures as shown in Eyring's plot (Figure 2.5). At 180-300 MPa, pressure generally increased the rate constant of inactivation of GOx, indicating a transition from pressure induced-stabilization to pressure induced-inactivation (Figure 2.5). These transitions have been reported for several proteins and enzymes and the theory is well established. An activation volume with a positive sign is the result of pressures that induce stabilization. In contrast, an activation volume with a negative sign is the result of pressures that induce inactivation of the enzyme (Smeller, 2002). Finally, a deviation from the Eyring model is observed at the transition from pressure induced-stabilization to pressure induced-inactivation (Grauwet et al., 2009). Therefore, in this study, the activation volume of the stabilization of the enzyme was calculated in the linear region (R^2 of 0.91 to 0.99) between 0.1 and 180 MPa. A positive apparent $\Delta V^{\neq}$ for all the studied temperatures (Table 2.2) indicated that GOx stability was favored by increasing pressure up to 180 MPa. The apparent $\Delta V^{\neq}$ increased from 22.8 ± 3.3 to 57.0 ± 12.0 $cm^3\,mol^{-1}$ as temperature increased from 58.8 °C to 74.5 °C. The apparent $\Delta V^{\neq}$ then decreased to 45.8 ± 3.5 $cm^3\,mol^{-1}$ at 80.0 °C (Table 2.2). At the lowest temperature of 58.8 °C, increasing pressure had a smaller protecting effect on the enzyme against thermal inactivation. The maximal protecting effect of pressure against GOx inactivation was at 74.5 °C. In a similar way, pressure favored stabilization of a pectinase cocktail was indicated by a positive $\Delta V^{\neq}$ at 0.1-400 MPa (Tomlin et al., 2013).

Glucose oxidase modification

A second method employed to increase the stability of GOx was chemical modification. Chemical modification, even with hydrophobic molecules, potentially can stabilize enzymes (Gupta, 1991; Mogharrab et al., 2007; Mozhaev et al., 1990; Stepankova et al., 2013). Glucose oxidase was modified with either benzoate or aniline using EDC to form an amide linkage

between the enzyme and the modifying molecule. Aniline and benzoate were chosen because the phenyl group can enhance the hydrophobicity of the enzyme, hence potentially increasing the enzyme thermal stability. Additionally, to explore the effects of modifying with both benzoate and aniline, several lots of modified enzyme were modified a second time. If GOx was modified initially with benzoate, then it would be modified in the second round with aniline. Similarly, some lots of the aniline-modified GOx were modified with benzoate (see the supplemental section for results).

Benzoate modification was quantified using a TNBS assay. Unmodified GOx was found to have 11 amines detectable out of the 16 total amines per GOx monomer (15 lysines plus the N-terminal amine). Modifying GOx with benzoate reduced the detectable amines to 2 ± 1. Therefore, there were 9 ± 1 benzoate modifications per GOx. This level of modification is reasonable as other groups have found 4-6 lysines per GOx monomer can be modified by hydrophobic groups (Jo et al., 2008; Kamyshny et al., 2002a; Kamyshny et al., 2002b). The number of anilines modifying GOx cannot be quantified using the TNBS assay because TNBS is sensitive only to the number of free amines, while anilines modify carboxylate groups.

Mass spectrometry can also be used to estimate the number of modifications. The higher mass of the modified GOx compared to unmodified GOx represents an increase due to the presence of modifying groups. Using MALDI-TOF mass spectrometry, an average of 28 ± 1 "lysine" residues per GOx monomer were modified by benzoate, while 20 ± 2 glutamate and aspartate residues were modified by aniline. Since there are only 15 lysines per GOx monomer, additional modifications may have occurred on tyrosine and reduced cysteine residues (Carraway and Koshland, 1968; Carraway and Triplett, 1970; Means and Feeney, 1971). As for aniline, there are 30 glutamates and 36 aspartates in GOx; 20 modifications per monomer are reasonable.

Effects of modifications on GOx

Circular dichroism spectra (Supplemental Figure S2.1) indicate the modifications do not alter GOx structure. The thermal stability of GOx was monitored by DSC and the thermograms for unmodified and modified GOx are shown in (Figure 2.6). Thermal denaturation of all the GOx samples was irreversible, and the thermograms were asymmetric. Despite the irreversibility of GOx thermal unfolding, the data can still be fit to a two-state (native to unfolded) mechanism (Zoldák et al., 2004). Due to the irreversibility of GOx unfolding, the thermodynamic parameters are apparent values (Table 2.3). Benzoate modification slightly destabilizes GOx, decreasing the T_m by 0.9 °C from 61.4 °C to 60.5 °C. The slight decrease in thermal stability of GOx suggests that GOx is not significantly affected by modification. Even more promising is when GOx was modified with aniline. It is quite clear from the thermograms (Figure 2.6) that modification of GOx with aniline has a large stabilizing effect with the T_m increasing by 8 °C to 69.4 °C. While it may seem counterintuitive that modifying an enzyme with hydrophobic molecules increases thermal stability, it depends upon what other potential interactions may occur with the modifying hydrophobic group and the surface of the enzyme (Gupta, 1991; Mozhaev et al., 1990). Presumably with aniline modification of GOx, some highly stabilizing interactions occur between the phenyl groups of aniline and nearby GOx residues. The large increase in thermal stability with aniline modification of GOx is very promising for future biosensor applications.

The amount of modification could have detrimental effects on the function of the enzyme. If key residues for activity get modified, the enzyme function could be lost. The activities of the unmodified and modified GOx species were determined by Michaelis-Menten kinetics (Table 2.4). For unmodified GOx, a k_{cat} of 446 ± 5 s^{-1} and K_M of 17.5 ± 0.8 mM concurred with literature values at pH 5 (Guo et al., 2010). Modifying GOx with aniline did not

perturb the efficiency of the enzyme. Both k_{cat} and K_M were unaffected, within error, when compared to unmodified GOx. Benzoate slightly altered the activity of GOx upon modification. While benzoate modification did not alter the k_{cat} of GOx, the K_M increased almost 2-fold compared to the unmodified enzyme. The minimal changes to k_{cat} and K_M for aniline modified GOx and only a slight increase in the K_M for the benzoate modified enzyme, without a change in k_{cat}, indicates that modification does not particularly perturb the enzyme's function.

How modification of GOx with aniline result in an increased T_m is unclear. How proteins accommodate hydrophobic groups on their surfaces is largely unexplored as hydropathy is typically proposed to lead to decreased solubility and/or increased aggregation. However aromatic groups possess a quadrupole moment, leading to their ability to interact with cations on the ring face (Dougherty, 1996; Gallivan and Dougherty, 1999) or anions on their ring edge (Jackson et al., 2007; Philip et al., 2011). In their study of protein stability, (Pace et al., 2011) state "The destabilizing force of most interest is conformational entropy". This leads to the possibility of solvent re-organization effects as numerous groups propose water near hydrophobic surfaces forms clathrate (ordered) structures (Head-Gordon, 1995; Teeter, 1984). Further, Petersen et al. (2009) find clathrate, hydration shells show a strong temperature dependence of water reorientation. Water can also have anomalous characteristics (Biela et al., 2012; Biela et al., 2013; Breiten et al., 2013; Chandler, 2005; Krimmer et al., 2014; Patel et al., 2012), thus its role is difficult to assess. A final comment considers the recent construction and analysis of a protein lacking charges (Hojgaard et al., 2016). This variant protein remains soluble and stable, indicating that electrostatic interactions are not required for its structure-function relationship. The different effects of modifying GOx with aniline vs. benzoate is likely due to the differences in the location of derivatized residues and the local environment.

Acknowledgment

This project was supported by USDA-NIFA-AFRI GRANT #11322452.

Table 2.1.

Analysis of average correlation coefficients for fitting data to zero, first and second-order models describing the relationship between GOx residual activity and treatment time for A) all processing pressures, and B) 180, 240, and 300 MPa.

A)

T (°C)	Correlation coefficient (R^2) for selected order models		
	Zero	First	Second
58.8	0.91	0.93	0.96
63.8	0.90	0.92	0.94
69.1	0.91	0.97	0.94
74.5	0.90	0.99	0.91
80.0	0.90	0.98	0.88
Average	0.91	0.96	0.93

B)

T (°C)	Correlation coefficient (R^2) for selected order models		
	Zero	First	Second
58.8	0.88	0.90	0.94
63.8	0.90	0.91	0.93
69.1	0.96	0.96	0.96
74.5	0.97	0.99	0.93
80.0	0.95	0.96	0.95
Average	0.93	0.95	0.94

Table 2.2.

Apparent first-order rate constant of inactivation of GOx ± the linear regression standard error and apparent activation energy and apparent activation volume obtained from apparent first-order rate constant of inactivation of GOx ± the linear regression standard error.

Pressure (MPa)	Temperature (°C)										E_a (kJ mol^{-1})	R^2
	58.8	R^2	63.8	R^2	69.1	R^2	74.5	R^2	80.0	R^2		
	k_{inact} (min^{-1}) × 10^{-2}											
0.1	0.64^{a} ±0.06	0.97	3.40^{a} ±0.29	0.98	42.67^{a} ±2.28	0.99	516.77^{a} ±31.81	0.99	1530.03^{a} ±36.71	1.00	378.1^{f} ±25.6	0.99
60	0.29^{b} ±0.03	0.97	1.21^{b} ±0.15	0.96	7.40^{b} ±0.56	0.98	62.33^{b} ±6.28	0.97	449.51^{b} ±27.28	0.99	342.4^{g} ±13.6	1.00
120	0.22^{c} ±0.03	0.94	0.52^{c} ±0.11	0.89	3.02^{c} ±0.44	0.94	24.50^{c} ±2.31	0.97	201.69^{c} ±15.35	0.98	320.4^{h} ±27.1	0.98
180	0.13^{d} ±0.02	0.94	0.43^{d} ± 0.08	0.91	2.15^{d} ±0.21	0.97	13.70^{d} ±0.48	1.00	88.36^{d} ±8.19	0.97	302.1^{i} ±15.2	0.99
240	0.14^{de} ±0.02	0.93	0.45^{d} ±0.07	0.93	2.33^{d} ±0.18	0.98	10.29^{d} ±0.66	0.99	73.13^{d} ±8.47	0.96	286.4^{j} ±14.4	0.99
300	0.16^{e} ±0.03	0.92	0.47^{d} ±0.09	0.90	1.90^{d} ±0.27	0.94	11.63^{d} ±0.56	0.99	69.55^{d} ±6.53	0.97	281.0^{k} ±17.4	0.99
$\Delta V^{\neq}$ (cm^3 mol^{-1})	22.8^{l} ± 3.3		32.9^{m} ± 6.3		46.8^{n} ± 10.6		57.0^{o} ± 12.0		45.8^{p} ± 3.5			
R^2	0.96		0.93		0.91		0.92		0.99			

[a, b, c, d, e] Differences in means of k_{inact} with different letter in each column (effect of pressure on k_{inact}) were significant ($p < 0.05$).

[f, g, h, i, j, k] Differences in means of E_a with different letter (effect of pressure on E_a) were significant ($p < 0.05$).

[l, m, n, o, p] Differences in means of $\Delta V^{\neq}$ with different letter (effect of temperature on $\Delta V^{\neq}$) were significant ($p < 0.05$).

Table 2.3.

Apparent thermodynamic parameters for thermal unfolding of GOx by DSC in 50 mM Na_2HPO_4, pH 7.1. Thermograms were fit to a two-state model with two unique unfolding transitions. The unfolding of GOx is irreversible, therefore the thermodynamic parameters obtained from fits of the data are apparent values.

Modification	T_{m1} (°C)	$\Delta H_{d,app1}$ (kJ mo1^{-1})[a]	T_{m2} (°C)	$\Delta H_{d,\,app2}$ (kJ mo1^{-1})[a]
None	61.4 ± 0.1	960 ± 40	61.4 ± 0.1	1000 ± 40
Aniline	69.4 ± 0.3	1090 ± 290	69.4 ± 0.3	630 ± 210
Benzoate	60.5 ± 0.2	1130 ± 80	60.5 ± 0.2	590 ± 170

[a] The apparent enthalpy of denaturation

Table 2.4.

Michaelis-Menten kinetic parameters for unmodified or modified GOx in 50 mM NaAcetate, pH 5.1 at 37 °C. The assay was performed as a coupled assay with peroxidase and o-dianisidine and the change in absorbance was measured at 500 nm.

Modification	k_{cat} (s^{-1})	K_M (mM)
None	446 ± 5	17.5 ± 0.8
Benzoate	434 ± 8	32.4 ± 3.7
Aniline	446 ± 14	23.2 ± 1.6

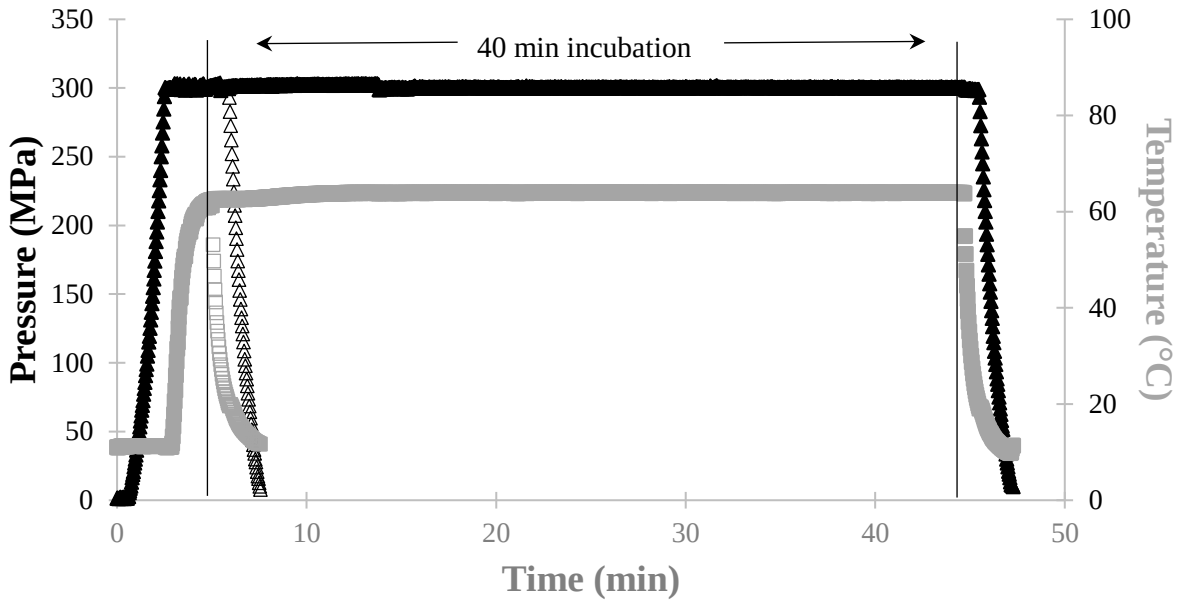

Figure 2.1. Pressure (▲) and temperature (■) profiles in high pressure reactor for treated sample at 63.8 °C, 300 MPa, and 40 min; as well as 0 min (100% residual activity) sample pressure (△) and temperature (□) profiles for treatment at 63.8 °C, 300 MPa, and 0 min.

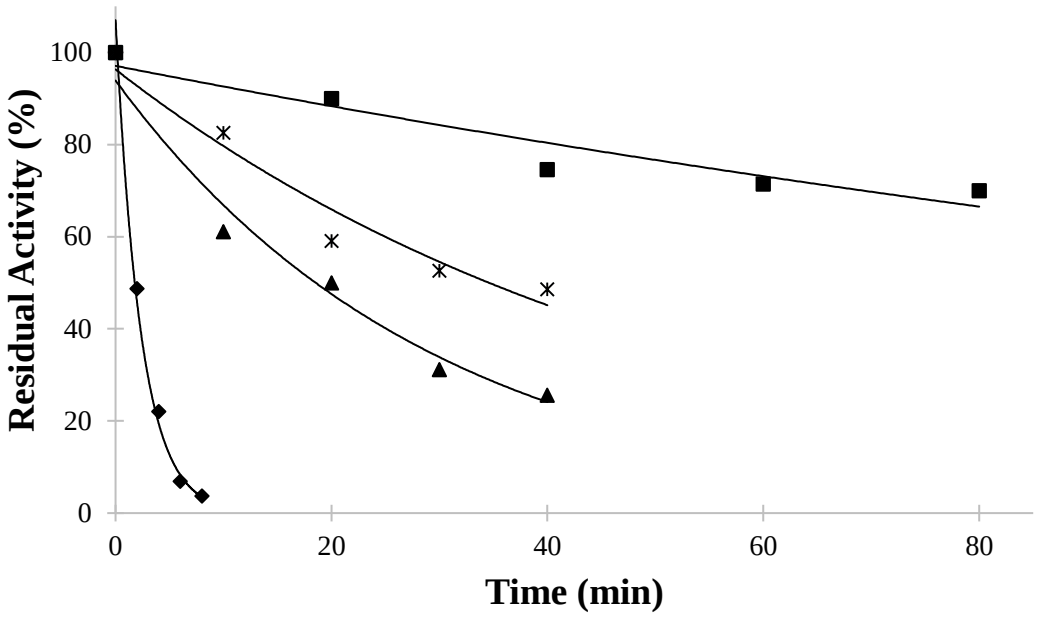

Figure 2.2. Effect of pressure and temperature on average GOx residual activity for treatments at (▲) 0.1 MPa and 63.8 °C, (■) 300 MPa and 63.8 °C, (◆) 0.1 MPa and 69.1 °C, and (✳) 300 MPa and 69.1 °C.

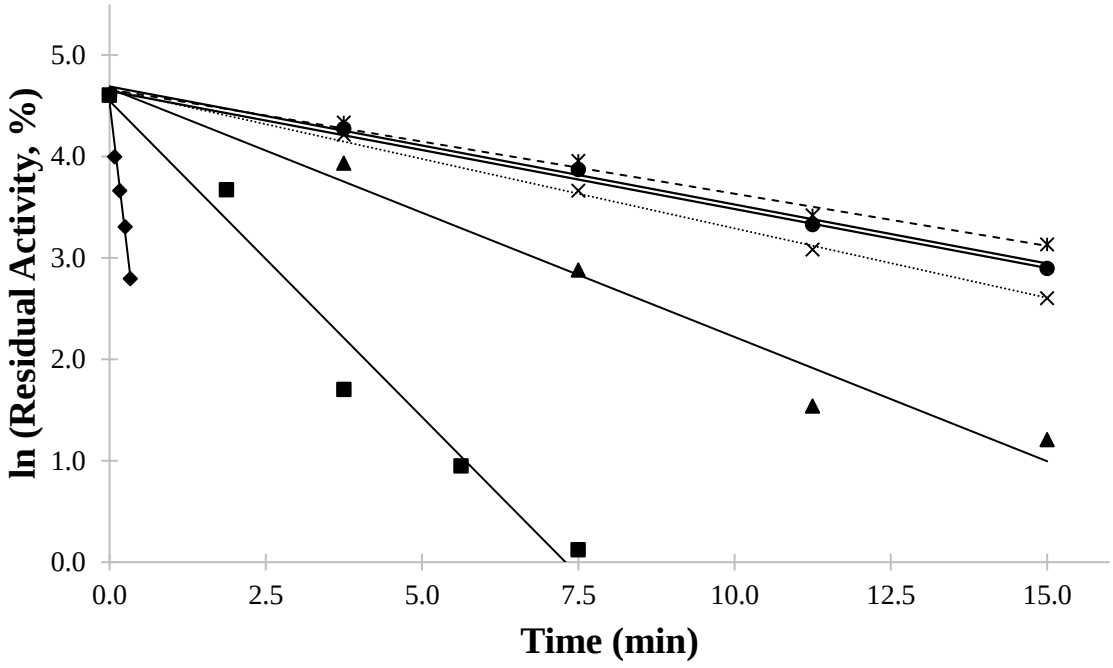

Figure 2.3. Linear behavior of rate constants for GOx inactivation at 74.5 ºC for samples treated at (◆) 0.1 MPa, (■) 60 MPa, (▲) 120 MPa, (×) 180 MPa, (∗) 240 MPa, and (●) 300 MPa. Trendlines at 180 MPa, 240 MPa, and 300 MPa are dotted, dashed, and double lined respectively to differentiate the last 3 pressures.

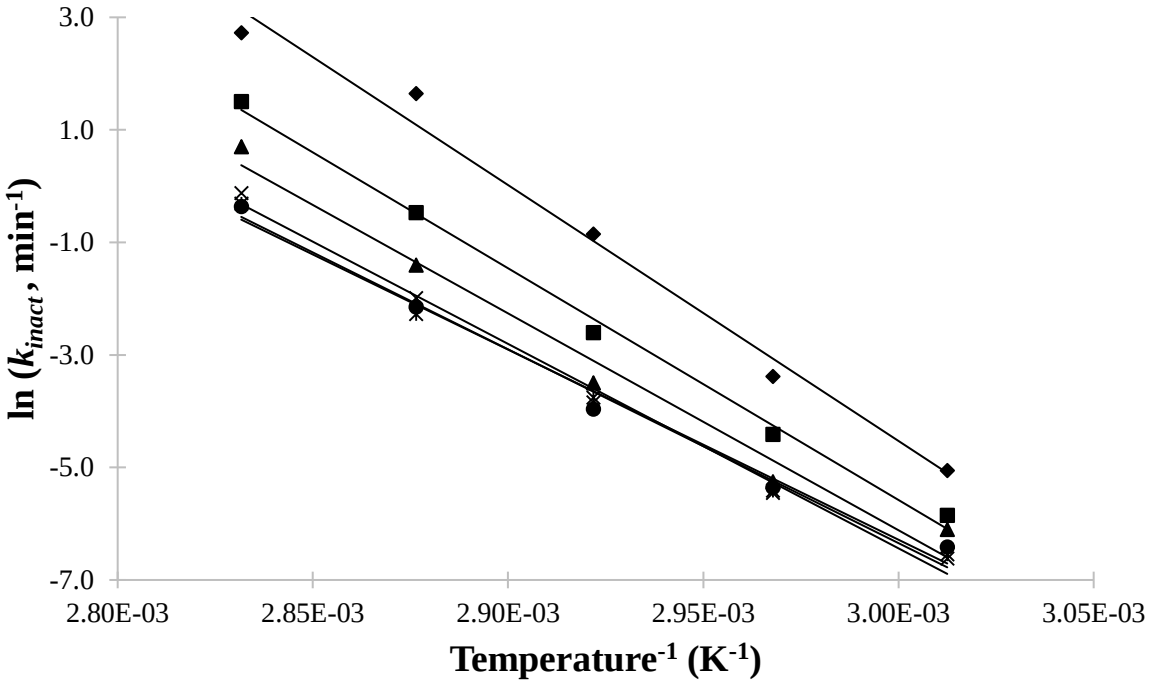

Figure 2.4. Arrhenius plots to obtain apparent activation energies from linear regression of ln k_{inact} versus inverse temperature for treatment at (◆) 0.1 MPa, (■) 60 MPa, (▲) 120 MPa, (×) 180 MPa, (∗) 240 MPa, and (●) 300 MPa.

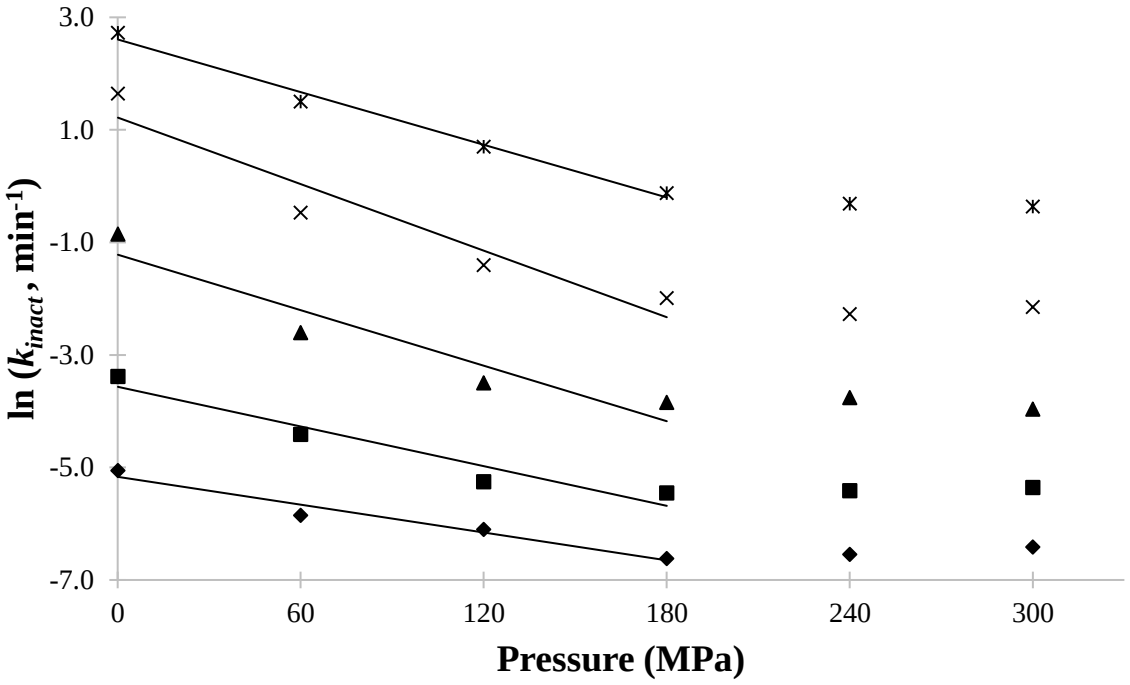

Figure 2.5. Eyring plots to obtain apparent activation volumes from linear regression of ln k_{inact} versus pressure for samples treated at (◆) 58.8 °C, (■) 63.8 °C, (▲) 69.1 °C, (×) 74.5 °C, and (∗) 80.0 °C.

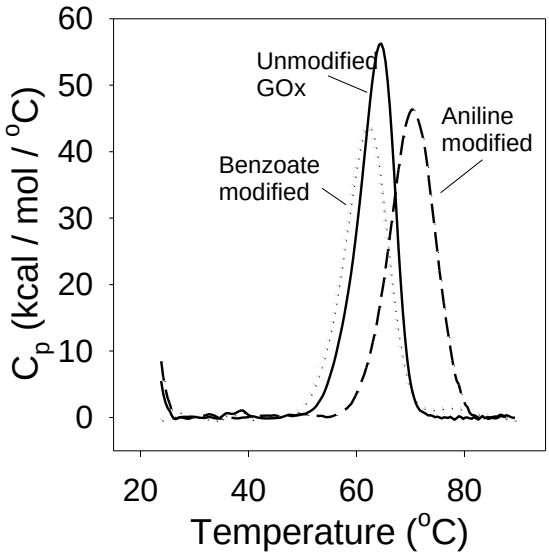

Figure 2.6. Thermograms for the thermal stability of 8-12 μM GOx examined by DSC in 50 mM Na_2HPO_4, pH 7.1 buffer. Scans were performed for unmodified GOx (solid line), aniline modified enzyme (dashed line) and benzoate modified enzyme (dotted line). Scans were performed from 20-90 °C at a scan rate of 1.5 °C min-1. Raw data were normalized to the protein concentration in each experiment and a baseline was subtracted from the normalized data. Unfolding of the enzymes was irreversible. Aniline modification thermally stabilized GOx, while benzoate modification destabilized the enzyme.

Appendix

2-I) High pressure system for stabilization study.

(a) **(b)**

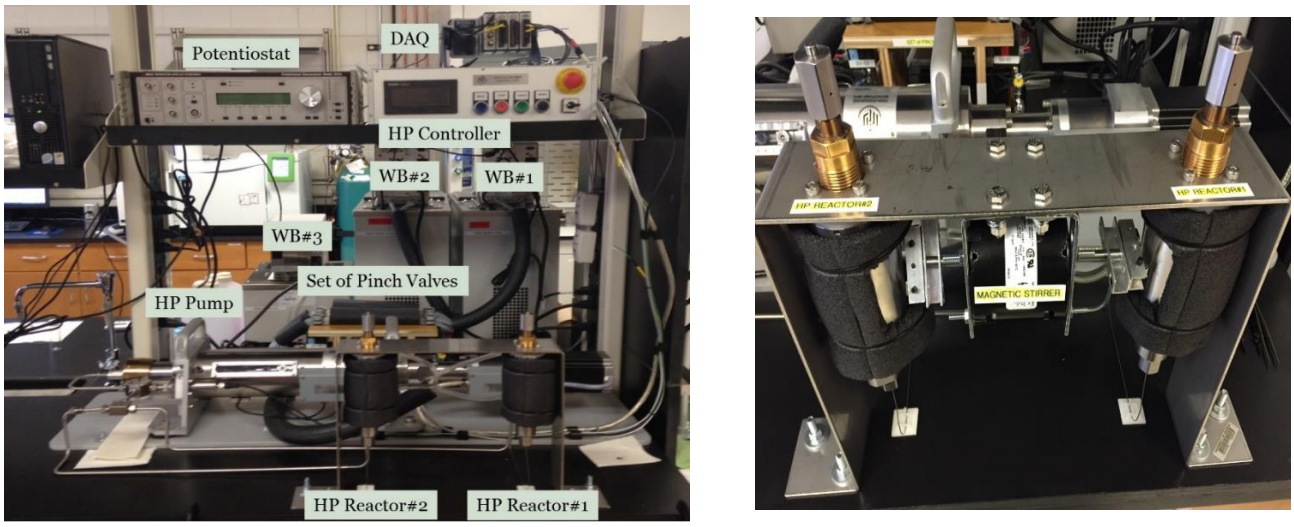

Figure A2.1. (a) High pressure equipment and (b) high pressure reactors model U111 used for the stabilization study.

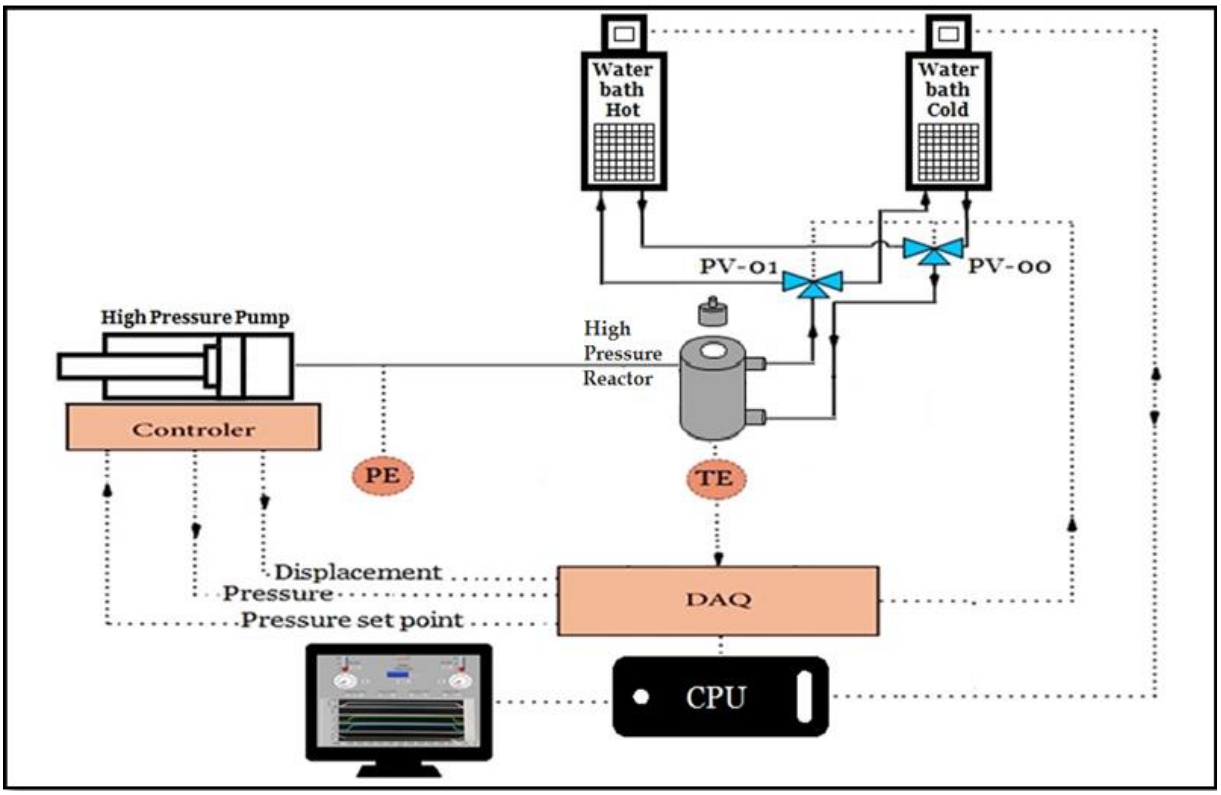

Figure A2.2. Schematic of the high pressure system used for the stabilization study.

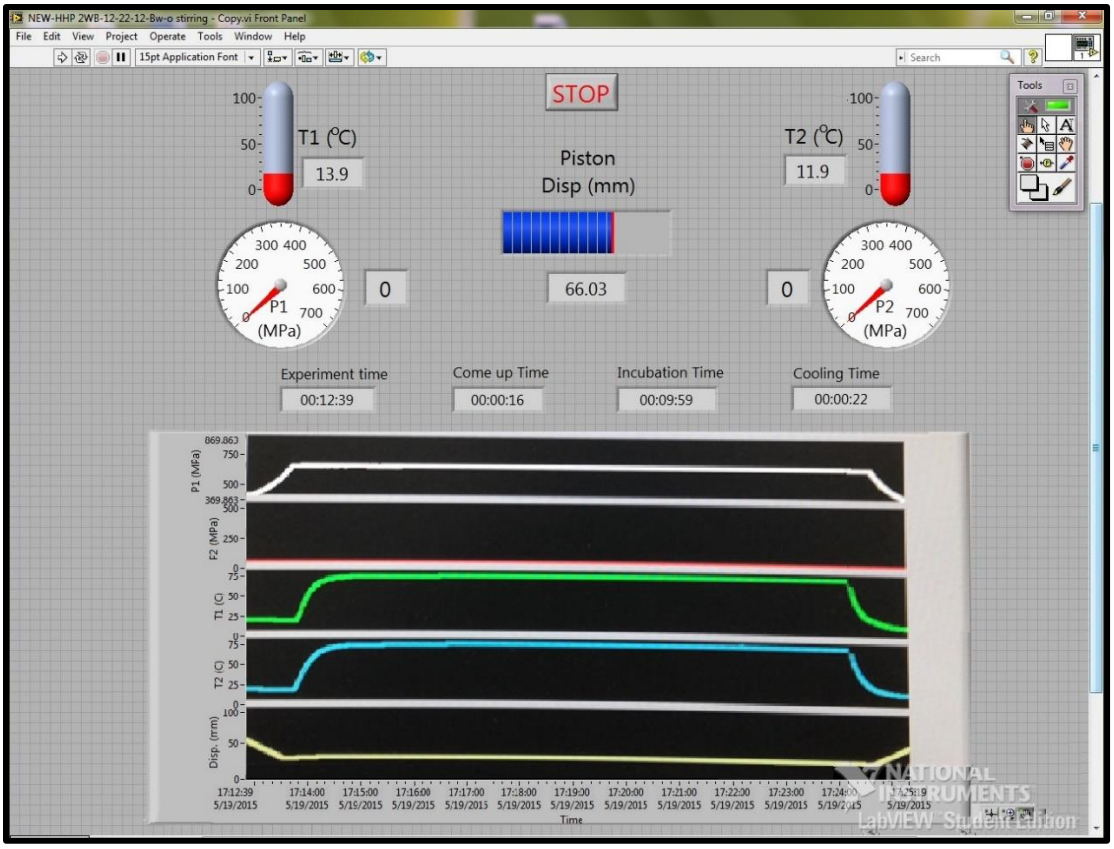

Figure A2.3. LabVIEW front panel window used to control and monitor the high pressure treatments.

2-II) Zero time activities

Table A2.1. The activity for the GOx samples at each pressure-temperature treatment with 0 min incubation time.

Pressure (MPa)	Temperature (°C)	$Activity_1$ (units mg^{-1})	$Activity_2$ (units mg^{-1})	Mean Activity (units mg^{-1})
0.1	58.8	87.94	86.44	87.19
	63.8	86.83	84.68	85.75
	69.1	63.17	64.72	63.95
	74.5	22.57	22.78	22.67
	80.0	6.99	8.13	7.56
60	58.8	93.14	91.58	92.36
	63.8	92.66	90.33	91.49
	69.1	79.58	80.44	80.01
	74.5	71.36	70.61	70.99
	80.0	49.33	51.60	50.47
120	58.8	94.34	93.14	93.74
	63.8	91.06	89.91	90.49
	69.1	81.57	79.19	80.38
	74.5	72.97	73.68	73.32
	80.0	68.27	67.17	67.72
180	58.8	95.26	93.31	94.29
	63.8	87.57	88.30	87.94
	69.1	82.95	81.87	82.41
	74.5	76.72	78.40	77.56
	80.0	69.76	71.03	70.39
240	58.8	91.64	90.41	91.03
	63.8	90.42	89.00	89.71
	69.1	85.38	87.55	86.47
	74.5	77.58	76.61	77.10
	80.0	66.82	68.02	67.42
300	58.8	89.39	89.93	89.66
	63.8	87.28	88.41	87.84
	69.1	86.67	87.99	87.33
	74.5	75.70	74.84	75.27
	80.0	68.83	67.27	68.05

2-III) Supplemental section

Effects of modification on Glucose Oxidase secondary structure

Near and far UV CD spectra for unmodified and modified GOx were monitored on an AVIV model 202 circular dichroism spectropolarimeter. At least three scans were performed on 9-11 μM enzyme in 50 mM Na_2HPO_4, pH 7.1 buffer using a 1 mm cuvette for far UV spectra and a 2 mm cuvette for near UV spectra. Data points were collected every 1 nm with a 10 second integration time. Data were normalized as the mean residue ellipticity using an average molecular weight per residue of 110 g/mol (Strader et al., 2001).

For modified enzymes to retain their activity, it is imperative that the structure of the enzyme remain intact. The effects of modification on the secondary structure of GOx were monitored by CD spectroscopy (Supplemental Figure S2.1). The far UV CD spectra for modified proteins had similar minima and intensities compared to the unmodified protein. The near UV spectra were superimposable for the modified and unmodified proteins. These results indicate that the structure of GOx is unaffected by the modification by either aniline or benzoate.

Double modification of GOx with aniline and benzoate

Buoyed by modifications having a lack of effects on protein structure, increasing GOx thermal stability in the case of aniline and minimal effects on enzyme activity, GOx was modified with both aniline and benzoate. Analyzing the number of modifications by MALDI-TOF MS yielded that benzoate-modified GOx is modified by 12 anilines, while 35 benzoates modify GOx previously modified with aniline. Fewer aniline modifications of the benzoate-modified GOx compared to unmodified GOx suggests that some of the aspartate and glutamate

groups available in the modified enzymes are no longer available in the benzoate-modified enzyme. Typically for the single modification reaction, a maximum number of modifications were reached after two hours of reaction. Perhaps in the case of the double modification, saturating modification are not obtain within two hours, especially if the modified groups from the first round of modification hinder access of the modifying molecule in the second round of modification. Alternately, more groups are available for benzoate modification when GOx is first modified by aniline.

The thermal stability of doubly modified GOx was also examined by DSC (Supplemental Figure S2.2). Doubly modified GOx samples had higher thermal stabilities compared to unmodified enzyme (Supplemental Table S2.1). An increase of approximately 5 °C was independent of the order in which GOx was modified. The increase in thermal stability is not quite as high as aniline modification alone. This may be because there are fewer anilines that modify GOx when the enzyme is previously modified by benzoate. Or, more likely, the benzoate groups that modify GOx may interfere with potentially stabilizing interactions that aniline groups form with GOx.

Modifying GOx with both aniline and benzoate decreases the activity of GOx (Supplemental Table S2.2). A 33% decrease in the k_{cat} of benzoate-modified GOx modified with aniline, along with a slight increase in the K_M are noted. Likewise, aniline-modified GOx modified with benzoate had a 15% loss in k_{cat} compared to unmodified enzyme. The K_M also increases from 17.5 mM to 25.1 mM. The decrease in the activity of the doubly modified enzymes. However, enough activity remains that doubly modified GOx would still be a viable option for biosensor use.

Supplemental Table S2.1.

Apparent thermodynamic parameters for thermal unfolding of GOx by DSC in 50 mM Na_2HPO_4, pH 7.1. Thermograms were fit to a two-state model with two unique unfolding transitions. The unfolding of GOx is irreversible, therefore the thermodynamic parameters obtained from fits of the data are apparent values.

Modification	T_{m1} (°C)	$\Delta H_{d,app1}$ (kJ mo1^{-1})[c]	T_{m2} (°C)	$\Delta H_{d,app2}$ (kJ mo1^{-1})[c]
Benzoate-Aniline[a]	65.4 ± 0.1	1300 ± 80	65.4 ± 0.1	590 ± 80
Aniline-Benzoate[b]	66.2 ± 0.2	1170 ± 80	66.2 ± 0.2	590 ± 40

[a]GOx was modified first with benzoate, then modified a second time with aniline.
[b]GOx was first modified with aniline, then modified with benzoate.
[c]The apparent enthalpy of denaturation.

Supplemental Table S2.2.

Michaelis-Menten kinetic parameters for unmodified or modified GOx in 50 mM NaAcetate, pH 5.1 at 37 °C. The assay was performed as a coupled assay with POx and o-dianisidine and the change in absorbance was measured at 500 nm.

Modification	k_{cat} (s^{-1})	K_M (mM)
Benzoate-Aniline[a]	299 ± 5	20.9 ± 1.5
Aniline-Benzoate[b]	368 ± 6	25.1 ± 1.3

[a]GOx was modified first with benzoate, then modified a second time with aniline.
[b]GOx was first modified with aniline, then modified with benzoate.

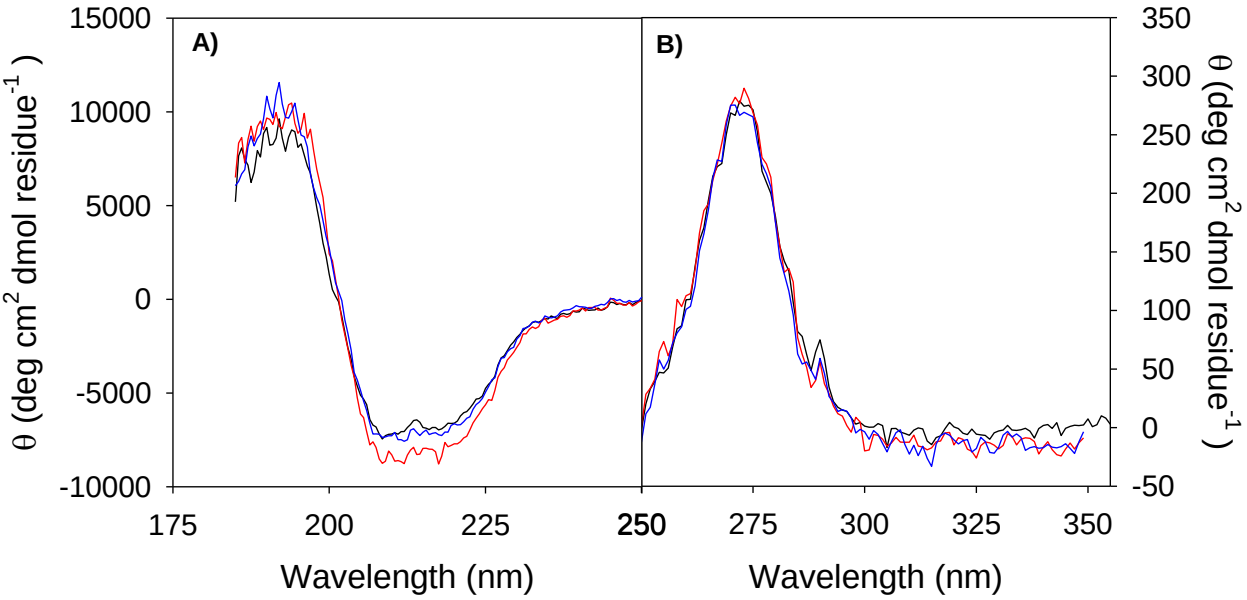

Supplemental Figure S2.1. The secondary structure of 9-11 μM GOx is unaffected by modification. A) Far UV spectra of GOx unmodified (black line), modified with benzoate (red line) and modified with aniline (blue line). B) Near UV spectra for unmodified GOx (black line), GOx modified with benzoate (red line) and GOx modified with aniline (blue line).

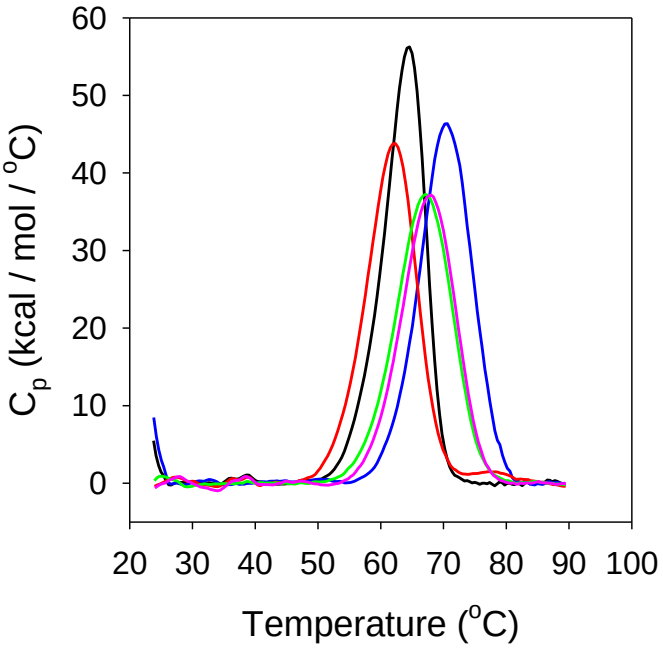

Supplemental Figure S2.2. The thermal stability of 8-12 μM GOx measured by DSC in 50 mM Na2HPO4, PH 7.1 buffer. Thermograms for GOx unmodified (black line), modified with benzoate (red line), modified with aniline (blue line), doubly modified with benzoate first and aniline second (green line) and doubly modified with aniline first and benzoate second (magenta line). Samples modified with aniline increase the thermal stability of GOx. Benzoate modifications decrease the stability relative to unmodified GOx (singly modified enzyme) or aniline-modified GOx (doubly modified enzymes).

CHAPTER 3

EFFECT OF HIGH HYDROSTATIC PRESSURE AND HYDROPHOBIC MODIFICATION ON THERMAL STABILITY OF XANTHINE OXIDASE [1]

[1] A. Halalipour, M.R. Duff, E.E. Howell, J.I. Reyes-De-Corcuera. To be submitted to *Enzyme and Microbial Technology*.

Abstract

The effect of high hydrostatic pressure (HHP) on the kinetics of thermal inactivation of xanthine oxidase (XOx) from bovine milk was studied. Inactivation of XOx followed pseudo-first-order kinetics at 0.1-300 MPa and 55.0-70.0 °C. High pressure up to at least 300 MPa stabilized XOx at all the studied temperatures. The highest stabilization effect of HHP on XOx was at 200 to 300 MPa at 55.0 and 58.6 °C, and at 250 to 300 MPa at 62.3 to 70.0 °C. The stability of XOx increased 9.5 times at 300 MPa and 70.0 °C compared to atmospheric pressure at the same temperature. The activation energy of inactivation of XOx decreased with pressure and was 1.9 times less at 300 MPa (97.0 ± 8.2 kJ mol^{-1}) than at 0.1 MPa (181.7 ± 12.1 kJ mol^{-1}). High pressure decreased the dependence of the rate constant of inactivation to temperature effects compared to atmospheric pressure. The stabilizing effect of HHP on XOx was highest at 70.0 °C where the activation volume of inactivation of XOx was 28.9 ± 2.9 cm^3 mol^{-1}. A second approach to increase XOx stability involved hydrophobic modification using aniline or benzoate. The thermal stability of XOx remained unaffected after 8 ± 1 modifications of carboxyl side groups per XOx monomer with aniline, or 12 ± 5 modifications of amino side groups per XOx monomer with benzoate.

Introduction

Bovine xanthine oxidase (XOx) consists of one molecule of flavin adenine dinucleotide (FAD), one atom of molybdenum, and four atoms of iron per enzyme subunit (Olson et al., 1974). As an oxidoreductase, XOx mainly catalyzes the oxidation of xanthine to uric acid by producing hydrogen peroxide in the presence of oxygen. The oxidation occurs using the molybdopterin center, the pair of iron-sulfur clusters, and bound FAD (Bray et al., 1961; Olson et al., 1974). Xanthine oxidase ability to catalyze different substrates has been used to fabricate biosensors to evaluate the freshness of fish by detection of hypoxanthine levels which imparts a bitter spoiled taste to dead fish (Dervisevic et al., 2015; Devi et al., 2011; Nakatani et al., 2005), and to detect of the caffeine (1,3,7-trimethylxanthine) for evaluation of the quality of commercial instant tea and coffee (Babu et al., 2007). In addition, XOx has also been used as biosensor to detect theophylline (1,3-dimethylxanthine) content which is one of the most common medications for chronic asthma (Mao et al., 2001; Stredansky et al., 2000).

Xanthine oxidase stabilization has been studied by procedures including immobilization onto polymeric supports (Araujo et al., 1997; Johnson and Coughlan, 1978; Neri et al., 2011), application of organic media (Amini et al., 2011; Rashidi et al., 2009), and utilization of cosolute (trehalose) and osmolyte (betaine) additives (Zhang et al., 2014). However, the effect of high hydrostatic pressure (HHP) on XOx stability at elevated temperatures has not yet been explored. High hydrostatic pressure has stabilized several enzymes (Eisenmenger and Reyes-De-Corcuera, 2009b). Recent reports include the effect of HHP on β-glucosidase (Terefe et al., 2013; Vila-Real et al., 2010), pectinases (Tomlin et al., 2013), polyphenoloxidase (Huang et al., 2014), inulin fructotransferase (Li et al., 2015), and glucose oxidase (Halalipour et al., 2016). Therefore, the

objective of this research was to elucidate the effect of HHP on the stability of XOx at selected temperatures.

Materials and methods

Materials and equipment

Xanthine oxidase from bovine milk (EC 1.17.3.2, Product No. X4376), N-(3-dimethylaminopropyl)-N'-ethylcarbodiimide (EDC), N-hydroxysulfosuccinimide, sodium benzoate and aniline were purchased from Sigma-Aldrich (St. Louis, MO, USA). Xanthine was obtained from either MP Biomedical (Solon, OH, USA) or Sigma-Aldrich. Potassium phosphate and potassium hydroxide were purchased from Fisher Scientific (Pittsburg, PA, USA). The HHP system used in this research is described in a previous report (Halalipour et al., 2016). Absorbance measurements were made in a multi-mode microplate reader (Model Synergy HTX) controlled by Gen5 data analysis software both from BioTek Instruments (Winooski, VT, USA).

Methods

Thermal stability treatments at HHP

A volume of 100 µL of 0.15 units mL^{-1} (0.21 mg mL^{-1}) untreated XOx in 50 mM potassium phosphate buffer pH 7.5 was transferred into a 15×15 mm polyethylene plastic pouch. The pouch was then heat-sealed and placed in the high-pressure reactor held at 10 °C. The pressure was then raised to 50, 100, 150, 200, 250, or 300 MPa. Experiments at 0.1 MPa served as a control. The temperature was then raised to 55.0 °C, 58.6 °C, 62.3 °C, 66.1 °C, or 70.0 °C. Incubation temperatures were selected to achieve even increments of the reciprocal of the absolute temperature based on an Arrhenius approach. The incubation time began when 95% of

the temperature set point was reached. Five incubation times were selected to obtain the kinetics of XOx inactivation under HHP for each incubation temperature. Upon completion of the incubation time, the samples were first cooled down to 15 °C and then the reactor was depressurized to ambient conditions (0.1 MPa). Figure 3.1 illustrates heating/cooling and pressurizing/depressurizing sequences for a XOx sample treated at 200 MPa, 66.1 °C, for 0-min (open symbols) or 20-min (filled symbols) incubation.

The activity of the processed sample was measured immediately after it was removed from the HHP reactor at ambient conditions at 29 °C. The enzyme activity was determined by monitoring the formation of uric acid at 295 nm for 3 min following the Bergmeyer et al. (1974b) method but adapted to the microplate reader by reducing 10-fold the volume of the reaction mixture. The residual enzyme activity was calculated as a percent relative to the initial activity. The initial activity was determined as the activity of a sample at the same pressure-temperature condition but with 0 min incubation time, as shown in Figure 3.1 (Table A3.1 presents XOx activity at 0 min time for each treatments). This accounted for the possible changes in the activity during the heating/cooling and pressurizing/depressurizing transient periods.

Treatments were duplicated and performed in a randomized block design. Pressure and incubation time were randomly chosen while treatments were blocked by incubation temperature.

Kinetics of thermal inactivation at HHP

The thermal inactivation kinetics of bovine milk XOx were evaluated utilizing a first-order kinetics model. The rate constant of inactivation of XOx (k_{inact}) was calculated by linear regression analysis of the relationship between the natural logarithm of residual activity and

incubation time. Experimental error in the calculation of k_{inact} was determined utilizing the standard error of the linear regression. To analyze whether there were significant differences in k_{inact} among pressure levels at each temperature, general linear model (GLM) was applied evaluating "pressure" and "incubation time" as random factors as well as the "pressure" × "incubation time" interaction with "incubation time" selected as covariate. Linear regression analysis and GLM were done using SAS statistical software (Cary, NC, USA). The R^2 values were used as indicators of the quality of the regression fit.

Effect of temperature on k_{inact}

Arrhenius equation was used to quantify the effect of temperature on k_{inact} (Van den Broeck et al., 2000; Weemaes et al., 1998). Therefore, the activation energy of inactivation (E_a) in the Arrhenius equation was calculated by linear regression analysis of the natural logarithm of k_{inact} of XOx and the reciprocal of the absolute temperature. The error in the calculation of the E_a was reported as the standard error of the linear regression of the Arrhenius plot. The comparison of E_a among HHP levels was performed using GLM using "pressure" and "1/temperature" as random factors and evaluating "pressure" × "1/ temperature" interaction with "1/temperature" selected as covariate.

Effect of pressure on k_{inact}

Eyring equation was used to assess the effect of pressure on the k_{inact} (Ludikhuyze et al., 1998; Van den Broeck et al., 2000). This allowed calculation of the activation volume of inactivation ($\Delta V^{\neq}$) by linear regression analysis of a plot of the natural logarithm of the rate constant of inactivation of XOx and pressure. The experimental error in the calculation of $\Delta V^{\neq}$

was determined utilizing the standard error of the linear regression. The comparison of $\Delta V^{\neq}$ among temperature levels was done using GLM, using "temperature" and "pressure" as random factors and evaluating the "temperature" × "pressure" interaction with "pressure" selected as covariate.

Modification of XOx for stability

Xanthine oxidase was chemically modified as described previously for glucose oxidase (Halalipour et al., 2016) with a few minor modifications. Briefly, 100 mM sodium benzoate, or aniline, was added to a 1-mL solution of 5 mg mL^{-1} XOx in 50 mM K_2HPO_4, pH 7.5. The solution was incubated on ice for five minutes before addition of N-(3-dimethylaminopropyl)-N'-ethylcarbodiimide (EDC) and N-hydroxysulfosuccinimide to concentrations of 10 mg mL^{-1} to initiate the covalent coupling of benzoate or aniline to XOx. The reaction proceeded on ice for five minutes. The reaction was stopped by immediately loading the solution onto a 10-DG Econopac column (BioRad) pre-equilibrated in the same 50 mM K_2HPO_4 buffer. This column removes excess reagents and products from the protein. Samples were stored at 4 °C until further use. Modification reactions performed for ≥ 30 minutes tended to completely abolish the activity of the enzyme.

Characterization of modified enzyme

Quantifying the level of modification of XOx was performed as previously reported (Halalipour et al., 2016). Briefly, a trinitrobenzene sulfonic acid (TNBS) assay was used to monitor labelling of the lysines and the N-terminal amine of XOx by benzoate. Additionally, the number of modifications by benzoate and aniline were estimated using a Bruker MicroFlex

MALDI-TOF mass spectrometer. The difference in mass between the modified and unmodified enzyme was divided by the mass of benzoate or aniline, minus the mass of water (18 Da).

Effects of modification on the thermal stability of XOx were measured on a MicroCal VP differential scanning calorimeter (DSC). Scans were performed on 0.5-1.5 μM XOx in 50 mM Na_2HPO_4, pH 8.0 from 25-95 °C at a scan rate of 1.5 °C min^{-1}. Origin v7.0 software supplied by MicroCal controlled the instrument and was also used to fit the data. All values were the average of two independent modification batches.

Michaelis-Menten kinetics analysis was performed at 25ºC in 50 mM K_2HPO_4, pH 7.5 buffer by directly monitoring the oxidation of xanthine to urate at 295 nm (Bergmeyer et al., 1974b). Concentrations of xanthine between 0.3 and 50 μM were used to measure the activity of 10-20 nM native or phenyl-modified XOx. The change in the absorbance of the sample at 295 nm was monitored on a Perkin Elmer λ35 UV-vis spectrometer. An extinction coefficient of $\varepsilon_{295\ nm}$ = 9600 M^{-1} cm^{-1} was used to process the data (Avis et al., 1956). All values were the average of two independent modification batches.

Results and discussion

Rate constant of inactivation

After all HHP treatments at the studied temperatures, the residual XOx activity was greater compared to treatments at atmospheric pressure and the corresponding temperature. This is illustrated in Figure 3.2 which contrasts treatments at 58.6 and 66.1 °C at 300 MPa (open symbols) against treatments at the same temperatures but at 0.1 MPa (filled symbols). This behavior indicates the stabilizing effects of HHP on XOx against thermal inactivation. The residual activity of XOx decreased over time for all the processing temperatures. The decrease in

XOx residual activity followed an apparent or pseudo-first-order inactivation model with an R^2 in the range of 0.95 to 1.00 as summarized in Table 3.1 and illustrated in Figure 3.3 for 70 °C and 0.1-300 MPa conditions. This is consistent with other studies of thermal inactivation kinetics of XOx at ambient pressure. Amini et al. (2011) reported a first-order inactivation kinetics of XOx from rat liver in the presence or absence of pyridine in the 35 to 65 °C temperature range, with an R^2 in the range of 0.95 to 1.00. Zhang et al. (2014) also suggested first-order inactivation kinetics of XOx from *Arthrobacter* M3 in the presence or absence of cosolute and osmolyte at 50 °C; however, analyses of the quality of the regression fits were not reported. The rate constant of inactivation of XOx was significantly ($p < 0.0001$) affected by pressure. An increase in pressure resulted in slower inactivation as indicated by a decrease in k_{inact} for all the studied temperatures (Table 3.1). The lowest value of k_{inact} was $(0.49 \pm 0.04)\times10^{-2}$ min^{-1} observed at 300 MPa and 55.0 °C. Temperature also had a significant effect on k_{inact} of XOx ($p < 0.0001$). However, in contrast to the effect of pressure, an increase in temperature increased k_{inact} at each pressure level as summarized in Table 3.1. Increase in temperature to 70.0 °C resulted in the highest k_{inact} of $(20.76 \pm 2.10)\times10^{-2}$ min^{-1} at atmospheric pressure.

The k_{inact} of XOx were significantly lower at all high pressures compared to atmospheric pressure at the same temperature ($p < 0.05$) as determined by pairwise comparison of the linear regression using GLM as described in materials and methods. Therefore, in the selected pressure range, HHP slowed down the k_{inact} of the enzyme, indicating greater thermal stability compared to atmospheric inactivation. Significant differences in the k_{inact} were more pronounced between 0.1 to 100 MPa ($p < 0.05$) as indicated with different letters within columns on Table 3.1. Therefore, at the pressure range of 0.1 to 100 MPa the greatest level of the reduction in the k_{inact} were observed. Increase in pressure from 100 to 300 MPa decreased the k_{inact} for all the studied

temperatures except at 66.1 °C and from 200 to 250 MPa. The level of reduction in the k_{inact} from 100 to 300 MPa decreased compared to 0.1 to 100 MPa because of approaching to the pressure induced-inactivation region. At 66.1 °C and 200 MPa, the two determined k_{inact} values were 2.19×10^{-2} and 1.89×10^{-2} min^{-1} where only the first replicate follows the decreasing trend of the k_{inact} by pressure from 200 to 250 MPa (2.08×10^{-2} min^{-1}). However, the differences in the two observation were not sufficient to exclude one of the replicates as an outlier. No significant differences were observed in the k_{inact} at 55.0 and 58.6 °C at the higher range of studied pressures of 200 to 300 MPa. The changes in the k_{inact} were more pronounced when subjected to increasing temperature. This was in agreement with another study using glutamate dehydrogenases from *Thermococcus litoralis* at 86 to 104 ºC where the effect of pressure on increasing thermal stability of the enzymes was greater at higher temperature (Sun et al., 2001). As the result, the lowest k_{inact} were at the range of 250 to 300 MPa at 62.3 to 70.0 °C. Fraeye et al. (2007) reported a shift in pressure with the highest stability from 200 to 300 MPa by increasing the temperature from 45 to 50 ºC for study on *Aspergillus aculeatus* pectinmethylesterase. Similarly, Halalipour et al. (2016) also reported an increase in the stabilizing effect of pressure at higher temperatures and an apparent shift in the pressure with the highest stability from 180 MPa at 58.8 ºC to 300 MPa at 80.0 ºC observed for glucose oxidase from *Aspergillus niger*.

The observed inhibition of thermal inactivation of XOx by the use of HHP can potentially enable enzymatic reaction at higher temperatures. Consequently, one can hypothesize that higher reaction rates would be feasible at higher temperatures than it is possible under atmospheric pressure due to XOx inactivation.

Thermal inactivation of XOx at atmospheric pressure has been previously studied. Machida and Nakanishi (1981) reported no change in XOx activity from *Enterobacter cloacae*

for 30 min of incubation below 50 °C to complete inactivation for 30 min of incubation at 70 °C. Additionally, the k_{inact} of XOx from rat liver at 55 °C was reported as 0.91×10^{-2} min^{-1} (Amini et al., 2011), which indicated a slower inactivation compared to our reported k_{inact} of XOx from bovine milk in of 1.21×10^{-2} min^{-1} at 55.0 °C. In our study and at 300 MPa, HHP resulted to decrease the k_{inact} of XOx 2.4, 2.8, 4.6, 5.5, or 9.5 times compared to atmospheric pressure at 55.0 °C, 58.6 °C, 62.3 °C, 66.1 °C, or 70.0 °C respectively.

An increase in thermostability of some other enzymes under HHP treatments has also been reported. The stability of inulin fructotransferase from *Arthrobacter aurescens* increased at HHP up to 200 MPa against inactivation at 70 and 80 °C (Li et al., 2015). The thermostability of carrot pectinmethylesterase was enhanced at HHP up to 300 MPa for treatments at 40 and 60 °C (Sila et al., 2007). High pressures in the range of 200-400 MPa stabilized a commercial pectinase cocktail against thermal inactivation processed in the range of 55.0-85.0 °C (Tomlin et al., 2013).

Increases in rigidity and decreases in the fluctuation of enzyme structures under pressure were hypothesized to enhance the thermostability of enzymes at high pressure (Sun et al., 1999). Further, Sun et al. (2001) proposed that a pressure of about 50 MPa shifted equilibrium between substates of glutamate dehydrogenases from *Thermococcus litoralis* toward producing a more compact conformational structure. The resulted structure at high pressure inhibited irreversible aggregation and hence enhanced thermostability. Wilton et al. (2009) reported that the cavities buried inside the ribonuclease enzyme barnase were the most compressible part of protein at pressures up to 200 MPa, performed by a pressure dependent NMR study. Therefore, reducing cavity size can reduce the water penetration into a protein structure, which is the main unfolding route of staphylococcal nuclease as detected by NMR spectroscopy (Roche et al., 2012). One can also hypothesize that reducing the amount of water molecules inside cavities can reduce

fluctuations in the structure of a protein at elevated temperatures. This can consequently enhance the ability of pressure to guard against thermal denaturation (Cioni and Strambini, 1996). However, despite the growing number of studies on the high pressure stabilization of proteins, the mechanisms of pressure-induced stabilization are yet to be resolved (Royer, 2015).

In our previous study, HHP increased 50-fold the stability of glucose oxidase from *Aspergillus niger* at 58.8-80.0 °C at 0.1-300 MPa (Halalipour et al., 2016). The highest stabilization level of XOx in this study was 9.5-fold in the range of 55.0-70.0 °C at 0.1-300 MPa. Glucose oxidase from *Aspergillus niger* has a smaller molecular mass of 160 kDa (O'Malley and Weaver, 1972) compared to bovine XOx with a molecular mass of 290 kDa (Pauff and Hille, 2009). Other studies (Krebbers et al., 2002; Wang et al., 2012) suggested the smaller molecular mass of peroxidase resulted in the higher stability at high pressures. One can also hypothesize that smaller molecular size reduces the possibility of water penetration as the main effect of protein unfolding (Roche et al., 2012) through the folded enzyme structure and hence protects the native enzyme structure. The grand average of hydropathicity (GRAVY) of both glucose oxidase from *Aspergillus niger* (-0.189) and bovine XOx (-0.196) are similar (Gasteiger et al., 2005), suggesting that GRAVY is not a good indicator of the ability of HHP to induce enzyme stabilization. However, the packing of hydrophobic groups is different in both enzymes; thus, hydrophobicity may still play an important role but one can speculate that the location of the hydrophobic groups along with the protein folding also have an impact in stability and the ability of HHP to stabilize enzymes. Finally, HHP studies were conducted at the range of isoelectric points of XOx and glucose oxidase. Therefore, net electrical charges of XOx and glucose oxidase were neutral and did not play a role in the differences of the observed ability of HHP induce-stabilization.

Effect of pressure on k_{inact}

The effect of pressure on the k_{inact} of XOx at each studied temperature was calculated as the activation volume of inactivation, or $\Delta V^{\neq}$, using the Eyring model. Figure 3.4 illustrates the linearized effect of pressure on the rate of inactivation of XOx. The relationship between the natural logarithm of the k_{inact} and pressure was linear up to 200 MPa with an R^2 in the range of 0.91 to 1.00. Calculation of $\Delta V^{\neq}$ using pressures greater than 200 MPa caused a deviation from linearity, suggesting that while pressure stabilized XOx below 200 MPa, it destabilized the enzyme at higher pressures (Grauwet et al., 2009; Smeller, 2002). Similarly, lipoxygenase was inactivated above 300 MPa (Rodrigo et al., 2005; Terefe et al., 2014) and stabilized below 300 MPa (Heinisch et al., 1995; Rodrigo et al., 2005). Table 3.1 reports the $\Delta V^{\neq}$ calculated at pressures between 0.1 to 200 MPa ± the standard error of the linear regression in this pressure range. A positive $\Delta V^{\neq}$ for all the studied temperatures indicated that HHP favored stabilization of XOx. An increase in temperature from 55.0 to 70.0 °C increased $\Delta V^{\neq}$ from 9.5 ± 0.2 to 28.9 ± 2.9 $cm^3\ mol^{-1}$ indicating that stabilization by HHP was least pronounced at the lowest temperature of 55.0 °C. Activation volumes with positive sign were also reported for a study of inactivation of a pectinase cocktail at 55.0-85.0 °C at 0.1-400 MPa (Tomlin et al., 2013). In a similar way, positive $\Delta V^{\neq}$ values were reported for glucose oxidase treated between 58.8 °C to 80.0 °C at 0.1 MPa to 300 MPa (Halalipour et al., 2016).

Pairwise comparison of slopes used to determine $\Delta V^{\neq}$ using GLM were done to identify significant differences between $\Delta V^{\neq}$ at different temperatures, as presented with superscript letters in Table 3.1. The $\Delta V^{\neq}$ significantly increased at temperatures between 58.6 to 70.0 °C ($p < 0.05$). However, the $\Delta V^{\neq}$ were not significantly different between 55.0 and 58.6 °C ($p > 0.05$)

indicating a smaller effect of pressure on the k_{inact} at the lower temperatures of this study as discussed earlier.

Effect of temperature on k_{inact}

The temperature effect on the k_{inact} was quantified by determination of the activation energy of inactivation (E_a), from the Arrhenius model at 0.1 MPa to 300 MPa. As illustrated by Figure 3.5, the relationship between the natural logarithm of the k_{inact} of XOx and reciprocal of the absolute temperature was linear for all the studied pressures with $R^2 > 0.97$. At HHP, the inactivating effect of temperature was less pronounced than at atmospheric pressure. In other words, increasing HHP decreased the dependence of the k_{inact} on temperature as summarized in the far right column of Table 3.1. The E_a decreased with pressure except from 150 to 250 MPa and 200 to 250 MPa. The smallest E_a was observed at 300 MPa. The E_a at 300 MPa was 97.0 ± 8.2 kJ mol^{-1} or, 1.9 times smaller than at atmospheric pressure (181.7 ± 12.1 kJ mol^{-1}).

Similar results have been observed for other enzymes. For example, the E_a of carrot pectinmethylesterase for treatment at 30-55 °C decreased from 48.9 to 31.6 kJ mol^{-1} upon increasing pressure from 0.1 to 200 MPa respectively. However, the E_a increased from 31.6 to 81.4 kJ mol^{-1} by increasing pressure from 200 to 500 MPa respectively due to the induced inactivation effect of HHP at higher pressure range (Sila et al., 2007). The E_a of a commercial pectinase formulation studied at 0.1-400 MPa and 55.0–85.0 °C was lowest at 400 MPa (107.3 kJ mol^{-1}) and highest at atmospheric pressure (195.9 kJ mol^{-1}) (Tomlin et al., 2013). Similarly, inactivation at 58.8-80.0 °C decreased the E_a of glucose oxidase at HHP (60-300 MPa) compared to atmospheric pressure (Halalipour et al., 2016). The glucose oxidase E_a decreased from 378.1 to 281.0 kJ mol^{-1} by increasing pressure from 0.1 to 300 MPa respectively. Furthermore, the E_a

of XOx from rat liver was 14.2 kJ mol^{-1} at 35 to 55 ºC at atmospheric pressure (Amini et al., 2011). This E_a was lower than our obtained E_a at atmospheric pressure of 181.7 ± 12.1 kJ mol^{-1}. The lower value may be because of the higher enzyme stability against thermal inactivation at lower temperature range and also due to the differences in the source of the studied enzymes, buffer and pH.

Pairwise comparison of slopes used to determine E_a using GLM were done to identify whether there were a significant differences between the E_a at different pressures, as presented with superscript letters in Table 3.1. The E_a at atmospheric pressure was significantly different at all studied high pressures ($p < 0.05$). Therefore, processing at HHP significantly decreased the dependence of the k_{inact} to temperature, compared to atmospheric inactivation. Significant differences in the E_a were more pronounced in the range of 0.1 to 150 MPa ($p < 0.05$). That said, no significant differences were found between 150 to 300 MPa ($p > 0.05$), due to the decreased effect of temperature on the k_{inact} at higher pressures.

Covalent modification of XOx

Previous studies with glucose oxidase found that covalently modifying the enzyme with aniline increased thermal stability, while benzoate modification decreased thermal stability (Halalipour et al., 2016). Chemical modification, even with hydrophobic groups, can increase the stability of proteins (Gupta, 1991; Mogharrab et al., 2007; Mozhaev et al., 1990). Therefore, we examined the effects of chemical modifications on XOx. Amide bond formation by EDC coupling of benzoate or aniline was used to covalently modify XOx.

The number of benzoate molecules that modify XOx can be determined using a TNBS assay, which quantifies the number of primary amines on a protein. Benzoate will mostly modify

primary amines, such as lysines and the N-terminal amine, although cysteines and tyrosines can also be modified (Carraway and Koshland, 1968; Carraway and Triplett, 1970). For unmodified XOx, 33 ± 3 amines were detected per monomer (out of 89 lysines and the N-terminus). When modified with benzoate, the number of amines per monomer decreased to 23 ± 2 amines. This indicated that, on average, 10 amines per monomer of XOx were modified with benzoate. Similar levels of modification were seen for glucose oxidase when covalently linked to benzoate (Halalipour et al., 2016). The TNBS assay cannot be used to quantify aniline modification of XOx, as the assay is only sensitive to primary amines. Aniline modifies carboxylate groups on the protein.

An estimate of the number of modifications of XOx was also obtained by MALDI-TOF mass spectrometry (MS). A peak around 146 kDa, equivalent to the XOx monomer, was used for quantification. For benzoate-modified XOx, 12 ± 5 modifications per monomer could be detected. This matches fairly well with the TNBS assay results of 10 modifications. For aniline, MALDI-TOF analysis estimated 8 ± 1 modifications per monomer of XOx. There are 56 aspartates and 88 glutamates per XOx monomer.

Effects of Modifying XOx

Xanthine oxidase thermal stability was measured by DSC. The enzyme thermal unfolding was irreversible for the both the modified and unmodified XOx. The data were fit to a two-state model with three transitions in Origin v7.0 (Supplemental Figure S3.1). Fits of the thermograms are given in Table 3.2. The enzyme has previously been characterized to have three transitions when undergoing thermal denaturation, and the T_ms obtained from our DSC match well with literature (62 °C, 68 °C, and 73 °C) (Burnier and Low, 1985). Thermal stability of XOx,

measured by DSC, remained unperturbed by the modification with either benzoate or aniline (Supplemental Figure S3.2). All three T_ms for the unmodified and modified proteins were within error. This indicates that, unlike glucose oxidase (Halalipour et al., 2016), XOx is not thermally stabilized by chemical modification by aniline. Nor is it destabilized by benzoate modification. Overall, chemical modification of XOx by either benzoate or aniline does not affect the thermal stability of the enzyme.

The effect of modification on the activity of XOx was measured by Michaelis-Menten kinetics (Supplemental Figure S3.3). A k_{cat} of 44 ± 1 min^{-1} and a K_m of 2.2 ± 0.2 μM were obtained for unmodified XOx (Table 3.3). The K_m is close to the reported values of 1.2-3.3 μM at pH 7.4 or 7.8 (Greenlee and Handler, 1964; Pauff and Hille, 2009). While the k_{cat} is an order of magnitude lower than what has been reported (600 to 1200 min^{-1}) (Hille and Massey, 1986; Massey et al., 1969; Pauff and Hille, 2009), it is similar to the values provided by Sigma-Aldrich for their preparations. Inactivation of a molybdo-sulfide (Kim and Hille, 1993; Massey and Edmondson, 1970), and general loss of activity of XOx after purification (Avis et al., 1956) may account for the difference between our k_{cat} and that of the literature. The effect of modification on XOx activity was also examined (Table 3.3). Modification of XOx with either aniline or benzoate did not affect the K_m. The k_{cat} for aniline-modified XOx was also relatively unaffected, decreasing by only 10%. Covalent modification by benzoate had a larger effect, the enzyme's catalytic efficiency decreased by around 30%. While the activity of XOx decreased with modification, its substrate affinity did not change, and the enzyme stability remained unaffected by modification.

Acknowledgment

This project was supported by USDA-NIFA-AFRI GRANT 11322452.

Table 3.1.

Pseudo-first-order rate constant of inactivation of XOx, activation energy of inactivation of XOx, and activation volume of inactivation of XOx ± the linear regression standard errors.

Pressure (MPa)	Temperature (°C)										E_a (kJ mol^{-1})	R^2
	55.0	R^2	58.6	R^2	62.3	R^2	66.1	R^2	70.0	R^2		
	k_{inact} (min^{-1}) × 10^{-2}											
0.1	1.21 [a] ± 0.07	0.99	1.80 [a] ± 0.15	0.98	3.99 [a] ± 0.24	0.99	8.79 [a] ± 1.03	0.96	20.76[a] ± 2.10	0.97	181.7 [g] ± 12.1	0.99
50	0.97 [b] ± 0.10	0.97	1.36 [b] ± 0.07	0.99	2.87 [b] ± 0.17	0.99	4.84 [b] ± 0.30	0.99	10.77[b] ± 0.51	0.99	151.8 [h] ± 10.6	0.99
100	0.83 [c] ± 0.09	0.97	1.01 [c] ± 0.10	0.97	1.97 [c] ± 0.21	0.97	3.67 [c] ± 0.30	0.98	6.13[c] ± 0.73	0.96	132.3 [i] ± 11.0	0.98
150	0.70 [cd] ± 0.08	0.97	0.96 [cd] ± 0.08	0.98	1.66 [c] ± 0.16	0.97	2.50 [d] ± 0.26	0.97	3.58[d] ± 0.35	0.97	105.2 [j] ± 5.0	0.99
200	0.60 [de] ± 0.08	0.95	0.79 [de] ± 0.08	0.97	1.33 [d] ± 0.09	0.99	2.04 [d] ± 0.16	0.98	2.86[e] ± 0.22	0.98	102.0 [j] ± 5.1	0.99
250†	0.50 [e] ± 0.05	0.98	0.68 [e] ± 0.08	0.95	1.16 [de] ± 0.05	0.99	2.08 [d] ± 0.13	0.99	2.43[ef] ± 0.07	1.00	107.4 [j] ± 10.2	0.97
300†	0.49 [e] ± 0.04	0.98	0.65 [e] ± 0.04	0.99	0.87 [e] ± 0.06	0.99	1.61 [e] ± 0.10	0.99	2.19[f] ± 0.15	0.99	97.0 [j] ± 8.2	0.98
$\Delta V^{\neq}$ (cm^3 mol^{-1})	9.5 [k] ± 0.2		11.1 [k] ± 1.0		15.3 [l] ± 1.2		20.2 [m] ± 2.6		28.9 [n] ± 2.9			
R^2	1.00		0.96		0.97		0.91		0.95			

[a, b, c, d, e, f] Different superscript letter within each column indicated k_{inact} were significantly different ($p < 0.05$).

[g, h, i, j] Different superscript within the column letter indicated E_a were significantly different ($p < 0.05$).

[k, l, m, n] Different superscript within the row letter indicated $\Delta V^{\neq}$ were significantly different ($p < 0.05$).

† Rate constatns at this pressure was not used for the calculation of the activation volume because they deviated from linearity in Eyring's plot indicating the transition between pressure-induced stabilization and pressure induced inactivation.

Table 3.2.

Apparent thermal stability of modified XOx in 50 mM Na_2HPO_4, pH 8.0 measured by DSC. Data were fit to three transitions in a two-state model. Unfolding of XOx was irreversible, therefore the fits to the data yield apparent values.

Modification	$T_{m\,1}$ (°C)	$\Delta H_{d,\,app\,1}$ (kJ mol^{-1})[a]	$T_{m\,2}$ (°C)	$\Delta H_{d,\,app\,2}$ (kJ mol^{-1})[a]	$T_{m\,3}$ (°C)	$\Delta H_{d,\,app\,3}$ (kJ mol^{-1})[a]
None	59.1 ± 0.2	15 ± 1	65.3 ± 0.1	78 ± 12	75.0 ± 0.2	23 ± 6
Aniline	59.0 ± 0.1	15 ± 5	65.3 ± 0.4	83 ± 11	74.6 ± 0.4	36 ± 12
Benzoate	59.6 ± 0.1	12 ± 1	64.8 ± 0.4	41 ± 7	74.5 ± 0.2	10 ± 1

[a] Apparent enthalpy of thermal denaturation.

Table 3.3.

Michaelis-Menten kinetic values for modified XOx measured in 50 mM K_2HPO_4, pH 7.5 at 25 °C. Assays were performed by measuring the formation of urate by the change in absorbance at 295 nm.

Modification	k_{cat} (min^{-1})	K_m (μM)
None	44 ± 1	2.2 ± 0.2
Aniline	40 ± 1	1.8 ± 0.2
Benzoate	30 ± 1	2.2 ± 0.2

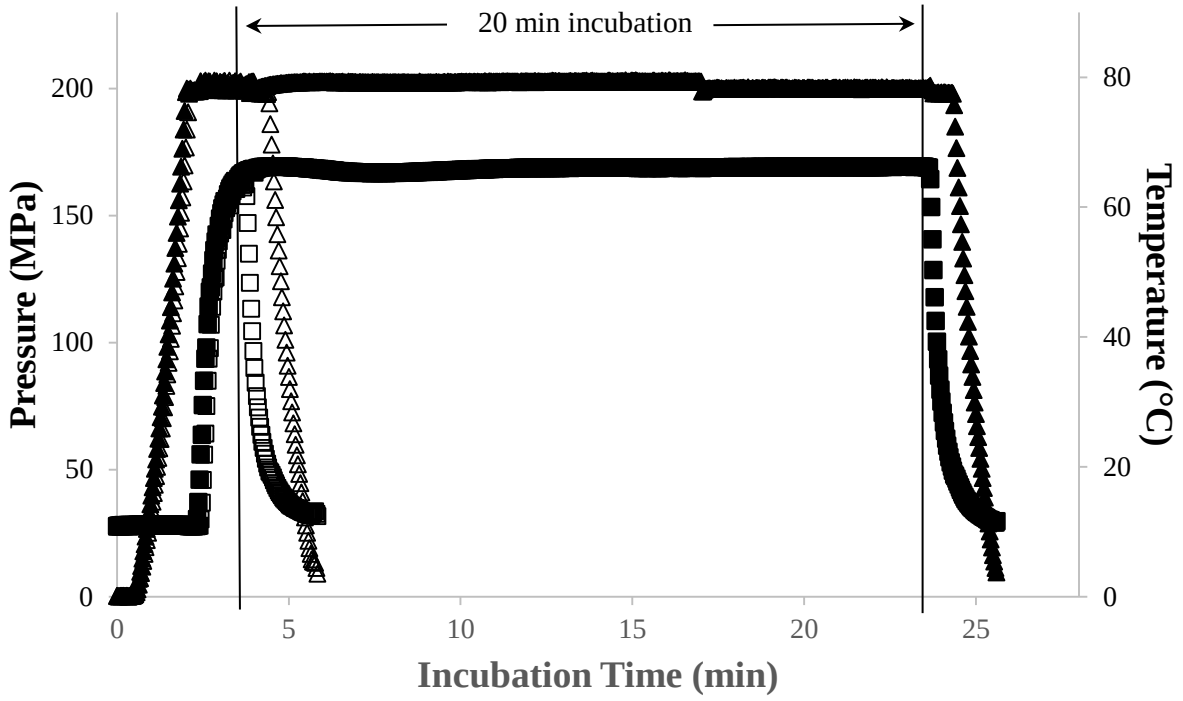

Figure 3.1. High pressure reactor temperature (■) and pressure (▲) profiles for a 20 min incubation time at 66.1 °C and 200 MPa; and temperature (□) and pressure (△) profiles for a 0 min incubation time at 66.1 °C and 200 MPa.

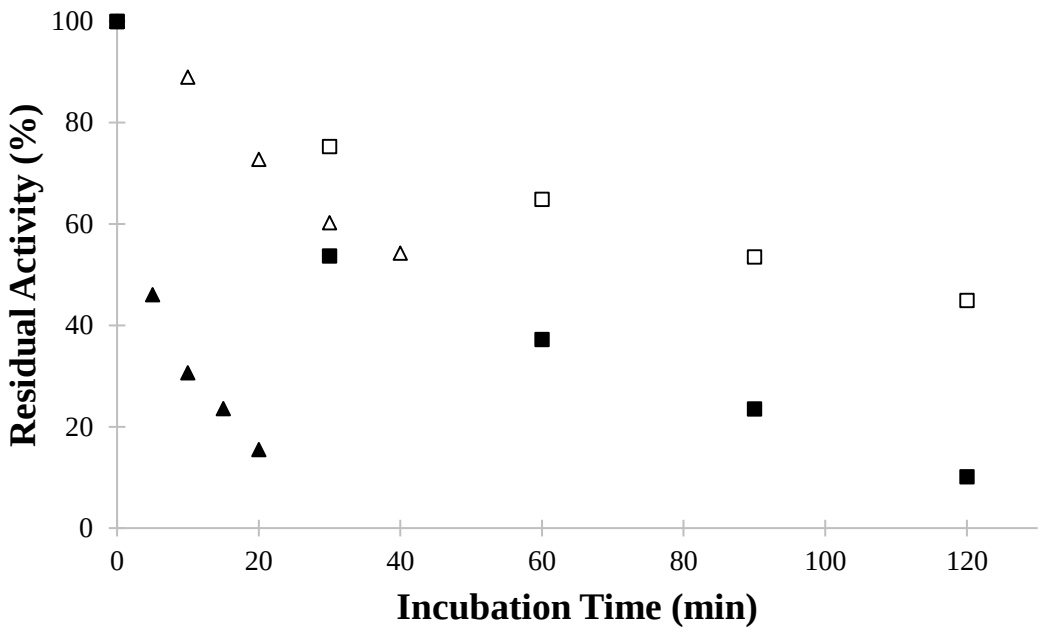

Figure 3.2. Average (*n*=2) residual activity of XOx for treatments at (■) 0.1 MPa and 58.6 °C, (□) 300 MPa and 58.6 °C, (▲) 0.1 MPa and 66.1 °C, (△) 300 MPa and 66.1 °C.

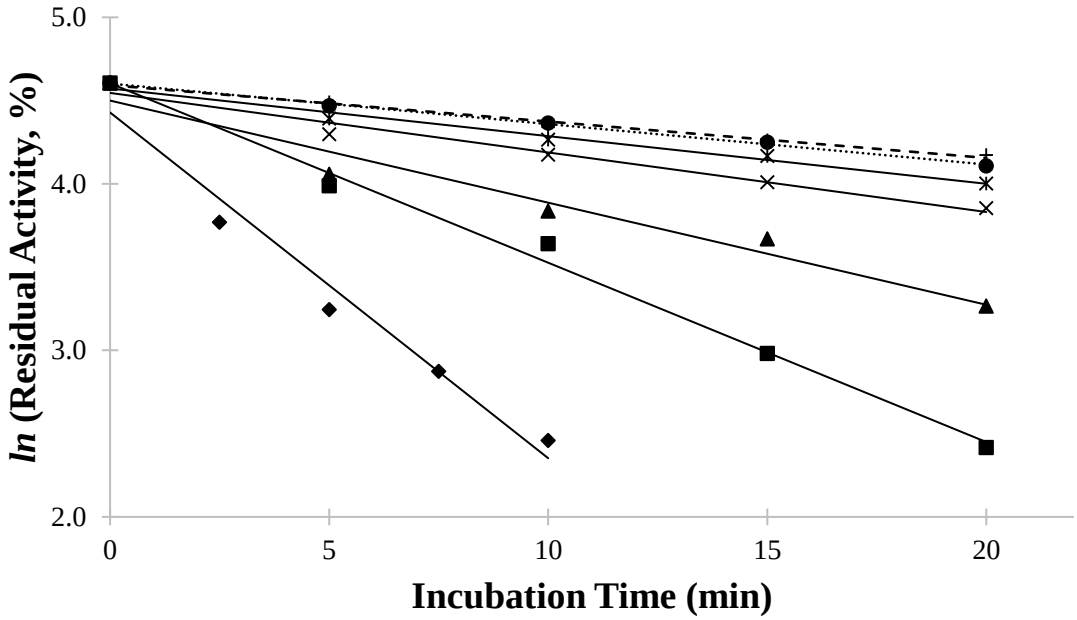

Figure 3.3. Xanthine oxidase thermal inactivation with pseudo-first-order linear regression trend lines used to calculate k_{inact} for samples treated at (◆) 0.1 MPa, (■) 50 MPa, (▲) 100 MPa, (×) 150 MPa, (∗) 200 MPa, (●, dotted) 250 MPa, and (+, dashed) 300 MPa at 70.0 ºC.

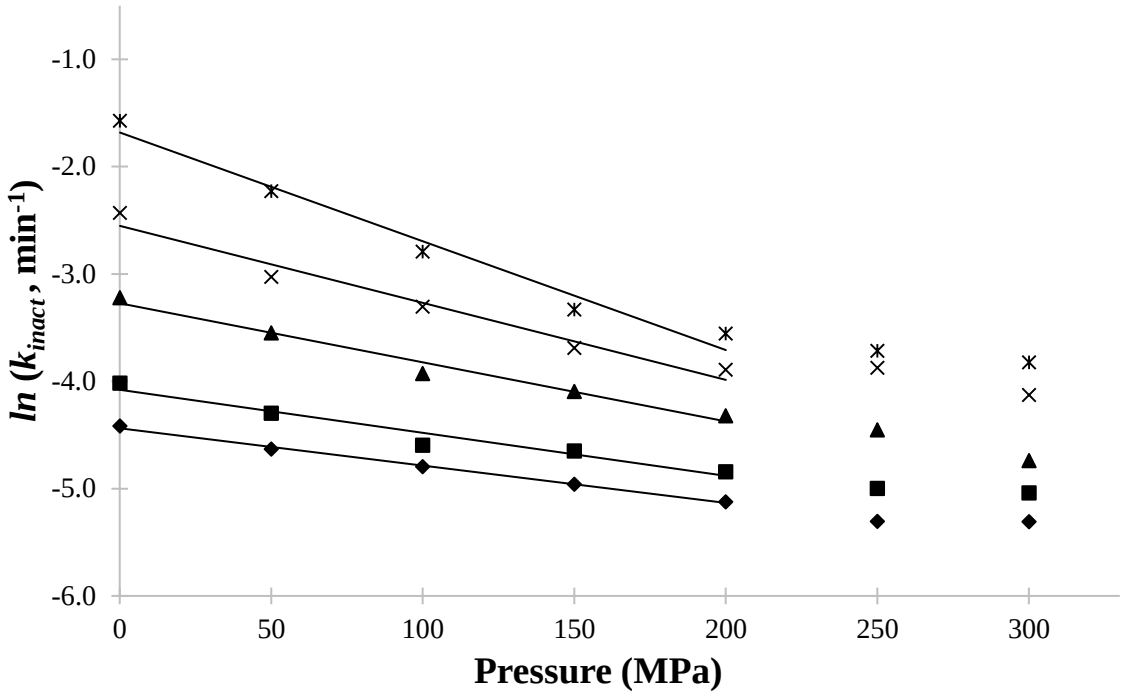

Figure 3.4. Eyring plot for the rate constant of inactivation of XOx at (◆) 55.0 °C, (■) 58.6 °C, (▲) 62.3 °C, (×) 66.1 °C, and (∗) 70.0 °C.

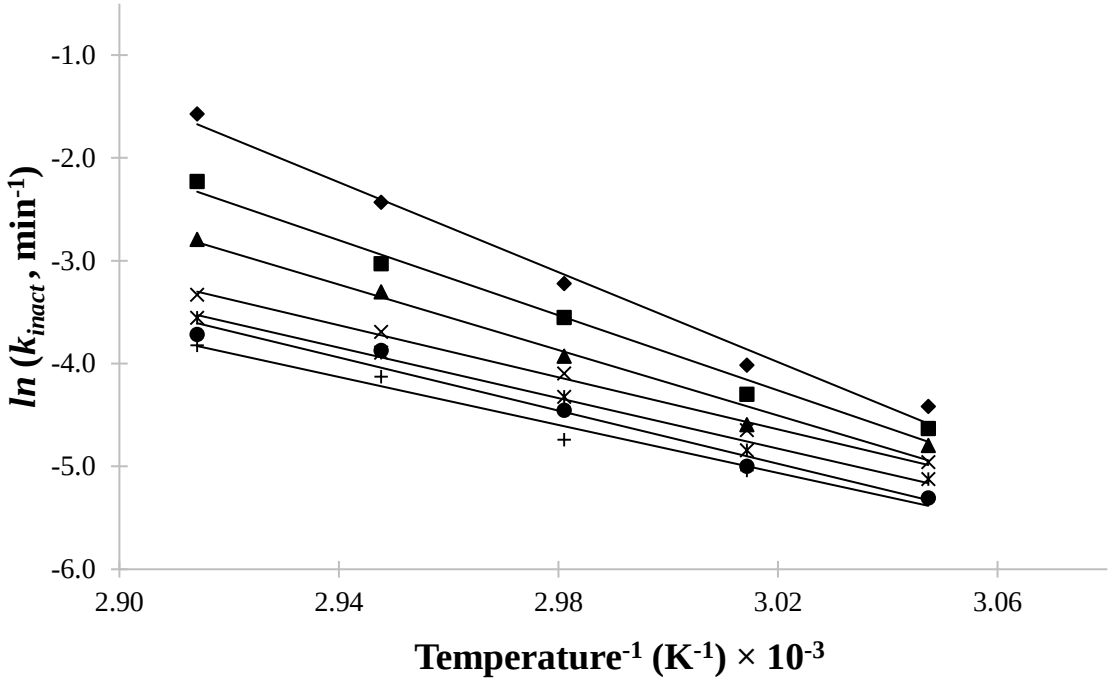

Figure 3.5. Arrhenius plot to obtain the E_a at (◆) 0.1 MPa, (■) 50 MPa, (▲) 100 MPa, (×) 150 MPa, (∗) 200 MPa, (●) 250 MPa, and (+) 300 MPa.

Appendix

3-I) Zero time activities

Table A3.1. The activity for the XOx samples at each pressure-temperature treatment with 0 min incubation time.

Pressure (MPa)	Temperature (°C)	$Activity_1$ (units mg^{-1})	$Activity_2$ (units mg^{-1})	Mean Activity (units mg^{-1})
0.1	55.5	0.0522	0.0561	0.0542
	58.6	0.0512	0.0524	0.0518
	62.3	0.0479	0.0491	0.0485
	66.1	0.0445	0.0471	0.0458
	70.0	0.0416	0.0380	0.0398
50	55.5	0.0557	0.0569	0.0563
	58.6	0.0538	0.0549	0.0544
	62.3	0.0522	0.0538	0.0530
	66.1	0.0522	0.0505	0.0514
	70.0	0.0497	0.0472	0.0485
100	55.5	0.0598	0.0581	0.0590
	58.6	0.0590	0.0563	0.0576
	62.3	0.0559	0.0574	0.0567
	66.1	0.0549	0.0561	0.0555
	70.0	0.0538	0.0523	0.0530
150	55.5	0.0591	0.0582	0.0587
	58.6	0.0549	0.0560	0.0554
	62.3	0.0567	0.0556	0.0562
	66.1	0.0569	0.0544	0.0557
	70.0	0.0519	0.0533	0.0526
200	55.5	0.0590	0.0574	0.0582
	58.6	0.0547	0.0560	0.0554
	62.3	0.0550	0.0535	0.0543
	66.1	0.0541	0.0512	0.0526
	70.0	0.0524	0.0501	0.0512
250	55.5	0.0576	0.0594	0.0585
	58.6	0.0561	0.0587	0.0574
	62.3	0.0551	0.0545	0.0548
	66.1	0.0549	0.0536	0.0542
	70.0	0.0501	0.0514	0.0507
300	55.5	0.0575	0.0561	0.0568
	58.6	0.0560	0.0536	0.0548
	62.3	0.0521	0.0540	0.0531
	66.1	0.0522	0.0502	0.0512
	70.0	0.0515	0.0503	0.0509

3-II) Supplemental section

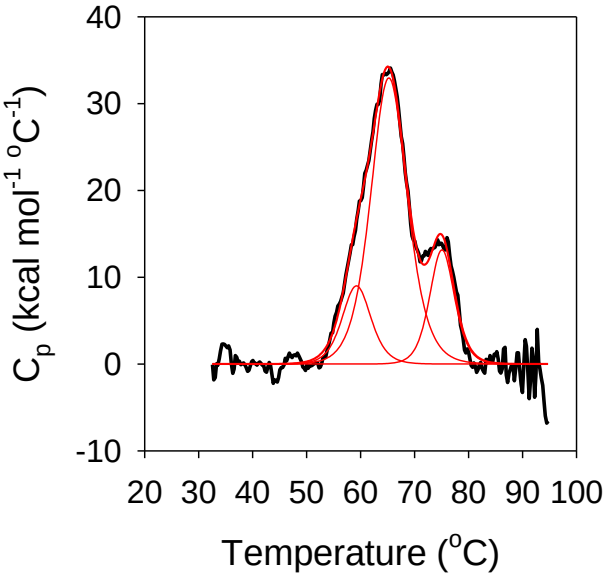

Supplemental Figure S3.1. Fit of a DSC thermogram for unmodified 2.2 μM of XOx monomer (thick black line) in 50 mM Na_2HPO_4, pH 8.0 buffer. Scans were performed from 25-95 °C at a scan rate of 1.5 °C min^{-1}. The fit of the data is shown as thin red lines. The data could be fit to three different transitions.

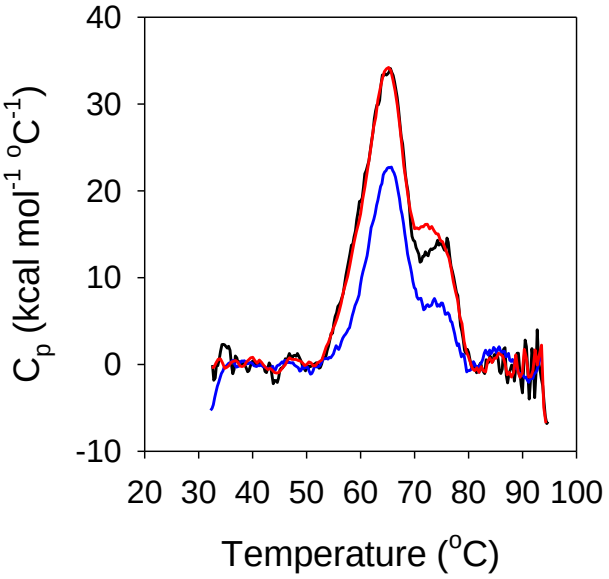

Supplemental Figure S3.2. DSC thermograms for the thermal denaturaiton of unmodified (black line), aniline modified (red line) and benzoate modified (blue line) XOx. Protein concentrations were 2-2.4 μM monomer.

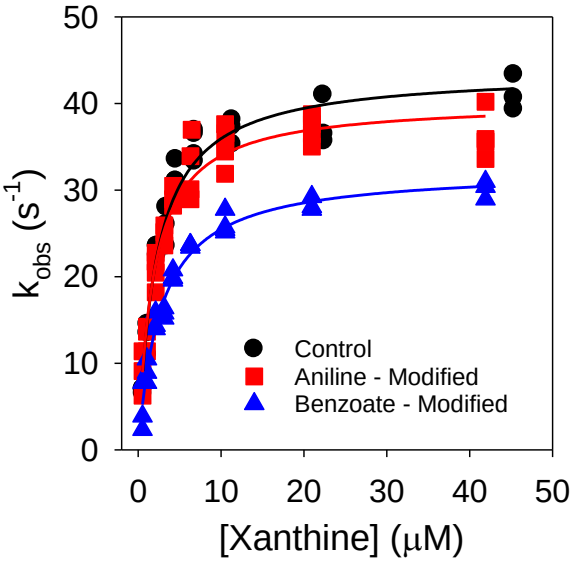

Supplemental Figure S3.3. Michaelis-Menten kinetics of unmodified (●), aniline modified (■) and benzoate modified (▲) XOx measured in 50 mM K_2HPO_4, pH 7.5 buffer at 25 °C.

CHAPTER 4

STABILIZATION AND CATALYTIC ACTIVITY OF NATIVE OR PHENYL-MODIFIED GLUCOSE OXIDASE AT HIGH HYDROSTATIC PRESSURE [1]

[1] A. Halalipour, M.R. Duff, E.E. Howell, J.I. Reyes-De-Corcuera. To be submitted to *Biotechnology and Bioengineering*.

Abstract

High hydrostatic pressure (HHP) stabilized the aniline-, and benzoate-modified glucose oxidase (GOx) at all the studied temperatures compared to atmospheric pressure. At HHP, the thermal stability of the aniline- or benzoate-modified GOx was higher than that of the native GOx. At 240 MPa and 80.0 °C, aniline-modified GOx was 3.7 times more stable than the native GOx; and benzoate-modified GOx was 2.8 times more stable than the native GOx. At 80.0 °C, aniline-modified GOx was 69 times more stable than the enzyme at 0.1 MPa. Similarly, at 80.0 °C, benzoate-modified GOx was 63 times more stable at 240 MPa than the enzyme at 0.1 MPa. In addition, the catalytic activity of the native, aniline-, or benzoate-modified GOx increased at HHP compared to atmospheric pressure and was highest at around 180 MPa for all the enzymes at all the studied temperatures. At 180 MPa and 69.1 °C, aniline-modified GOx produced the fastest catalytic rate followed by benzoate-modified GOx and native GOx. At 180 MPa and 69.1 °C, aniline-modified GOx catalyzed the oxidation of glucose 11 times faster than at atmospheric pressure and room temperature. For the activity enhancement studies, increase in temperature increased the activation volume of reaction and the highest values were -38.5 ± 10.2, -37.3 ± 9.3, or -33.5 ± 7.8 cm^3 mol^{-1} for the aniline-, benzoate-, or native GOx treated at 69.1 °C respectively. The highest value of activation energy was 34.7 ± 2.7, 42.3 ± 3.7, or 39.4 ± 2.4 kJ mol^{-1} at 180 MPa for the native, aniline-, or benzoate-modified GOx respectively.

Introduction

Glucose oxidase (GOx) is a homodimeric glycoprotein with a molecular mass of ~160 kDa that consisting of two tightly bound flavin adenine dinucleotide (FAD) per dimer (O'Malley and Weaver, 1972). The enzyme catalyzes the oxidation of β-D-glucose to δ-gluconolactone with simultaneous production of the hydrogen peroxide in the presence of molecular oxygen (Leskovac et al., 2005). The produced δ-gluconolactone is spontaneously hydrolyzed into gluconic acid in aqueous solution (Wohlfahrt et al., 1999). Glucose oxidase has been studied for over 50 years with applications in research, biomedical diagnostic and industrial processing (Caves et al., 2011). For instance, GOx has been applied for glucose removal in the processing of liquid egg and reduced-alcohol wine (Gómez et al., 1995; Pickering et al., 1998; Sisak et al., 2006). The catalytic activity of GOx is also important for the production of gluconic acid which has important food applications, such as cheese curd formation and prevention of milkstone in dairy industry, and formulation of donuts. Moreover, gluconic acid has been used for pharmaceutical applications such as prevention of iron and calcium deficiency (Ramachandran et al., 2006). Gluconic acid is mainly produced by microbial fermentation (Singh et al., 2005). However, the slow production of gluconic acid and presence of unwanted by-products during microbial fermentation (Wong et al., 2008) led to proposing a bioreactor using GOx (Godjevargova et al., 2004; Nakao et al., 1997).

Previously, we reported the stabilization of native GOx against thermal inactivation by high hydrostatic pressure (HHP) as well as hydrophobic modification of the native enzyme (Halalipour et al., 2016); and hence proposed the possibility of further stabilization of the modified GOx at HHP as well as conducting the enzymatic reaction of the native and modified enzyme at elevated temperatures. Catalytic activity enhancement of some enzymes at HHP has

been documented (Eisenmenger and Reyes-De-Corcuera, 2009b). Recent reports include the activation effect of pressure on polyphenol oxidase from strawberry puree and apple juice (Buckow et al., 2009; Terefe et al., 2010), *Candida antarctica* lipase B (Eisenmenger and Reyes-De-Corcuera, 2010), pectinase formulation from *Aspergillus niger* (Tomlin et al., 2014), protease from *Bacillus* species (Senyay-Oncel et al., 2014), and α-chymotrypsin from bovine pancreas (Levin et al., 2016). Here we report the effect of HHP on the stability of the aniline- or benzoate-modified GOx as well as the catalytic activity of the native, aniline-, or benzoate-modified GOx.

Materials and methods

Materials and equipment

Glucose oxidase from *Aspergillus niger* (EC 1.1.3.4, Product No. G7141), horseradish peroxidase (POx, EC 1.11.1.7, Product No. P8250), glucose, and o-Dianisidine dihydrochloride were obtained from Sigma-Aldrich Chemical Company (St. Louis, MO, USA).

The same high pressure pump and temperature control system as previously reported (Halalipour et al., 2016) were used. However, for the catalytic activity study instead of the U111 high pressure reactor, a high pressure optical cell (model U103) from Unipress Equipment (Warsaw, Poland) was used to monitor the reaction progress *in situ*. The optical cell is a cylindrical HHP reactor into which a quartz cuvette can be snuggly fitted. It has aligned sapphire windows that allow a fiber optic spectrometer model USB2000+ and an UV−vis−NIR light source (model DH-2000-BAL) from Ocean Optics (Dunedin, FL, USA) to be connected via optic fibers to monitor the enzyme reaction continuously. Cylindrical reaction cuvettes (2.1 cm length × 0.74 cm ID × 0.96 cm OD) use two Teflon rod caps with O-rings to enclose the reaction

mixture and prevent mixing of the reaction solution with the silicon oil pressurization fluid. A thermocouple inserted through the side of the reactor measured the temperature inside the high pressure optical cell adjacent to the quartz cuvette. Absorbance data collection was performed at 500 nm using OceanView 1.5.0 software also from Ocean Optics. The data acquisition system and LabVIEW program (National Instruments, Austin, TX, USA) were described previously (Halalipour et al., 2016) and were used to control and monitor the pressure, temperature, and process time during the treatments.

Methods

Sample preparation and reaction conditions

The same procedure that was used to stabilize the native GOx was followed for the stabilization of the aniline-, or benzoate-modified GOx under HHP (Halalipour et al., 2016). However, the highest pressure set point increased to 360 MPa to better monitor the possible pressure-induced inactivation. Therefore, the incubation pressure was set to 0.1, 60, 120, 240, or 360 MPa. The incubation temperature was set to 69.1 °C, 74.5 °C, or 80.0 °C which stabilization were more pronounced in our previous report.

For the catalytic activity study native, aniline-, or benzoate-modified GOx were diluted in 50 mM sodium acetate buffer pH 5.1 to ~0.12 units mL^{-1}. Aliquots of 10 µL of enzyme were then added to 310 µL of chilled reaction cocktail in a quartz cuvette. In the 320 µL reaction mix, the final concentrations were 5 pM GOx, 0.16 mM o−Dianisidine, 90 mM β-D-glucose, 233 µM oxygen, and 26 µM of POx. The cuvette was sealed with the cap avoding the inclusion of air bubbles. The reaction vial was immersed in the high pressure fluid kept at 5 °C, and the pressure cell closed. The initial temperature was kept at 5 ± 0.1 °C to minimize the reaction progress

before starting the desired treatments. Moreover, to ensure consistency of all the experiments, pressurizing always started 90 s after the addition of GOx to the reaction vial. Using the program written in LabVIEW, the pressure was set to 0.1 MPa as control, 60, 120, 180, or 240 MPa. The temperature was set to 25.0, 53.9, 58.8, 63.8, or 69.1 °C. The reaction progress was monitored for 10 min as the pressure set point and then 95% of the temperature set point was reached. Pressurizing was performed before increasing temperature to minimize the possible thermal inactivation of the enzymes during the heating period (Eisenmenger and Reyes-De-Corcuera, 2009a).

A randomized block design was used for the design of the experiments. Temperature was selected as block while pressure and processing time were randomly chosen for the duplicated treatments. General linear model (GLM) was used to determine the differences between inactivation rates, catalytic rates, activation volumes, activation energies, or extinction coefficients due to pressure-temperature treatments utilizing SAS statistical software as explained in previous chapter (Cary, NC, USA).

Effect of HHP on enzyme activity

Glucose oxidase catalyzed reaction follows a Ping-Pong Bi-Bi mechanism and described by the Equation (1) and the scheme below (Leskovac et al., 2005; Romero et al., 2012):

$$v = \frac{v_{max}[\text{Glucose}][O_2]}{[\text{Glucose}][O_2]+K_{m,\,\text{Glucose}}[O_2]+K_{m,\,O_2}[\text{Glucose}]} \quad (1)$$

$$\text{GOx} + \text{Glucose} \leftrightarrow^{k_1}_{k_{-1}} \text{GOx-Glucose} \xrightarrow{k_2} \text{GOx}_{\text{reduced}} + \text{Glucono-1,5-Lactone}$$

$$\text{GOx}_{\text{reduced}} + O_2 \leftrightarrow^{k_3}_{k_{-3}} \text{GOx}_{\text{reduced}}\text{-}O_2 \xrightarrow{k_4} \text{GOx} + H_2O_2$$

where v is the velocity of the reaction, v_{max} is the maximal velocity of the reaction, [Glucose] and [O_2] are glucose and oxygen concentrations, $K_{m,\ Glucose}$ and $K_{m,\ O_2}$ are the Michaelis-Menten constants for the glucose and O_2 respectively, k_1 and k_3 are the enzyme and substrate association rate constants, k_{-1} and k_{-3} are the enzyme and substrate dissociation rate constants, and k_2 and k_4 are the rate constants of the formation of the products. The v_{max} in Ping-Pong Bi-Bi mechanism defined as:

$$v_{max} = [GOx]\ k_2\ k_4 / (k_2 + k_4) = [GOx]\ k_{cat} \quad (2)$$

where [GOx] is the enzyme concentration and k_{cat} is the catalytic rate of reaction (Romero et al., 2012). In the excess of glucose and oxygen to enzyme, Equation (1) was simplified to:

$$v = v_{max} = [GOx]\ k_{cat} \quad (3)$$

The $K_{m,\ Glucose}$ was 17.5, 32.4, or 23.2 mM for the native, aniline-, or benzoate-modified GOx respectively (Halalipour et al., 2016). The $K_{m,\ O_2}$ was 20 µM for native GOx (Nakamura et al., 1976). To ensure that glucose and oxygen are in excess, the linearity of the reaction progress was monitored at all the studied pressure-temperature treatments. The R^2 value was used as the indicator of the linearity and it was in the range of 0.93 to 1.00 at all the studied pressure-temperature treatments. Moreover, the greatest change in the [Glucose] and [O_2] was 16.4 µM at all the studied pressure-temperature treatments which is <1% of the initial [Glucose] and 8% of the initial [O_2].

The produced H_2O_2 oxidizes o-Dianisidine in the reaction vial in the presence of POx (Bergmeyer et al., 1974a). The oxidized o-Dianisidine was detectable in the high pressure optical cell by absorbance at 500 nm. The absorbance at this wavelength was then correlated to the concentration of the produced oxidized o-Dianisidine in the high pressure optical cell. The velocity of the reaction was then calculated as the concentration of the oxidized o-Dianisidine

over time over the linear range of the curve of absorbance at 500 nm versus time with $R^2 > 0.93$. Experimental error in the calculation of the velocity was calculated as the standard error of the linear regression of the concentration of the oxidized o-Dianisidine *vs.* time.

Increases in pressure and decreases in temperature decrease the volume of solution (V). Decreases in V results in increasing solute concentration and thus, absorbance at 500 nm. Therefore, the concentrations obtained from the absorbance of the solutions were corrected by multiplying to the ratio of the known $V_{p,\,T} / V_{0.1\ \text{MPa},\ 25\ ^\circ\text{C}}$ of water listed in Table 4.1 (USNIST, 2008) in the range of 0.92 to 1.02. These corrections allowed us to determine the concentration of the oxidized o-Dianisidine only due to pressure-temperature treatments.

In addition, the extinction coefficient of the oxidized o-Dianisidine ($\varepsilon_{\text{o-Dianisidine}}$) was obtained for each selected pressure-temperature treatments. It is important to correct the extinction coefficient values because changes in the extinction coefficients by pressure-temperature variations can result in errors in the determination of the concentration. For example, the importance of changes in the haemoglobin extinction coefficients by temperature variation was studied for the accurate spectrophotometric determination of haemoglobin concentration (Kim and Liu, 2007). The $\varepsilon_{\text{o-Dianisidine}}$ calculated from the linear regression of the absorbance at 500 nm *vs.* five different concentrations of o-Dianisidine over the path-length of the quartz cuvette multiplied by the ratio of the known $V_{p,\,T} / V_{0.1\ \text{MPa},\ 25\ ^\circ\text{C}}$ of water. Samples were duplicated and the error in calculation of $\varepsilon_{\text{o-Dianisidine}}$ was estimated using the standard error of the linear regression.

Dependence of enzyme activity on temperature

The apparent activation energy (E_a) of the native, aniline-, or benzoate-modified GOx reaction was calculated from the Arrhenius equation to quantify the temperature effect on the enzyme activity:

$$\left(\frac{\partial ln\, k}{\partial(\frac{1}{T})}\right)_P = -\frac{E_a}{R} \quad (4)$$

where R is the ideal gas constant, T the absolute temperature, P is the pressure, and k is the reaction rate constant. The error in the calculation of the E_a was reported as the standard error of the linear regression of ln(k) *vs.* 1/T multiplied by R.

Dependence of enzyme activity on pressure

The apparent activation volume ($\Delta V^{\neq}$) of the native, aniline-, or benzoate-modified GOx reaction was quantified from the Eyring model to determine the pressure dependence of the enzyme activity:

$$\left(\frac{\partial ln\, k}{\partial P}\right)_T = -\frac{\Delta V^{\neq}}{RT} \quad (5)$$

The error in the calculation of the $\Delta V^{\neq}$ was reported as the standard error of the linear regression of the slope of ln(k) *vs.* P multiplied by RT.

Results and discussion

Effect of HHP on modified enzyme stability

The inactivation kinetics of the aniline- or benzoate-modified GOx followed an apparent first-order model with the quality of the regression fit of R^2 in the range of 0.92 to 1.00 as

summarized in Table 4.1. Decreases in R^2 were more pronounced at higher studied pressures which is consistent with the native GOx inactivation study at HHP and with the fact that greatest correlation coefficients are obtained for grater slopes under similar data dispersion (Halalipour et al., 2016). The rate constant of inactivation (k_{inact}) for both aniline- or benzoate-modified GOx was significantly ($p < 0.0001$) affected by pressure. An increase in pressure resulted in slower inactivation as indicated by a decrease in the k_{inact} up to 240 MPa for all the studied temperatures (Table 4.1). This indicates that HHP stabilized aniline- and benzoate-modified GOx against thermal inactivation. Temperature also presented significant effect on the k_{inact} of modified GOx ($p < 0.0001$). However, in contrast to pressure, temperature increased the k_{inact} of the aniline- and benzoate-modified GOx at all the studied pressures. At 0.1 MPa, the inactivation was fastest for both of the aniline- or benzoate-modified GOx at all the studied temperatures. At 0.1 MPa, the reported k_{inact} was $(28.60 \pm 2.02)\times10^{-2}$ or $(36.80 \pm 1.79)\times10^{-2}$ min^{-1}, $(426.99 \pm 30.54)\times10^{-2}$ or $(557.57 \pm 29.04)\times10^{-2}$ min^{-1}, or $(1343.70 \pm 76.01)\times10^{-2}$ or $(1625.68 \pm 98.36)\times10^{-2}$ min^{-1} for the aniline- or benzoate-modified GOx at 69.1, 74.5, or 80.0 °C respectively. The atmospheric k_{inact} of the native GOx was $(42.67 \pm 2.28)\times10^{-2}$, $(516.77 \pm 31.81)\times10^{-2}$, or $(1530.03 \pm 36.71)\times10^{-2}$ min^{-1} at 69.1, 74.5, or 80.0 °C respectively (Halalipour et al., 2016). This indicated that the aniline-modified GOx inactivated slowest compared to the native or the benzoate-modified GOx at atmospheric pressure at each corresponding temperature which is consistent with the DSC results of our previous study. The benzoate-modified GOx inactivated at a slower rate than the native GOx at 69.1 °C; however, it inactivated faster than the native GOx at 74.5 or 80.0 °C. Previous DSC study indicated benzoate modification slightly but insignificantly decreased the stability of the enzyme which was consistent with the current rate of inactivation at 74.5 and 80.0 °C.

At 240 MPa, k_{inact} was slowest for both aniline- and benzoate-modified GOx compared to all the studied pressures. The slowest k_{inact} for the aniline-modified GOx were $(1.48 \pm 0.07)\times10^{-2}$, $(7.36 \pm 0.59)\times10^{-2}$, or $(19.58 \pm 2.70)\times10^{-2}$ min^{-1} at 69.1, 74.5, or 80.0 °C respectively. The k_{inact} for the benzoate-modified GOx were $(2.04 \pm 0.14)\times10^{-2}$, $(10.22 \pm 1.26)\times10^{-2}$, or $(25.79 \pm 3.95)\times10^{-2}$ min^{-1} at 69.1, 74.5, or 80.0 °C respectively. The k_{inact} at 240 MPa of the native GOx was $(2.33 \pm 0.18)\times10^{-2}$, $(10.29 \pm 0.66)\times10^{-2}$, or $(73.13 \pm 8.47)\times10^{-2}$ at 69.1, 74.5, or 80.0 °C respectively (Halalipour et al., 2016). This indicated that the aniline-modified GOx followed by the benzoate-modified GOx inactivated slower compared to the native GOx at 240 MPa at each corresponding temperature. Therefore, HHP stabilized the aniline-modified GOx by 19, 58, or 69 times compared to the aniline-modified GOx at 0.1 MPa at 69.1, 74.5, or 80.0 °C respectively. Compared to the native GOx inactivation at atmospheric pressure, HHP stabilized aniline-modified GOx by 29, 70, or 78 at 69.1, 74.5, or 80.0 °C respectively. Moreover, HHP stabilized benzoate-modified GOx by 18, 55, or 63 times compared to the benzoate-modified GOx at 0.1 MPa at 69.1, 74.5, or 80.0 °C respectively. Compared to the native GOx inactivation at atmospheric pressure, HHP stabilized benzoate-modified GOx by 21, 51, or 59 at 0.1 MPa at 69.1, 74.5, or 80.0 °C respectively.

Activation energy of the inactivation was evaluated to determine the effect of temperature on k_{inact} at each studied pressure. The E_a of inactivation (Table 4.1), decreased with pressure up to 240 MPa and increased from 240 MPa to 360 MPa. At 240 MPa, the E_a was 238.4 ±19.0 or 233.8 ±19.9 kJ mol^{-1} for the aniline- or benzoate-modified GOx respectively. Decrease in the E_a (slope of Arrhenius plot) at HHP indicated the smaller changes in the k_{inact} at HHP by increasing temperature. The smaller changes in the k_{inact} at HHP by temperature indicated that the

inactivating effect of temperature was decreased at HHP. The obtained E_a of the aniline- and benzoate-modified GOx were not significantly different among the studied pressures ($p < 0.10$).

The activation volume of inactivation was quantified to determine the temperature effect on k_{inact} at each studied temperature. The $\Delta V^{\neq}$ of inactivation (Table 4.1), increased with temperature which indicated the greater decrease in k_{inact} at higher temperature. In other words, the stabilizing effect of HHP increased with temperature. At 80.0 °C, $\Delta V^{\neq}$ was 86.0 ± 6.6 or 83.6 ±8.9 cm^3 mol^{-1} for the aniline- or benzoate-modified GOx respectively. The calculated $\Delta V^{\neq}$ of the aniline- or benzoate-modified GOx were not significantly different among the studied temperatures ($p > 0.10$).

Effect of HHP on enzyme activity

The $\varepsilon_{\text{o-Dianisidine}}$ values changed at different pressure-temperature treatments as reported on Table 4.2. Pressure and temperature had antagonistic effects on the extinction coefficient. As explained in the Materials and methods, the contribution of pressure and temperature on volume changes (hence concentration) was corrected using the the known $V_{p,\,T} / V_{0.1\text{ MPa},\,25\text{ °C}}$ of water. This allowed us to determine the $\varepsilon_{\text{o-Dianisidine}}$ only because of the changes in the optical absorbance at the studied pressure-temperature conditions. The $\varepsilon_{\text{o-Dianisidine}}$ values were significantly smaller at 0.1 MPa compared to all the studied HHP, whereas the $\varepsilon_{\text{o-Dianisidine}}$ values were not significantly different between different level of pressures at HHP. Therefore, the $\varepsilon_{\text{o-Dianisidine}}$ at HHP was calculated using results from pressure in the range of 60 to 240 MPa at each specific temperature as listed in the last row of Table 4.2. The $\varepsilon_{\text{o-Dianisidine}}$ was lowest at 0.1 MPa and 69.1 °C (6.90 ± 0.12 mM^{-1} cm^{-1}) and highest at HHP and 25.0 °C (8.49 ± 0.30 mM^{-1} cm^{-1}) at our process conditions. The importance of temperature effect on changing the optical absorbance

spectra and extinction coefficients were discussed in order to obtain more accurate values of the concentration changes (Kim and Liu, 2007). The report from Cordone et al. (1986) showed decrease in temperature from 25 to -73 °C increased the $\varepsilon_{deoxyhaemoglobin}$ at 758 nm by ~0.22 mM^{-1} cm^{-1}.

At all the HHP treatments, the production of oxidized o-Dianisidine using native, aniline-, or benzoate-modified GOx was faster compared to the treatments at atmospheric pressure and the corresponding temperature. The changes in the concentration of oxidized o-Dianisidine at 0.1 MPa and 25.0 °C for the native GOx as well as at 180 MPa and 69.1 °C for the native, aniline-, or benzoate-modified GOx are plotted in Figure 4.1. The deviation from linearity at the initial of the reaction was attributed to slow mixing and reagent diffusion in the quartz cuvette. The final concentrations of oxidized o-Dianisidine increased at HHP and the aniline-modified GOx resulted in the highest concentration of the product followed by the benzoate-modified GOx and the native GOx at 180 MPa and 69.1 °C. Therefore, both HHP and temperature increased the rate of reaction of native, aniline-, or benzoate-modified GOx. To evaluate the velocity of reaction at the studied conditions, concentration of the produced oxidized o-Dianisidine over time was determined. Table 4.3 provides the velocity of the reaction at all the studied pressure and temperature treatment combinations for the native, aniline-, or benzoate-modified GOx. Decrease in the velocity and R^2 of the linear regression at atmospheric pressure at 63.8 or 69.1 °C indicated the thermal inactivation of the native, aniline-, or benzoate-modified enzyme at these conditions despite the stabilization effects of modification. In a similar way, the deviation from linearity for activity assessment of *Candida antarctica* lipase B at 0.1 and 400 MPa was suggested as thermal inactivation of the enzyme at temperatures above 63.5 °C (Eisenmenger and Reyes-De-Corcuera, 2009a). At atmospheric pressure at 63.8 or 69.1 °C, native GOx and

benzoate-modified GOx indicated similar deviation from linearity, whereas the deviation from linearity was smaller for the aniline-modified GOx. This agrees with our finding of the higher thermal stability of the aniline-modified GOx compared to the benzoate-modified or the native GOx, previously observed by differential scanning calorimetry method (Halalipour et al., 2016). At atmospheric pressure, increase in temperature from 25.0 °C to 53.9 °C increased the velocity of reaction for the native, aniline-, and benzoate-modified GOx by 2-fold. Similarly, activity of the GOx from *Aspergillus niger* increased 2-fold reported for increasing the temperature from 25 °C to 55 °C (Kalisz et al., 1991). However, the velocity of the reaction for the native, aniline-, and benzoate-modified at atmospheric pressure decreased at 58.8, 63.8, or 69.1°C compared to 53.9 °C because of the observed thermal inactivation of the enzymes.

At 60 to 240 MPa, increase in temperature always increased the velocity of the reaction for the native, aniline-, and benzoate-modified GOx. This indicated the enzymes were protected against thermal inactivation at these HHP in contrast to atmospheric pressure. As shown in Table 4.3, increase in pressure up to 180 MPa accelerated the reaction as indicated by an increase in the velocity of reaction at all the studied temperatures for the native, aniline-, and benzoate-modified GOx. However, this acceleration of reaction toward producing more products was not favored by increasing the pressure from 180 MPa to 240 MPa as indicated by a decrease in the velocity at 240 MPa for all the studied enzymes. Similarly, Mozhaev et al. (1996) reported enzymatic activity of α-chymotrypsin increased up to 360 MPa, whereas pressure higher than 360 MPa decreased the activity due to pressure-induced denaturation of the enzyme.

The slowest velocity of reaction was at atmospheric pressure, whereas the reactions at 180 MPa resulted in the highest velocity values for the native, aniline-, or benzoate-modified GOx at all the studied temperatures. The combined effects of temperature and pressure produced

the greatest increase in reaction velocity in aniline-modified GOx followed by the benzoate-modified GOx and the native GOx. The velocity of the reaction catalyzed by aniline-modified GOx increased 1.1, 4.1, 5.4, 6.6, or 11.3 times at 180 MPa at 25.0, 53.9, 58.8, 63.8, or 69.1 °C respectively compared to the velocity of the aniline-modified GOx at 0.1 MPa and 25.0 °C. Similarly, the velocity of the reaction for the benzoate-modified GOx was 1.1, 4.0, 5.0, 6.1, or 9.3 times higher at 180 MPa at 25.0, 53.9, 58.8, 63.8, or 69.1 °C respectively compared to the velocity of the benzoate-modified GOx at 0.1 MPa and 25.0 °C. Finally, the velocity of the reaction for the native GOx increased less than modified GOx at HHP and was 1.1, 3.4, 3.9, 4.8, or 7.3 times faster at 180 MPa at 25.0, 53.9, 58.8, 63.8, or 69.1 °C respectively compared to the velocity of the native GOx at 0.1 MPa and 25.0 °C. Treatments at 180 MPa at 25.0 °C resulted in the same level of acceleration for all the three enzymes where the changes in the velocity were less pronounced. The observed increase in HHP effect by increasing temperature was in agreement with study of activation of α-chymotrypsin for catalyzing analide where level of activation at HHP increased by temperature from 6.5-fold at 20 °C to 30-fold at 50 °C (Mozhaev et al., 1996). Therefore, the combination effects of temperature and pressure on the studied enzymes in our research resulted in up to 11-fold activation at 180 MPa and 69.1°C. Egg white is an important product in the food industry and de-sugaring the egg white (glucose content of 4.01 mg mL^{-1}) using GOx to 98% of the initial glucose content has been reported to take 3 h at 25 °C (Sisak et al., 2006). The observed 11-fold increase in activity of the aniline-modified GOx at 69.1°C at 240 MPa can suggest to possibly decrease the process time of egg white to under 20 min or the cost of enzyme usage by approximately 90%.

Increases in activity of some other enzymes under pressure have also been reported. Activity of β-glucosidase from strawberry increased by 76% at 400 MPa while HHP at 600 and

800 MPa inactivated the enzyme (Garcia-Palazon et al., 2004). Increase in pressure up to 400 MPa increased activity of polyphenol oxidase from apple juice by 44.0 ± 8.2 % compared to the activity of the enzyme in a freshly squeezed apple juice, whereas increase in activity of the enzyme reduced to 27.1 ± 1.9 % by increasing pressure from 400 MPa to 500 MPa (Buckow et al., 2009). The rate of viscosity reduction of pectin using a pectinase formulation from *Aspergillus niger* increased 2.6-fold at 300 MPa and 62.4 °C compared to the rate at atmospheric pressure at 45.0 °C (Tomlin et al., 2014).

Dependence of enzyme activity on temperature

The dependence of the enzyme activity on the temperature for each native, aniline-, and benzoate-modified GOx was assessed by evaluation of E_a at all the studied pressures. Error in the calculation of E_a at each pressure was expressed as the standard error of the linear regression as reported in Table 4.4 for each studied enzyme. Arrhenius plot was linear at HHP for the native and modified enzymes with the R^2 in the range of 0.90 to 0.99. The lowest R^2 was observed at 240 MPa for each enzyme due to pressure induced-inactivation. Moreover, calculation of E_a at 0.1 MPa was not applicable using Arrhenius model because of deviation from linearity due to thermal inactivation of the enzymes. Therefore, only at HHP increase in temperature always favored the enzymes activation. For all three enzymes, the highest value of E_a was at 180 MPa (34.7 ± 2.7, 42.3 ± 3.7, or 39.4 ± 2.4 kJ mol^{-1} for the native, aniline-, or benzoate-modified GOx respectively). As listed in Table 4.4, E_a values then decreased by increasing pressure from 180 MPa to 240 MPa due to decrease in activation at this pressure. Moreover, E_a values were higher for the aniline-modified GOx, followed by the benzoate-modified GOx and the native enzyme at all the studied pressures. Similarly, Tomlin et al. (2014) observed an increase in the E_a at 300

MPa (42.4 ± 11.3 kJ mol^{-1}) due to activation of a pectinase formulation from *Aspergillus niger* at high pressure.

Pairwise comparison tests determined the significant difference between the E_a due to the pressures for each native, aniline-, and benzoate-modified GOx (Table 4.4). The E_a significantly increased from 60 MPa to 180 MPa for all the studied enzymes. Therefore, HHP significantly increased the acceleration of the reaction of the enzymes by temperature up to 180 MPa. However, the decrease in E_a values at 240 MPa for all the three enzymes resulted in no significant difference in E_a. Pairwise comparisons were also conducted to assess the significant differences in E_a due to modification at each studied pressure. Results are presented with subscript Greek letters in each column of Table 4.4. Aniline modification of GOx significantly increased the effect of temperature on the acceleration of the reaction compared to the native enzyme. In addition, the effect of temperature on the acceleration of the reaction by the benzoate modification was not significantly different than the native GOx. The higher effect of temperature on the aniline-modified GOx reaction can also be attributed to the higher stability of the aniline-modified GOx against thermal inactivation compared to the native and benzoate-modified GOx.

Dependence of enzyme activity on pressure

The dependence of the enzyme activity on the pressure for each native, aniline-, or benzoate-modified GOx was assessed by quantification of the activation volume ($\Delta V^{\neq}$) at all the studied temperatures. Error in the calculation of the $\Delta V^{\neq}$ at each temperature was the standard error of the linear regression as reported in Table 4.5 for each studied enzyme. Since the purpose of this study was to evaluate the activation effect of HHP on the enzymatic reaction, only

pressures up to 180 MPa were used in calculation of the $\Delta V^{\neq}$. As mentioned in pervious section, pressure at 240 MPa reduced the velocity of the reaction which indicated pressure induced-inactivation. Therefore, the $\Delta V^{\neq}$ of each studied enzyme was calculated in the pressure range of 0.1 to 180 MPa with the R^2 in the range of 087 to 0.99. The $\Delta V^{\neq}$ evaluation resulted in negative values for native, aniline-, or benzoate-modified GOx at all the selected temperatures which indicated activation was favored by increasing pressure up to 180 MPa. The lowest calculated $\Delta V^{\neq}$ values for native and modified GOx were at 25 °C where -0.8 ± 0.2, -0.9 ± 0.3, or -1.0 ± 0.2 $cm^3\,mol^{-1}$ obtained for native, aniline-, or benzoate-modified GOx respectively. A similar small value of -2.2 $cm^3\,mol^{-1}$ has been reported as the $\Delta V^{\neq}$ of α-chymotrypsin indicating activating effect of pressure for treatment at 0.1 to 200 MPa at 20 °C (Luong and Winter, 2015). Similarly, pressure enhanced catalytic activity of naringinase as indicated by a negative $\Delta V^{\neq}$ of -9.0 ± 2.8 $cm^3\,mol^{-1}$ studied at 0.1-160 MPa at 30 °C (Pedro et al., 2007). Increase in temperature increased the $\Delta V^{\neq}$ and the highest values were -38.5 ± 10.2, -37.3 ± 9.3, or -33.5 ± 7.8 $cm^3\,mol^{-1}$ for aniline-, benzoate-, or native GOx treated at 69.1 °C respectively. In other words, effect of pressure on the catalytic activity of the native, aniline-, and benzoate-modified GOx was highest at the highest studied temperature. Beside effect of pressure on activation of enzyme, increase in activity at elevated temperatures was also attributed to the pressure induced-stabilization reported for *Candida antarctica* lipase B at 80 °C (Eisenmenger and Reyes-De-Corcuera, 2009a). Similar trend in $\Delta V^{\neq}$ compared to our study was also reported where temperature increased the effect of pressure on the catalytic activity of thermolysin protease as indicated by increasing $\Delta V^{\neq}$ from -71 $cm^3\,mol^{-1}$ at 25 °C to -95 $cm^3\,mol^{-1}$ at 45 °C (Kunugi et al., 1997).

Pairwise comparison tests of linear regressions using GLM determined the significant difference between $\Delta V^{\neq}$ due to temperatures for each native, aniline-, or benzoate-modified GOx

(Table 4.5). The $\Delta V^{\neq}$ significantly increased from 25.0 °C to 69.1 °C for the aniline-modified GOx. Same trend were observed for the native and benzoate-modified GOx, however, $\Delta V^{\neq}$ between 53.9 and 58.8 °C was not significantly different for native and benzoate-modified GOx. This was due to less pronounced effect of temperature on the velocity of the reaction at lower temperatures. Pairwise comparison tests were also conducted to assess the significant differences between $\Delta V^{\neq}$ due to modification at each studied temperature. The $\Delta V^{\neq}$ values were not significantly different due to enzyme modification as presented with subscript Greek letters in each column of Table 4.5. One can hypothesize that although the aniline-modified GOx presented the highest velocity of the reaction at HHP, the level of changes in the velocity by pressure are independent from the hydrophobic modification of the surface residues. In other words, increase in pressure from 0.1 to 180 MPa resulted in similar level of acceleration of the reaction regardless of hydrophobic modifications.

The effect of pressure on the activation of enzymes has been discussed from the relationship between the activation volume and the rate of catalyzing substrate. More negative activation volume attributed to the greater activity enhancement under HHP (Boonyaratanakornkit et al., 2002). Frye and Royer (1998) suggested that pressure affects the rate of reaction by changing native protein structure due to solvation of hydrophobic groups, electrostriction of charged and polar groups, and compression of structure. However, the pressure-induced the level of acceleration of the reaction was similar regardless of modification and hence the hydrophobic effects might not play the main role in pressure induced-activation. Moreover, Michels et al. (1996) suggested presence of substrate increases enzyme activity by protecting the structure of enzyme at high pressure against unfolding. However, different substrates may result in different pressure effect where Kunugi et al. (1997) observed pressure

range with highest activity of thermolysin protease changed from 100-120 MPa for a heptapeptide substrate to 200-250 MPa for a dipeptide amide substrate. Finally, Schuabb et al. (2016) reported that the effect of pressure on the catalytic activity of α-chymotrypsin and peroxidase strongly depends on the interfacial properties of the adsorbed enzyme on different adsorbent materials. However, they did not observe changes in the structure of the adsorbed enzymes at the studied surfaces using Fourier transform infrared method. Despite the numerous reports on the effect of HHP on enzyme stability and activity, the exact mechanisms of pressure induced activation of enzymes have yet to be elucidated.

Acknowledgment

This project was supported by USDA-NIFA-AFRI GRANT 11322452.

Table 4.1.

The k_{inact} of modified GOx ± the linear regression standard error and $\Delta V^{\neq}$ and E_a of inactivation ± the linear regression standard error. Bolded values are given indicating the slowest k_{inact}, greatest $\Delta V^{\neq}$, and smallest E_a.

Pressure (MPa)	Modification	Temperature (°C) 69.1	R^2	74.5	R^2	80.0	R^2	E_a (kJ mol^{-1})	R^2
		k_{inact} (min^{-1}) × 10^{-2}							
0.1	Aniline	$28.60^{a}{}_{\alpha}$ ±2.02	0.99	$426.99^{e}{}_{\alpha}$ ±30.54	0.98	$1343.70^{i}{}_{\alpha}$ ±76.01	0.99	$355.2^{E}{}_{\alpha}$ ±32.7	0.95
	Benzoate	$36.80^{m}{}_{\beta}$ ±1.79	0.99	$557.57^{q}{}_{\beta}$ ±29.04	0.99	$1625.68^{v}{}_{\beta}$ ±98.36	0.99	$349.6^{H}{}_{\alpha}$ ±34.0	0.94
60	Aniline	$4.94^{b}{}_{\alpha}$ ±0.23	0.99	$59.23^{f}{}_{\alpha}$ ±2.47	0.99	$172.36^{j}{}_{\alpha}$ ±10.76	0.99	$327.8^{EF}{}_{\alpha}$ ±30.6	0.95
	Benzoate	$6.36^{n}{}_{\beta}$ ±0.27	0.99	$73.83^{r}{}_{\beta}$ ±5.55	0.98	$202.06^{w}{}_{\beta}$ ±5.18	1.00	$319.2^{HI}{}_{\alpha}$ ±31.0	0.95
120	Aniline	$1.91^{c}{}_{\alpha}$ ±0.15	0.98	$15.36^{g}{}_{\alpha}$ ±1.58	0.97	$35.79^{k}{}_{\alpha}$ ±1.78	0.99	$270.3^{FG}{}_{\alpha}$ ±28.0	0.95
	Benzoate	$2.49^{o}{}_{\beta}$ ±0.26	0.97	$22.36^{s}{}_{\beta}$ ±1.61	0.98	$48.07^{x}{}_{\beta}$ ±2.64	0.99	$273.3^{IJ}{}_{\alpha}$ ±30.9	0.93
240	Aniline	**$1.48^{d}{}_{\alpha}$ ±0.07**	0.99	**$7.36^{h}{}_{\alpha}$ ±0.59**	0.98	**$19.58^{l}{}_{\alpha}$ ±2.70**	0.95	**$238.4^{G}{}_{\alpha}$ ±19.0**	0.98
	Benzoate	$2.04^{p}{}_{\beta}$ ±0.14	0.99	$10.22^{u}{}_{\beta}$ ±1.26	0.96	$25.79^{y}{}_{\beta}$ ±3.95	0.93	$233.8^{J}{}_{\alpha}$ ±19.9	0.98
360	Aniline	$2.09^{c}{}_{\alpha}$ ±0.23	0.97	$12.93^{g}{}_{\alpha}$ ±1.70	0.95	$39.29^{k}{}_{\alpha}$ ±6.67	0.92	$270.5^{G}{}_{\alpha}$ ±20.2	0.98
	Benzoate	$2.93^{o}{}_{\beta}$ ±0.30	0.97	$15.88^{t}{}_{\beta}$ ±1.71	0.97	$53.39^{x}{}_{\beta}$ ±7.38	0.95	$267.7^{J}{}_{\alpha}$ ±16.8	0.99
$\Delta V^{\neq}$ (cm^3 mol^{-1})	Aniline	$62.3^{A}{}_{\alpha}$ ±10.8	0.97	$77.7^{AB}{}_{\alpha}$ ±8.5	0.99	**$86.0^{B}{}_{\alpha}$ ±6.6**	0.99		
	Benzoate	$62.0^{C}{}_{\alpha}$ ±10.9	0.96	$75.1^{CD}{}_{\alpha}$ ±11.2	0.98	$83.6^{D}{}_{\alpha}$ ±8.9	0.98		

[a - l] Differences in the k_{inact} of aniline-modified GOx with different letter (effect of pressure on k_{inact}) were significant ($p < 0.10$).

[m - y] Differences in the k_{inact} of benzoate-modified GOx with different letter (effect of pressure on k_{inact}) were significant ($p < 0.10$).

[A - B] Differences in the $\Delta V^{\neq}$ of aniline-modified GOx with different letter (effect of temperature on $\Delta V^{\neq}$) were significant ($p < 0.10$).

[C - D] Differences in the $\Delta V^{\neq}$ of benzoate-modified GOx with different letter (effect of temperature on $\Delta V^{\neq}$) were significant ($p < 0.10$).
[E - G] Differences in the E_a of aniline-modified GOx with different letter (effect of pressure on E_a) were significant ($p < 0.10$).
[H - J] Differences in the E_a of benzoate-modified GOx with different letter (effect of pressure on E_a) were significant ($p < 0.10$).
[α - β] Differences in the aniline- and benzoate-modified GOx with different Greek letter (effect of modification on the k_{inact} at each pressure-temperature treatments, effect of modification on the $\Delta V^{\neq}$ at each temperature, and effect of modification on the E_a at each pressure) were significant ($p < 0.10$).

Table 4.2.

Average extinction coefficient (n=2) of the o-Dianisidine at each pressure-temperature treatments ± the linear regression standard error. Numbers in parentheses are the $V_{p,\,T}$ / $V_{0.1\ \mathrm{MPa},\ 25\ ^{\circ}\mathrm{C}}$ of water used for correction of the collected absorbance at each studied pressure-temperature treatments.

Pressure (MPa)	Temperature (°C)				
	25.0	53.9	58.8	63.8	69.1
	$\varepsilon_{\text{o-Dianisidine}}$ ($\mathrm{mM^{-1}\ cm^{-1}}$)				
0.1	7.72[a] ± 0.13 (1.00)	7.38[a] ± 0.09 (1.01)	7.10[a] ± 0.09 (1.01)	7.05[a] ± 0.11 (1.02)	6.90[a] ± 0.12 (1.02)
60	8.47[b] ± 0.14 (0.98)	8.39[b] ± 0.14 (0.99)	8.27[b] ± 0.16 (0.99)	8.23[b] ± 0.07 (0.99)	8.14[b] ± 0.08 (0.99)
120	8.51[b] ± 0.34 (0.95)	8.44[b] ± 0.17 (0.97)	8.36[b] ± 0.14 (0.97)	8.29[b] ± 0.11 (0.97)	8.13[b] ± 0.09 (0.97)
180	8.53[b] ± 0.33 (0.94)	8.44[b] ± 0.16 (0.95)	8.26[b] ± 0.16 (0.95)	8.20[b] ± 0.15 (0.95)	8.10[b] ± 0.22 (0.95)
240	8.45[b] ± 0.31 (0.92)	8.28[b] ± 0.22 (0.93)	8.23[b] ± 0.22 (0.93)	8.22[b] ± 0.29 (0.94)	8.21[b] ± 0.27 (0.94)
60-240	8.49 ± 0.30	8.39 ± 0.32	8.28 ± 0.29	8.24 ± 0.33	8.15 ± 0.35

[a - b] Differences in the $\varepsilon_{\text{o-Dianisidine}}$ in each column with different letter were significant ($p < 0.10$).

Table 4.3.

The velocity of the reaction for the native, aniline-, and benzoate-modified GOx at each pressure-temperature treatments ± the linear regression standard error. Bolded numbers are given representing the highest value of the velocity at each temperature.

Pressure (MPa)	Modification	Temperature (°C)									
		25.0	R^2	53.9	R^2	58.8	R^2	63.8	R^2	69.1	R^2
		v ($\times 10^{-4}$, mM^{-1} min^{-1})									
0.1	None	1.52± 0.01	0.99	3.12± 0.03	0.99	2.91± 0.04	0.99	1.94± 0.05	0.97	1.15± 0.06	0.93
	Aniline	1.54± 0.02	0.99	3.32± 0.03	0.99	3.06± 0.03	0.99	2.12± 0.05	0.98	1.38± 0.05	0.95
	Benzoate	1.49 ± 0.02	1.00	3.22± 0.04	0.99	2.93± 0.06	0.99	1.98± 0.05	0.97	1.17± 0.05	0.93
60	None	1.54± 0.02	0.99	3.21± 0.03	0.99	3.34± 0.04	0.99	4.01± 0.04	0.98	4.67± 0.05	0.98
	Aniline	1.55± 0.03	1.00	4.05± 0.04	0.99	4.42± 0.03	0.99	6.19± 0.04	0.99	7.15± 0.05	0.98
	Benzoate	1.55± 0.03	0.99	3.41± 0.04	0.99	3.54± 0.05	0.99	4.30± 0.03	0.99	5.60± 0.06	0.96
120	None	1.56± 0.02	0.99	3.57± 0.04	0.99	3.86± 0.03	0.99	4.89± 0.05	0.99	6.29± 0.04	0.99
	Aniline	1.56± 0.03	1.00	4.45± 0.04	0.99	5.43± 0.03	1.00	6.97± 0.04	0.98	12.20± 0.03	0.98
	Benzoate	1.56± 0.03	1.00	4.04± 0.04	0.99	4.43± 0.04	0.99	5.95± 0.04	0.99	9.06± 0.05	0.98
180	None	1.61± 0.01	1.00	5.15± 0.05	0.99	5.96± 0.04	0.99	7.31± 0.03	0.99	11.02± 0.07	0.99
	Aniline	**1.65± 0.02**	0.99	**6.37± 0.04**	0.99	**8.25± 0.04**	0.99	**10.21± 0.03**	1.00	**17.34± 0.09**	0.98
	Benzoate	1.59± 0.01	0.99	5.94± 0.05	0.99	7.41± 0.06	0.99	8.98± 0.03	0.99	13.67± 0.05	0.99
240	None	1.54± 0.02	1.00	3.25± 0.04	0.99	3.46± 0.04	1.00	4.30± 0.04	0.99	6.50± 0.06	0.98
	Aniline	1.57± 0.02	1.00	3.60± 0.05	0.99	4.73± 0.06	0.99	6.95± 0.04	0.99	12.32± 0.05	0.99
	Benzoate	1.52± 0.03	0.99	3.34± 0.06	0.98	3.94± 0.04	0.99	5.02± 0.03	0.99	8.97± 0.04	0.99

Table 4.4.

Dependence of the enzyme activity on temperature presented by the E_a calculated at each studied pressure for the native, aniline-, and benzoate-modified GOx ± the linear regression standard error.

Modification	Pressure (MPa)									
	0.1†	R^2†	60	R^2	120	R^2	180	R^2	240	R^2
	E_a (kJ mol^{-1})									
None	-	-	$20.8^{a}{}_{\alpha}$ ± 1.1	0.99	$25.4^{b}{}_{\alpha}$ ± 2.2	0.97	$34.7^{c}{}_{\alpha}$ ± 2.7	0.98	$24.6^{b}{}_{\alpha}$ ± 4.0	0.93
Aniline	-	-	$28.9^{d}{}_{\beta}$ ± 2.1	0.98	$35.7^{e}{}_{\beta}$ ± 5.1	0.94	$42.3^{fg}{}_{\beta}$ ± 3.7	0.98	$35.1^{eg}{}_{\beta}$ ± 7.5	0.90
Benzoate	-	-	$23.2^{h}{}_{\alpha}$ ± 2.1	0.98	$30.9^{i}{}_{\alpha\beta}$ ± 4.1	0.95	$39.4^{j}{}_{\alpha\beta}$ ± 2.4	0.99	$30.1^{i}{}_{\alpha\beta}$ ± 6.0	0.91

† The E_a and R^2 cannot be calculated at 0.1 MPa using Arrhenius model because of deviation from linearity due to enzyme inactivation.

$^{a-c}$ Differences in the E_a of native GOx with different letter (effect of pressure on E_a) were significant ($p < 0.10$).

$^{d-g}$ Differences in the E_a of aniline-modified GOx with different letter (effect of pressure on E_a) were significant ($p < 0.10$).

$^{h-j}$ Differences in the E_a of benzoate-modified GOx with different letter (effect of pressure on E_a) were significant ($p < 0.10$).

$_{\alpha-\beta}$ Differences in the E_a of native, aniline-, and benzoate-modified GOx with different Greek letter in each column (effect of modification on E_a) were significant ($p < 0.10$).

Table 4.5.

Dependence of the enzyme activity on pressure presented by the $\Delta V^{\neq}$ calculated at each studied temperature for the native, aniline-, and benzoate-modified GOx ± the linear regression standard error.

Modification	Temperature (°C)									
	25.0	R^2	53.9	R^2	58.8	R^2	63.8	R^2	69.1	R^2
	$\Delta V^{\neq}$ ($cm^3\ mol^{-1}$)									
None	$-0.8^{a}{}_{\alpha} \pm 0.2$	0.91	$-7.3^{b}{}_{\alpha} \pm 2.5$	0.81	$-10.6^{b}{}_{\alpha} \pm 2.4$	0.91	$-19.5^{c}{}_{\alpha} \pm 3.4$	0.94	$-33.5^{d}{}_{\alpha} \pm 7.8$	0.90
Aniline	$-0.9^{e}{}_{\alpha} \pm 0.3$	0.87	$-9.3^{f}{}_{\alpha} \pm 1.7$	0.94	$-14.7^{g}{}_{\alpha} \pm 1.3$	0.99	$-22.5^{h}{}_{\alpha} \pm 6.5$	0.86	$-38.5^{i}{}_{\alpha} \pm 10.2$	0.88
Benzoate	$-1.0^{j}{}_{\alpha} \pm 0.2$	0.90	$-9.1^{k}{}_{\alpha} \pm 2.4$	0.88	$-13.8^{k}{}_{\alpha} \pm 2.5$	0.94	$-22.7^{l}{}_{\alpha} \pm 3.2$	0.96	$-37.3^{m}{}_{\alpha} \pm 9.3$	0.89

[a - d] Differences in the $\Delta V^{\neq}$ of native GOx with different letter (effect of temperature on $\Delta V^{\neq}$) were significant ($p < 0.10$).

[e - i] Differences in the $\Delta V^{\neq}$ of aniline-modified GOx with different letter (effect of temperature on $\Delta V^{\neq}$) were significant ($p < 0.10$).

[j - m] Differences in the $\Delta V^{\neq}$ of benzoate-modified GOx with different letter (effect of temperature on $\Delta V^{\neq}$) were significant ($p < 0.10$).

[α] Differences in the $\Delta V^{\neq}$ of native, aniline-, and benzoate-modified GOx with same Greek letter in each column (effect of modification on $\Delta V^{\neq}$) were not significant ($p > 0.10$).

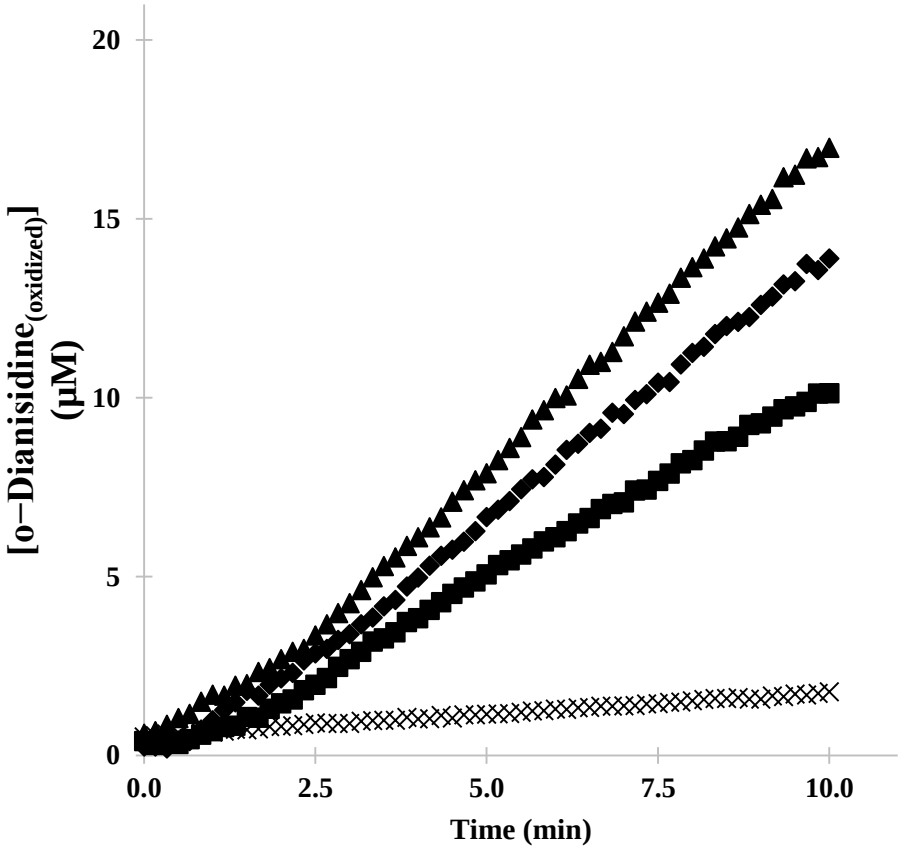

Figure 4.1. Progress of the production of oxidized o-Dianisidine during 10 min treatment using (×) native GOx at 0.1 MPa and 25.0 °C, (■) native GOx at 180 MPa and 69.1 °C, (◆) benzoate-modified GOx at 180 MPa and 69.1 °C, and (▲) aniline-modified GOx at 180 MPa and 69.1 °C.

Appendix

4-I) High pressure system for activation study.

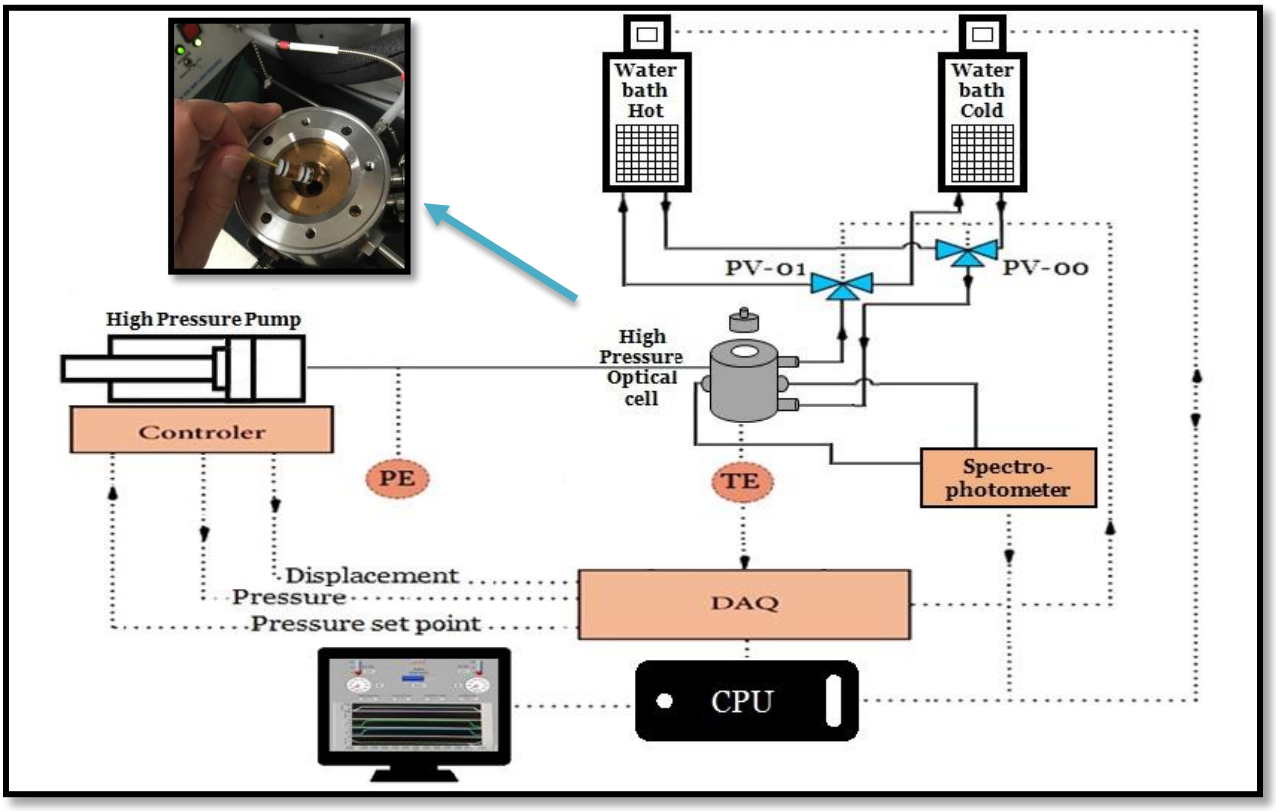

Figure A4.1. Schematic of the high pressure system using optical cell model U103.

4-II) Arrhenius plots to obtain the E_a of native, aniline-, and benzoate-modified GOx.

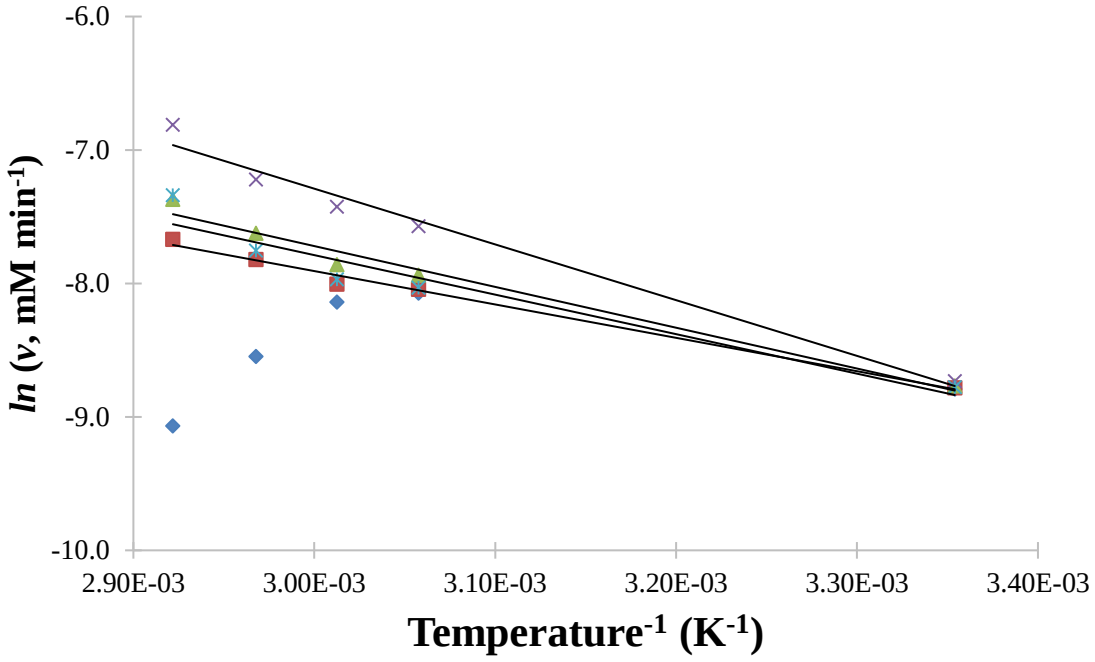

Figure A4.2. Arrhenius plots to obtain the E_a of native GOx for treatment at (◆) 0.1 MPa, (■) 60 MPa, (▲) 120 MPa, (×) 180 MPa, and (∗) 240 MPa.

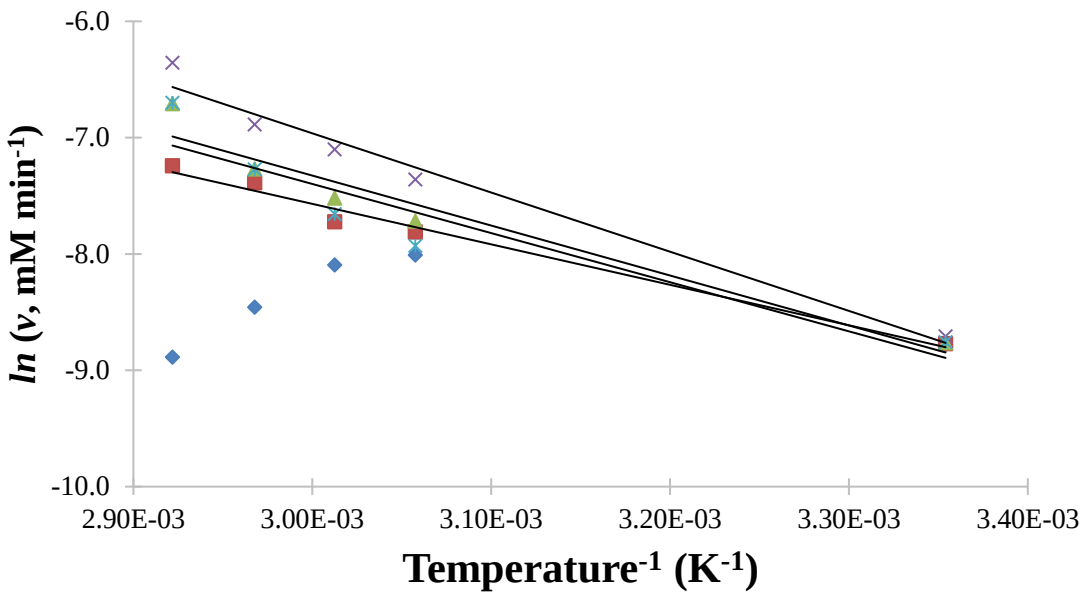

Figure A4.3. Arrhenius plots to obtain the E_a of the aniline-modified GOx for treatment at (◆) 0.1 MPa, (■) 60 MPa, (▲) 120 MPa, (×) 180 MPa, and (∗) 240 MPa.

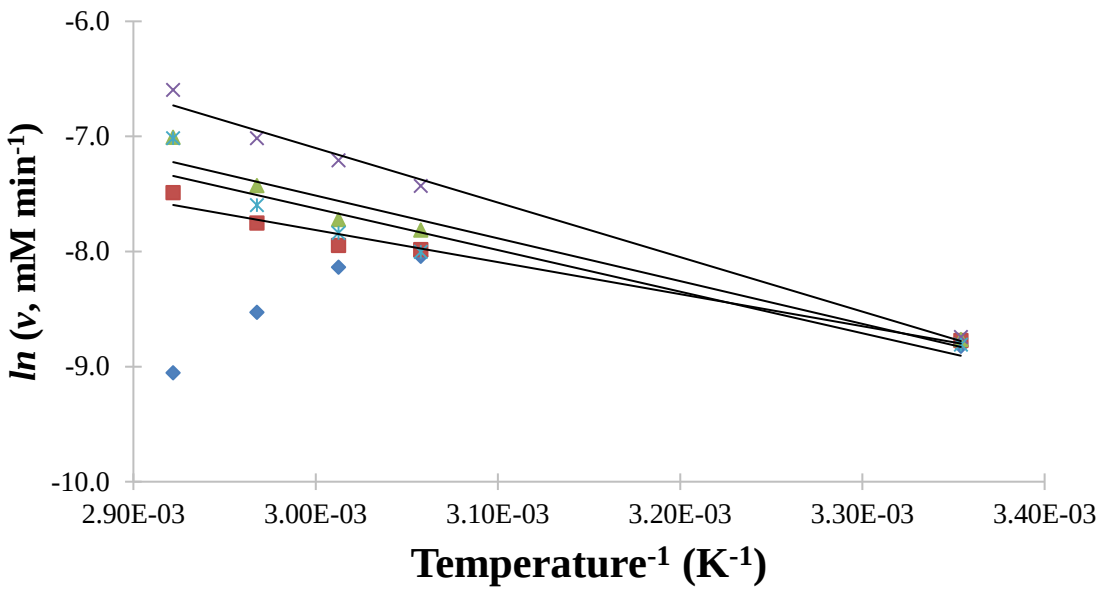

Figure A4.4. Arrhenius plots to obtain the E_a of the benzoate-modified GOx for treatment at (◆) 0.1 MPa, (■) 60 MPa, (▲) 120 MPa, (×) 180 MPa, and (✳) 240 MPa.

CHAPTER 5

OVERALL DISCUSSION AND SUGGESTED FUTURE STUDIES

Overall discussion

We studied the effects of HHP and chemical modification of GOx and XOx with phenyl groups. Overall, at the studied temperatures, HHP increased the thermal stability of GOx and XOx compared to treatments at atmospheric pressure. The stabilization effect of HHP increased with temperature for GOx and XOx up to 74.5 and 70.0 °C respectively, and the differences in rate of inactivation was more pronounced at higher temperatures. The pressure that induced the greatest stability changed from 180 to 300 MPa as temperature increased from 58.8 to 80.0 °C whereas it was consistent at 300 MPa for XOx at all the studied temperatures, however, there were no significant differences in the rate of inactivation among the highest pressures ranges. In addition, the relative extent to which HHP stabilized GOx was greater than XOx. Moreover, under pressure, the rate of reaction of the native or the modified GOx catalyzed reaction were faster compared to treatments at atmospheric pressure. The aniline-modified GOx catalyzed the fastest reaction at all the studied conditions. From one enzyme to the other enzyme the reported results are different for studies of: pressure that results in the greatest stability or activity; the level of stabilization for each enzyme; the effect of pressure on modified enzymes; and the changes in the effect of pressure by temperature. However, no supportive mechanism of these phenomena under pressure were documented. Insights into the mechanisms of pressure effects on proteins are critical to further explore the application of HHP for the enzyme enhancement.

It is important to understand why and how the effect of pressure is different from one enzyme to the other. However, despite the increasing number of investigations on effect of pressure on proteins, the mechanism of how pressure affects proteins has yet to be elucidated (Royer, 2015). Important structural changes such as penetration of water into the structure or conformational changes in the active sites under pressure most likely explain the mechanism of pressure effects on enzymes. Relevant structural considerations and studies include:

1. Subunit interaction under pressure: subunit interaction of oligomeric proteins such as dimeric GOx and XOx, or octameric alcohol oxidase under pressure is of great importance. Subunit interaction can produce intermediate forms of the dissociated monomers under pressure with higher stability and activity. Tetrameric structure of pig heart lactate dehydrogenase with four identical subunits dissociated into dimers reversibly up to 200 MPa and further pressure resulted in irreversible dissociation from dimers to monomers detected by high pressure small-angle X-ray scattering which employed double flat crystal monochromators and a bent cylindrical mirror with 1:1 magnification (Fujisawa et al., 1999). Subunit interaction was reported reversible and it can possibly explain the reason of the deviation of GOx inactivation from a first-order model at higher pressures. One can hypothesize the duration of exposure to HHP affects the extent to which conformation of enzyme is modified. Also, upon depressurization, refolding or re-association of subunits may not be instantaneous. Therefore, the dynamics and reversibility of the effects of HHP needs to be considered when analyzing residual activity or performing any structural measurement. In another study, during high pressure denaturation of met-myoglobin, high pressure small-angle X-ray scattering has been successfully applied to detect the intermediate, partially unfolded, and formation of dimers of met-myoglobin under pressure at HHP up to 200 MPa and at 10, 20, 30, or 45 °C using a

high pressure cell with two diamond windows of 3.0 mm diameter and 1 mm thickness that can take pressure up to 200 MPa (Spinozzi et al., 2007).

2. Structural cavities under pressure: cavities (void spaces in the folded structure associated with the tertiary or quaternary structure of a protein) buried inside the ribonuclease enzyme barnase were the most compressible part of protein at pressure up to 200 MPa, detected by a high pressure NMR spectroscopy (Wilton et al., 2009). One can hypothesize that, under pressure, a reduction in the cavity size can reduce the fluctuation of the structure and protect the enzyme against thermal denaturation.
3. Solvent interaction under pressure: effects of pressure on the hydrogen bonding in the solvent can also result in stabilization and denaturation of the protein structure. In the study of lysozyme up to 400 MPa using high pressure small-angle X-ray scattering method, pressure up to 200 MPa resulted in small changes in the water structure, however, structural changes in the solvent water at pressure higher than 200 MPa correlated to the very sensitive changes in intermolecular interactions between the protein molecules at higher pressure range (Schroer et al., 2012). At pressure about 200 MPa, the solvent structure changed by disruption of the second water hydration layer. Moreover, by measurement of the potential of intermolecular interactions of lysozyme using small-angle X-ray scattering method, structural changes in the solvent water affected the intermolecular interactions the highest compared to the ionic strength, temperature, and protein concentration up to 400 MPa (Möller et al., 2012).
4. Hydration of cavities under pressure: changes in the cavities and solvent interaction under pressure can define the significance of the hydration of cavities. Penetration of water molecules inside the structural cavities was reported as the main cause of unfolding of

staphylococcal nuclease at pressure up to 300 MPa in the presence of denaturant detected by high pressure NMR spectroscopy (Roche et al., 2012).

5. Water molecules buried in cavities under pressure: using NMR chemical shift methodology, volume changes in the structure of lysozyme close to the buried water molecules were interestingly reported mostly as expansion under pressure up to 200 MPa, although the overall effect of pressure was compression of the structure (Refaee et al., 2003). In this study, they suggested increasing in structural mobility due to the buried water can cause the pressure induced channel opening or denaturation at elevated pressures. Therefore, one can hypothesize that different level of stabilization for different enzymes is related to the presence of buried water molecules and the ability of the water to diffuse through the cavities.
6. Hydrogen bonds under pressure: hydrogen bonds are important for the correct folding of the protein structure. Shortening of hydrogen bonds in ubiquitin protein up to 250 MPa have been detected using high pressure NMR spectroscopy (Nisius and Grzesiek, 2012). Moreover, hydrogen bonds in the GB1 domain of protein G were shortened up to 200 MPa as detected by high pressure NMR spectroscopy (Wilton et al., 2008). Therefore, HHP stabilized hydrogen bonds and hence the protein structure at the reported pressure range.
7. Hydrophobic core under pressure: site-directed mutagenesis used to alter the hydrophobicity of azurin core. The free energies of unfolding of the wild-type and mutant azurins were measured under pressure up to 240 MPa using steady state and dynamic fluorescence techniques (Mei et al., 1999). Their results indicated a positive correlation between pressure stabilization and hydrophobicity of the core of azurins. One can also hypothesize that the

possibility of the water penetration or presence of water molecules inside the protein structure can decrease due to the hydrophobicity of the core.

8. Active sites under pressure: pressure induced structural changes and compressibility were greatest in the loop 10-16 where the active site of the bovine pancreatic trypsin inhibitor is located detected by NMR chemical shift methodology at 200 MPa (Williamson et al., 2003). Therefore, one can hypothesize that the compression of the active site and residues at the position of the active site effects the dissociation or association constants and equilibrium of enzyme-substrate bindings at HHP. Also at HHP the enzyme-substrate interactions can be a factor of the substrate molecular size because of high compression of the active site.

Suggested future studies

1. Determine the most stable dissociated monomers or dimers of GOx and XOx under pressure using high pressure small-angle X-ray scattering.
    a. Application of crosslinking or entrapment techniques under pressure to retain the structure with the greatest stability.
    b. Fabrication of GOx and XOx biosensors at the pressure with the highest stability of the enzymes to retain the stable structure on the surface of the electrode.
2. Determine the location and number of the structural cavities in GOx and XOx and their effects on the compressibility and level of stabilization of the enzymes using a high pressure NMR spectroscopy.
3. Characterize the effect of solvent interaction on the enhancement of GOx and XOx under HHP.
    a. To answer if water-water interactions are increased under HHP or water-protein interactions.

4. Determine the pressure that water penetrated in cavities and the structural changes of GOx and XOx by increasing pressure all the way to the unfolding of the enzyme.
    a. Determine if enzyme surface with hydrophobic group, positively charged, or negatively charged modifications can alter the water penetration and hence results in different behavior of different enzymes.
5. Determine the location and number of the buried water in the GOx and XOx structure and if extraction of the buried water molecule in an organic solvent increase or decrease the stability and activity of the enzymes.
6. Study the different inter- and intra-molecular hydrogen bonds in the structure of GOx and XOx and how shortening or expansion of each effects the behavior of the under pressure structure.
7. Determine if mutagenesis (at a controlled level to keep the folded structure unaffected) of proteins with same type and number hydrophobic residue (hence same hydropathy index) but at different position (hence different hydrophobicity in the protein core after folding) can clarify the effect of pressure on the proteins hydropathy.
8. Determine the compressibility of the active sites of GOx and XOx under pressure.
    a. Determine if hydrophobic/hydrophilic modification of residue close to the active site can change the substrates binding efficiency at HHP in the compressed active site.
    b. Determine if the compressed enzyme is affected by substrate sizes due to impacts on:
        i. the native structure of the enzyme protected by presence of substrate against unfolding and
        ii. the diffusion of the substrate to the active site of enzyme at HHP.

REFERENCES

Adler, I., Bazerque, P.M., Crivelli, M.R., Aguas, S., Quarracino, C., (1993). Effect of a toothpaste containing amyloglucosidase and glucose oxidase on recurrent aphthous ulcers. Acta odontológica latinoamericana 7(2), 33-38.

Altikatoglu, M., Basaran, Y., Arioz, C., Ogan, A., Kuzu, H., (2010). Glucose Oxidase-dextran Conjugates with Enhanced Stabilities Against Temperature and pH. Applied Biochemistry and Biotechnology 160(8), 2187-2197.

Amini, K., Sorouraddin, M.H., Rashidi, M.R., (2011). Activity and stability of rat liver xanthine oxidase in the presence of pyridine. Canadian Journal of Chemistry 89(1), 1-7.

Araujo, A.M., Neves, M.T., Azevedo, W.M., Oliveira, G.G., Ferreira, D.L., Coelho, R.A.L., Figueiredo, E.A.P., Carvalho, L.B., (1997). Polyvinyl alcohol-glutaraldehyde network as a support for protein immobilisation. Biotechnology Techniques 11(2), 67-70.

Arica, M.Y., Hasirci, V., (1993). Immobilization of glucose oxidase: A comparison of entrapment and covalent bonding. Journal of Chemical Technology & Biotechnology 58(3), 287-292.

Atanasov, P., Wilkins, E., (1994). Biosensor for continuos glucose monitoring. Biotechnology and Bioengineering 43(3), 262-266.

Avis, P.G., Bergel, F., Bray, R.C., (1956). Cellular constituents. The chemistry of xanthine oxidase. Part III. Estimations of the co-factors and the catalytic activities of enzyme fractions from cow's milk. Journal of the Chemical Society (Resumed), 1219-1226.

Babu, V.R.S., Patra, S., Karanth, N.G., Kumar, M.A., Thakur, M.S., (2007). Development of a biosensor for caffeine. Analytica Chimica Acta 582(2), 329-334.

Balasubramaniam, V.M., Martínez-Monteagudo, S.I., Gupta, R., (2015). Principles and Application of High Pressure–Based Technologies in the Food Industry. Annual Review of Food Science and Technology 6(1), 435-462.

Balda, F.P., Aparicio, B.V., Samson, C.T., (2012). Industrial high pressure processing of foods: Review of evolution and emerging trends. Journal of Food Science and Engineering 2(10), 543-549.

Bergmeyer, H.U., Gawehn, K., Grassl, M., (1974a). Methods of enzymatic analysis, Second ed. New York: Academic Press Inc., pp. 457-458.

Bergmeyer, H.U., Gawehn, K., Grassl, M., (1974b). Methods of enzymatic analysis, Second ed. New York: Academic Press Inc., pp. 521-522.

Bhatti, H.N., Madeeha, M., Asgher, M., Batool, N., (2006). Purification and thermodynamic characterization of glucose oxidase from a newly isolated strain of Aspergillus niger. Canadian Journal of Microbiology 52(6), 519-524.

Biela, A., Betz, M., Heine, A., Klebe, G., (2012). Water Makes the Difference: Rearrangement of Water Solvation Layer Triggers Non-additivity of Functional Group Contributions in Protein–Ligand Binding. ChemMedChem 7(8), 1423-1434.

Biela, A., Nasief, N.N., Betz, M., Heine, A., Hangauer, D., Klebe, G., (2013). Dissecting the Hydrophobic Effect on the Molecular Level: The Role of Water, Enthalpy, and Entropy in Ligand Binding to Thermolysin. Angewandte Chemie International Edition 52(6), 1822-1828.

Boonyaratanakornkit, B.B., Park, C.B., Clark, D.S., (2002). Pressure effects on intra- and intermolecular interactions within proteins. Biochimica et Biophysica Acta (BBA) - Protein Structure and Molecular Enzymology 1595(1–2), 235-249.

Bouin, J.C., Hultin, H.O., (1982). Stabilization of glucose oxidase by immobilization/modification as a function of pH. Biotechnology and Bioengineering 24(5), 1225-1231.

Bray, R.C., Pettersson, R., Ehrenberg, A., (1961). The chemistry of xanthine oxidase. 7. The anaerobic reduction of xanthine oxidase studied by electron-spin resonance and magnetic susceptibility. Biochemical Journal 81(1), 178-189.

Breiten, B., Lockett, M.R., Sherman, W., Fujita, S., Al-Sayah, M., Lange, H., Bowers, C.M., Heroux, A., Krilov, G., Whitesides, G.M., (2013). Water Networks Contribute to

Enthalpy/Entropy Compensation in Protein–Ligand Binding. Journal of the American Chemical Society 135(41), 15579-15584.

Buckow, R., Weiss, U., Knorr, D., (2009). Inactivation kinetics of apple polyphenol oxidase in different pressure–temperature domains. Innovative Food Science & Emerging Technologies 10(4), 441-448.

Burnier, R.C., Low, P.S., (1985). Identification and partial characterization of the xanthine oxidase transitions of the milk fat globule membrane. Archives of Biochemistry and Biophysics 240(1), 60-69.

Carraway, K.L., Koshland, D.E., (1968). Reaction of tyrosine residues in proteins with carbodiimide reagents. Biochimica et Biophysica Acta (BBA)-Protein Structure 160(2), 272-274.

Carraway, K.L., Triplett, R.B., (1970). Reaction of carbodiimides with protein sulfhydryl groups. Biochimica et Biophysica Acta (BBA)-Protein Structure 200(3), 564-566.

Caves, M.S., Derham, B.K., Jezek, J., Freedman, R.B., (2011). The mechanism of inactivation of glucose oxidase from Penicillium amagasakiense under ambient storage conditions. Enzyme and Microbial Technology 49(1), 79-87.

Chakraborty, S., Kaushik, N., Rao, P.S., Mishra, H.N., (2014). High-Pressure Inactivation of Enzymes: A Review on Its Recent Applications on Fruit Purees and Juices. Comprehensive reviews in food science and food safety 13(4), 578-596.

Chandler, D., (2005). Interfaces and the driving force of hydrophobic assembly. Nature 437(7059), 640-647.

Chaudhary, A., Raina, M., Harma, H., Hanninen, P., McShane, M.J., Srivastava, R., (2009). Evaluation of glucose sensitive affinity binding assay entrapped in fluorescent dissolved-core alginate microspheres. Biotechnology and Bioengineering 104(6), 1075-1085.

Chen, L.-Q., Zhang, X.-E., Xie, W.-H., Zhou, Y.-F., Zhang, Z.-P., Cass, A.E.G., (2002). Genetic modification of glucose oxidase for improving performance of an amperometric glucose biosensor. Biosensors and Bioelectronics 17(10), 851-857.

Cioni, P., Strambini, G.B., (1996). Pressure Effects on the Structure of Oligomeric Proteins Prior to Subunit Dissociation. Journal of Molecular Biology 263(5), 789-799.

Cordone, L., Cupane, A., Leone, M., Vitrano, E., (1986). Optical absorption spectra of deoxy- and oxyhemoglobin in the temperature range 300-20 K. Biophysical Chemistry 24(3), 259-275.

Dervisevic, M., Custiuc, E., Çevik, E., Şenel, M., (2015). Construction of novel xanthine biosensor by using polymeric mediator/MWCNT nanocomposite layer for fish freshness detection. Food Chemistry 181, 277-283.

Devi, R., Yadav, S., Pundir, C.S., (2011). Electrochemical detection of xanthine in fish meat by xanthine oxidase immobilized on carboxylated multiwalled carbon nanotubes/polyaniline composite film. Biochemical Engineering Journal 58–59, 148-153.

Dewan, S.S., (2014). Global markets for enzymes in industrial applications. BCC Research, BIO030H.

Dougherty, D.A., (1996). Cation-π interactions in chemistry and biology: a new view of benzene, Phe, Tyr, and Trp. Science 271(5246), 163-168.

Duff, M.R., Jr., Chopra, S., Strader, M.B., Agarwal, P.K., Howell, E.E., (2016). Tales of Dihydrofolate Binding to R67 Dihydrofolate Reductase. Biochemistry 55(1), 133-145.

Duong, T., Balaban, M., (2014). Optimisation of the process parameters of combined high hydrostatic pressure and dense phase carbon dioxide on enzyme inactivation in feijoa (Acca sellowiana) puree using response surface methodology. Innovative Food Science & Emerging Technologies 26, 93-101.

Earnshaw, R.G., Appleyard, J., Hurst, R.M., (1995). Understanding physical inactivation processes: combined preservation opportunities using heat, ultrasound and pressure. International Journal of Food Microbiology 28(2), 197-219.

Eisenmenger, M.J., Reyes-De-Corcuera, J.I., (2009a). High hydrostatic pressure increased stability and activity of immobilized lipase in hexane. Enzyme and Microbial Technology 45(2), 118-125.

Eisenmenger, M.J., Reyes-De-Corcuera, J.I., (2009b). High pressure enhancement of enzymes: A review. Enzyme and Microbial Technology 45(5), 331-347.

Eisenmenger, M.J., Reyes-De-Corcuera, J.I., (2010). Enhanced synthesis of isoamyl acetate using an ionic liquid–alcohol biphasic system at high hydrostatic pressure. Journal of Molecular Catalysis B: Enzymatic 67(1–2), 36-40.

Eryomin, A.N., Drozhdenyuk, A.P., Zhavnerko, G.K., Semashko, T.V., Mikhailova, R.V., (2004). Quartz sand as an adsorbent for purification of extracellular glucose oxidase from Penicillium funiculosum 46.1. Applied Biochemistry and Microbiology 40(2), 151-157.

Fiedurek, J., Gromada, A., (1997). Screening and mutagenesis of molds for improvement of the simultaneous production of catalase and glucose oxidase. Enzyme and Microbial Technology 20(5), 344-347.

Fraeye, I., Duvetter, T., Verlent, I., Ndaka Sila, D., Hendrickx, M., Van Loey, A., (2007). Comparison of enzymatic de-esterification of strawberry and apple pectin at elevated pressure by fungal pectinmethylesterase. Innovative Food Science & Emerging Technologies 8(1), 93-101.

Fridh, G., Koch, G., (1999). Effect of a mouth rinse containing amyloglucosidase and glucose oxidase on recurrent aphthous ulcers in children and adolescents. Swedish dental journal 23(2-3), 49-57.

Frye, K.J., Royer, C.A., (1998). Probing the contribution of internal cavities to the volume change of protein unfolding under pressure. Protein Science 7(10), 2217-2222.

Fujisawa, T., Kato, M., Inoko, Y., (1999). Structural Characterization of Lactate Dehydrogenase Dissociation under High Pressure Studied by Synchrotron High-Pressure Small-Angle X-ray Scattering. Biochemistry 38(20), 6411-6418.

Gallivan, J.P., Dougherty, D.A., (1999). Cation-π interactions in structural biology. Proceedings of the National Academy of Sciences 96(17), 9459-9464.

Garcia-Galan, C., Berenguer-Murcia, Á., Fernandez-Lafuente, R., Rodrigues, R.C., (2011). Potential of Different Enzyme Immobilization Strategies to Improve Enzyme Performance. Advanced Synthesis & Catalysis 353(16), 2885-2904.

Garcia-Palazon, A., Suthanthangjai, W., Kajda, P., Zabetakis, I., (2004). The effects of high hydrostatic pressure on β-glucosidase, peroxidase and polyphenoloxidase in red raspberry (Rubus idaeus) and strawberry (Fragaria × ananassa). Food Chemistry 88(1), 7-10.

Gasteiger, E., Hoogland, C., Gattiker, A., Duvaud, S.e., Wilkins, M.R., Appel, R.D., Bairoch, A., (2005). Protein Identification and Analysis Tools on the ExPASy Server, in: Walker, J.M. (Ed.), *The Proteomics Protocols Handbook*. Humana Press, Totowa, NJ, pp. 571-607.

Ge, L., Zhao, Y.S., Mo, T., Li, J.R., Li, P., (2012). Immobilization of glucose oxidase in electrospun nanofibrous membranes for food preservation. Food Control 26(1), 188-193.

Godjevargova, T., Dayal, R., Turmanova, S., (2004). Gluconic Acid Production in Bioreactor with Immobilized Glucose Oxidase Plus Catalase on Polymer Membrane Adjacent to Anion-Exchange Membrane. Macromolecular Bioscience 4(10), 950-956.

Gómez, E., Martínez, A., Laencina, J., (1995). Prevention of oxidative browning during wine storage. Food Research International 28(3), 213-217.

Gouda, M.D., Singh, S.A., Rao, A.G., Thakur, M.S., Karanth, N.G., (2003). Thermal inactivation of glucose oxidase. Mechanism and stabilization using additives. Journal of Biological Chemistry 278(27), 24324-24333.

Grauwet, T., Van der Plancken, I., Vervoort, L., Hendrickx, M., Van Loey, A., (2009). Investigating the potential of Bacillus subtilis alpha-amylase as a pressure-temperature-time indicator for high hydrostatic pressure pasteurization processes. Biotechnology Progress 25(4), 1184-1193.

Grauwet, T., Van der Plancken, I., Vervoort, L., Hendrickx, M.E., Van Loey, A., (2010). Solvent engineering as a tool in enzymatic indicator development for mild high pressure pasteurization processing. Journal of Food Engineering 97(3), 301-310.

Greenlee, L., Handler, P., (1964). Xanthine Oxidase: VI. Influence of pH on substrate specificity. Journal of Biological Chemistry 239(4), 1090-1095.

Guerrero-Beltrán, J.A., Barbosa-Cánovas, G.V., Swanson, B.G., (2005). High Hydrostatic Pressure Processing of Fruit and Vegetable Products. Food Reviews International 21(4), 411-425.

Guisán, J.M., Bastida, A., Cuesta, C., Fernandez-Lufuente, R., Rosell, C.M., (1991). Immobilization-stabilization of α-chymotrypsin by covalent attachment to aldehyde-agarose gels. Biotechnology and Bioengineering 38(10), 1144-1152.

Gulla, K.C., Gouda, M.D., Thakur, M.S., Karanth, N.G., (2004). Enhancement of stability of immobilized glucose oxidase by modification of free thiols generated by reducing disulfide bonds and using additives. Biosensors and Bioelectronics 19(6), 621-625.

Guo, Y., Lu, F., Zhao, H., Tang, Y., Lu, Z., (2010). Cloning and heterologous expression of glucose oxidase gene from Aspergillus niger Z-25 in Pichia pastoris. Appl Biochem Biotechnol 162(2), 498-509.

Gupta, M.N., (1991). Thermostabilization of proteins. Biotechnology and Applied Biochemistry 14(1), 1-11.

Haki, G.D., Rakshit, S.K., (2003). Developments in industrially important thermostable enzymes: a review. Bioresource Technology 89(1), 17-34.

Halalipour, A., Duff, M.R., Howell, E.E., Reyes-De-Corcuera, J.I., (2016). Glucose oxidase stabilization against thermal inactivation using high hydrostatic pressure and hydrophobic modification. Biotechnology and Bioengineering, In press.

Head-Gordon, T., (1995). Is water structure around hydrophobic groups clathrate-like? Proc Natl Acad Sci U S A 92(18), 8308-8312.

Heinisch, O., Kowalski, E., Goossens, K., Frank, J., Heremans, K., Ludwig, H., Tauscher, B., (1995). Pressure effects on the stability of lipoxygenase: Fourier transform-infrared spectroscopy (FT-IR) and enzyme activity studies. Zeitschrift für Lebensmittel-Untersuchung und Forschung 201(6), 562-565.

Hendrickx, M., Ludikhuyze, L., Van den Broeck, I., Weemaes, C., (1998). Effects of high pressure on enzymes related to food quality. Trends in Food Science & Technology 9(5), 197-203.

Hille, R., Massey, V., (1986). The equilibration of reducing equivalents within milk xanthine oxidase. Journal of Biological Chemistry 261(3), 1241-1247.

Hojgaard, C., Kofoed, C., Espersen, R., Johansson, K.E., Villa, M., Willemoes, M., Lindorff-Larsen, K., Teilum, K., Winther, J.R., (2016). A Soluble, Folded Protein without Charged Amino Acid Residues. Biochemistry 55(28), 3949-3956.

Huang, W., Ji, H., Liu, S., Zhang, C., Chen, Y., Guo, M., Hao, J., (2014). Inactivation effects and kinetics of polyphenol oxidase from Litopenaeus vannamei by ultra-high pressure and heat. Innovative Food Science & Emerging Technologies 26, 108-115.

Isaksen, A., Adler-Nissen, J., (1997). Antioxidative Effect of Glucose Oxidase and Catalase in Mayonnaises of Different Oxidative Susceptibility. I. Product Trials. LWT - Food Science and Technology 30(8), 841-846.

Iyer, P.V., Ananthanarayan, L., (2008). Enzyme stability and stabilization—Aqueous and non-aqueous environment. Process Biochemistry 43(10), 1019-1032.

Jackson, M.R., Beahm, R., Duvvuru, S., Narasimhan, C., Wu, J., Wang, H.-N., Philip, V.M., Hinde, R.J., Howell, E.E., (2007). A Preference for Edgewise Interactions between Aromatic Rings and Carboxylate Anions: The Biological Relevance of Anion−Quadrupole Interactions. The Journal of Physical Chemistry B 111(28), 8242-8249.

Jiang, Z., Ooraikul, B., (1989). Reduction of nonenzymatic browning in potato-chips and french fries with glucose-oxidase. Journal of food processing and preservation 13(3), 175-186.

Jo, S.-M., Xia, Y., Lee, H., Kim, Y., Kim, J.-C., (2008). Liposomes incorporating hydrophobically modified glucose oxidase. Korean Journal of Chemical Engineering 25(5), 1221-1225.

Johnson, D.B., Coughlan, M.P., (1978). Studies on the stability of immobilized xanthine oxidase and urate oxidase. Biotechnology and Bioengineering 20(7), 1085-1095.

Kalisz, H.M., Hecht, H.-J., Schomburg, D., Schmid, R.D., (1990). Crystallization and preliminary X-ray diffraction studies of a deglycosylated glucose oxidase from Aspergillus niger. Journal of Molecular Biology 213(2), 207-209.

Kalisz, H.M., Hecht, H.-J., Schomburg, D., Schmid, R.D., (1991). Effects of carbohydrate depletion on the structure, stability and activity of glucose oxidase from Aspergillus niger. Biochimica et Biophysica Acta 1080(2), 138-142.

Kalisz, H.M., Hendle, J., Schmid, R.D., (1997). Structural and biochemical properties of glycosylated and deglycosylated glucose oxidase from Penicillium amagasakiense. Applied Microbiology and Biotechnology 47(5), 502-507.

Kamyshny, A., Danino, D., Magdassi, S., Talmon, Y., (2002a). Transmission Electron Microscopy at Cryogenic Temperatures and Dynamic Light Scattering Studies of Glucose Oxidase Molecules and Self-Aggregated Nanoparticles. Langmuir 18(8), 3390-3391.

Kamyshny, A., Trofimova, D., Magdassi, S., Levashov, A., (2002b). Native and modified glucose oxidase in reversed micelles. Colloids and Surfaces B 24(3–4), 177-183.

Katano, H., Sugimoto, Y., Uematsu, K., Hibi, T., (2011). Kinetic study of the thermal inactivation of glucose oxidase in the presence of denaturant and stabilizer by means of bioelectrocatalysis method. Analytical Sciences 27(10), 979-983.

Katchalski-Katzir, E., (1993). Immobilized enzymes — learning from past successes and failures. Trends in Biotechnology 11(11), 471-478.

Katchalski-Katzir, E., Kraemer, D.M., (2000). Eupergit® C, a carrier for immobilization of enzymes of industrial potential. Journal of Molecular Catalysis B: Enzymatic 10(1–3), 157-176.

Katsaros, G.I., Katapodis, P., Taoukis, P.S., (2009). Modeling the effect of temperature and high hydrostatic pressure on the proteolytic activity of kiwi fruit juice. Journal of Food Engineering 94(1), 40-45.

Kim, J.G., Liu, H., (2007). Variation of haemoglobin extinction coefficients can cause errors in the determination of haemoglobin concentration measured by near-infrared spectroscopy. Physics in Medicine and Biology 52(20), 6295-6322.

Kim, J.H., Hille, R., (1993). Reductive half-reaction of xanthine oxidase with xanthine. Observation of a spectral intermediate attributable to the molybdenum center in the reaction of enzyme with xanthine. Journal of Biological Chemistry 268(1), 44-51.

Kirsch, C., Dahms, J., Kostko, A.F., McHugh, M.A., Smirnova, I., (2013). Pressure assisted stabilization of biocatalysts at elevated temperatures: Characterization by dynamic light scattering. Biotechnology and Bioengineering 110(6), 1674-1680.

Koide, S., Sidhu, S.S., (2009). The importance of being tyrosine: lessons in molecular recognition from minimalist synthetic binding proteins. ACS Chem Biol 4(5), 325-334.

Krebbers, B., Matser, A.M., Koets, M., Van den Berg, R.W., (2002). Quality and storage-stability of high-pressure preserved green beans. Journal of Food Engineering 54(1), 27-33.

Krimmer, S.G., Betz, M., Heine, A., Klebe, G., (2014). Methyl, ethyl, propyl, butyl: futile but not for water, as the correlation of structure and thermodynamic signature shows in a congeneric series of thermolysin inhibitors. ChemMedChem 9(4), 833-846.

Kunugi, S., Kitayaki, M., Yanagi, Y., Tanaka, N., Lange, R., Balny, C., (1997). The Effect of High Pressure on Thermolysin. European Journal of Biochemistry 248(2), 567-574.

Leskovac, V., Trivić, S., Wohlfahrt, G., Kandrač, J., Peričin, D., (2005). Glucose oxidase from Aspergillus niger: the mechanism of action with molecular oxygen, quinones, and one-electron acceptors. The International Journal of Biochemistry & Cell Biology 37(4), 731-750.

Levin, A., Erlkamp, M., Steitz, R., Czeslik, C., (2016). Volume profile of [small alpha]-chymotrypsin during adsorption and enzymatic reaction on a poly(acrylic acid) brush. Physical Chemistry Chemical Physics 18(13), 9070-9078.

Li, C., Ban, X., Gu, Z., Li, Z., (2013). Calcium Ion Contribution to Thermostability of Cyclodextrin Glycosyltransferase Is Closely Related to Calcium-Binding Site CaIII. Journal of Agricultural and Food Chemistry 61(37), 8836-8841.

Li, Y., Miao, M., Liu, M., Chen, X., Jiang, B., Feng, B., (2015). Enhancing the thermal stability of inulin fructotransferase with high hydrostatic pressure. International Journal of Biological Macromolecules 74, 171-178.

Longo, M.a.A., Combes, D., (1997). Influence of surface hydrophilic/hydrophobic balance on enzyme properties. Journal of Biotechnology 58(1), 21-32.

Ludikhuyze, L., Indrawati, Van den Broeck, I., Weemaes, C., Hendrickx, M., (1998). Effect of Combined Pressure and Temperature on Soybean Lipoxygenase. 2. Modeling Inactivation Kinetics under Static and Dynamic Conditions. Journal of Agricultural and Food Chemistry 46(10), 4081-4086.

Ludikhuyze, L., Van Loey, A., Indrawati, Smout, C., Hendrickx, M., (2003). Effects of Combined Pressure and Temperature on Enzymes Related to Quality of Fruits and Vegetables: From Kinetic Information to Process Engineering Aspects. Critical Reviews in Food Science and Nutrition 43(5), 527-586.

Luong, T.Q., Winter, R., (2015). Combined pressure and cosolvent effects on enzyme activity - a high-pressure stopped-flow kinetic study on [small alpha]-chymotrypsin. Physical Chemistry Chemical Physics 17(35), 23273-23278.

Ly-Nguyen, B., Van Loey, A.M., Smout, C., ErenÖzcan, S., Fachin, D., Verlent, I., Truong, S.V., Duvetter, T., Hendrickx, M.E., (2003). Mild-Heat and High-Pressure Inactivation of Carrot Pectin Methylesterase: A Kinetic Study. Journal of Food Science 68(4), 1377-1383.

Machida, Y., Nakanishi, T., (1981). Purification and Properties of Xanthine Oxidase from Enterobacter cloacae. Agricultural and Biological Chemistry 45(2), 425-432.

Mao, L., Xu, F., Xu, Q., Jin, L., (2001). Miniaturized Amperometric Biosensor Based on Xanthine Oxidase for Monitoring Hypoxanthine in Cell Culture Media. Analytical Biochemistry 292(1), 94-101.

Massey, V., Brumby, P.E., Komai, H., Palmer, G., (1969). Studies on milk xanthine oxidase Some spectral and kinetic properties. Journal of Biological Chemistry 244(7), 1682-1691.

Massey, V., Edmondson, D., (1970). On the mechanism of inactivation of xanthine oxidase by cyanide. Journal of Biological Chemistry 245(24), 6595-6598.

Massey, V., Harris, C.M., (1997). Milk xanthine oxidoreductase: the first one hundred years. Biochemical Society Transactions 25(3), 750-755.

Means, G.E., Feeney, R.E., (1971). Chemical modifications of proteins. Holden-Day, San Francisco, p. 254.

Mei, G., Di Venere, A., Campeggi, F.M., Gilardi, G., Rosato, N., De Matteis, F., Finazzi-Agrò, A., (1999). The effect of pressure and guanidine hydrochloride on azurins mutated in the hydrophobic core. European Journal of Biochemistry 265(2), 619-626.

Michels, P.C., Hei, D., Clark, D.S., (1996). Pressure Effects on Enzyme Activity and Stability at High Temperatures, in: Frederic M. Richards, D.S.E., Peter, S.K. (Eds.), *Advances in Protein Chemistry*. Academic Press, pp. 341-376.

Mogharrab, N., Ghourchian, H., Amininasab, M., (2007). Structural Stabilization and Functional Improvement of Horseradish Peroxidase upon Modification of Accessible Lysines: Experiments and Simulation. Biophysical Journal 92(4), 1192-1203.

Mohamadin, A.M., Abdel-Naim, A.B., (2003). In vitro activation of dibromoacetonitrile to cyanide: role of xanthine oxidase. Archives of Toxicology 77(2), 86-93.

Möller, J., Schroer, Martin A., Erlkamp, M., Grobelny, S., Paulus, M., Tiemeyer, S., Wirkert, Florian J., Tolan, M., Winter, R., (2012). The Effect of Ionic Strength, Temperature, and Pressure on the Interaction Potential of Dense Protein Solutions: From Nonlinear Pressure Response to Protein Crystallization. Biophysical Journal 102(11), 2641-2648.

Mozhaev, V.V., Lange, R., Kudryashova, E.V., Balny, C., (1996). Application of high hydrostatic pressure for increasing activity and stability of enzymes. Biotechnology and Bioengineering 52(2), 320-331.

Mozhaev, V.V., Melik-Nubarov, N.S., Siksnis, V., Martinek, K., (1990). Strategy for stabilizing enzymes part two: increasing enzyme stability by selective chemical modification. Biocatalysis 3(3), 189-196.

Nakamatsu, T., Akamatsu, T., Miyajima, R., Shiio, I., (1975). Microbial Production of Glucose Oxidase. Agricultural and Biological Chemistry 39(9), 1803-1811.

Nakamura, S., Hayashi, S., Koga, K., (1976). Effect of periodate oxidation on the structure and properties of glucose oxidase. Biochimica et Biophysica Acta 445(2), 294-308.

Nakao, K., Kiefner, A., Furumoto, K., Harada, T., (1997). Production of gluconic acid with immobilized glucose oxidase in airlift reactors. Chemical Engineering Science 52(21), 4127-4133.

Nakatani, H.S., Santos, L., Pelegrine, C.P., Gomes, M., Matsushita, M., Souza, N., Visentainer, J., (2005). Biosensor based on xanthine oxidase for monitoring hypoxanthine in fish meat. American Journal of Biochemistry and Biotechnology 1(2), 85-89.

Neri, D.F.M., Bernardino, D.P.B., Beltrão, E.I.C., Carvalho Jr, L.B., (2011). Purines oxidation by immobilized xanthine oxidase on magnetic polysiloxane–polyvinyl alcohol composite. Applied Catalysis A: General 401(1–2), 210-214.

Nisius, L., Grzesiek, S., (2012). Key stabilizing elements of protein structure identified through pressure and temperature perturbation of its hydrogen bond network. Nat Chem 4(9), 711-717.

O'Malley, J.J., Weaver, J.L., (1972). Subunit structure of glucose oxidase from Aspergillus niger. Biochemistry 11(19), 3527-3532.

Olson, J.S., Ballou, D.P., Palmer, G., Massey, V., (1974). The Mechanism of Action of Xanthine Oxidase. Journal of Biological Chemistry 249(14), 4363-4382.

Pace, C.N., Fu, H., Fryar, K.L., Landua, J., Trevino, S.R., Shirley, B.A., Hendricks, M.M., Iimura, S., Gajiwala, K., Scholtz, J.M., Grimsley, G.R., (2011). Contribution of hydrophobic interactions to protein stability. J Mol Biol 408(3), 514-528.

Parpinello, G.P., Chinnici, F., Versari, A., Riponi, C., (2002). Preliminary Study on Glucose Oxidase–Catalase Enzyme System to Control the Browning of Apple and Pear Purées. LWT - Food Science and Technology 35(3), 239-243.

Patel, A.J., Varilly, P., Jamadagni, S.N., Hagan, M.F., Chandler, D., Garde, S., (2012). Sitting at the Edge: How Biomolecules use Hydrophobicity to Tune Their Interactions and Function. The Journal of Physical Chemistry B 116(8), 2498-2503.

Pauff, J.M., Hille, R., (2009). Inhibition studies of bovine xanthine oxidase by luteolin, silibinin, quercetin, and curcumin. Journal of Natural Products 72(4), 725-731.

Pedro, H.A.L., Alfaia, A.J., Marques, J., Vila-Real, H.J., Calado, A., Ribeiro, M.H.L., (2007). Design of an immobilized enzyme system for naringin hydrolysis at high-pressure. Enzyme and Microbial Technology 40(3), 442-446.

Petersen, C., Tielrooij, K.-J., Bakker, H.J., (2009). Strong temperature dependence of water reorientation in hydrophobic hydration shells. The Journal of Chemical Physics 130(21), 214511-214516.

Philip, V., Harris, J., Adams, R., Nguyen, D., Spiers, J., Baudry, J., Howell, E.E., Hinde, R.J., (2011). A survey of aspartate-phenylalanine and glutamate-phenylalanine interactions in the protein data bank: searching for anion-pi pairs. Biochemistry 50(14), 2939-2950.

Pickering, G.J., Heatherbell, D.A., Barnes, M.F., (1998). Optimising glucose conversion in the production of reduced alcohol wine using glucose oxidase. Food Research International 31(10), 685-692.

Pluschkell, S., Hellmuth, K., Rinas, U., (1996). Kinetics of glucose oxidase excretion by recombinant Aspergillus niger. Biotechnology and Bioengineering 51(2), 215-220.

Ramachandran, S., Fontanille, P., Pandey, A., Larroche, C., (2006). Gluconic Acid: Properties, Applications and Microbial Production. Food Technology & Biotechnology 44(2), 185-195.

Rando, D., Kohring, G.W., Giffhorn, F., (1997). Production, purification and characterization of glucose oxidase from a newly isolated strain of Penicillium pinophilum. Applied Microbiology and Biotechnology 48(1), 34-40.

Rashidi, M.R., Soruraddin, M.H., Taherzadeh, F., Jouyban, A., (2009). Catalytic activity and stability of xanthine oxidase in aqueous-organic mixtures. Biochemistry (Moscow) 74(1), 97-101.

Rauf, S., Ihsan, A., Akhtar, K., Ghauri, M.A., Rahman, M., Anwar, M.A., Khalid, A.M., (2006). Glucose oxidase immobilization on a novel cellulose acetate–polymethylmethacrylate membrane. Journal of Biotechnology 121(3), 351-360.

Refaee, M., Tezuka, T., Akasaka, K., Williamson, M.P., (2003). Pressure-dependent Changes in the Solution Structure of Hen Egg-white Lysozyme. Journal of Molecular Biology 327(4), 857-865.

Riahi, E., Ramaswamy, H.S., (2004). High pressure inactivation kinetics of amylase in apple juice. Journal of Food Engineering 64(2), 151-160.

Roche, J., Caro, J.A., Norberto, D.R., Barthe, P., Roumestand, C., Schlessman, J.L., Garcia, A.E., García-Moreno E., B., Royer, C.A., (2012). Cavities determine the pressure unfolding of proteins. Proceedings of the National Academy of Sciences 109(18), 6945-6950.

Rodrigo, D., Jolie, R., Van Loey, A., Hendrickx, M., (2005). Combined thermal and high pressure inactivation kinetics of tomato lipoxygenase. European Food Research and Technology 222(5), 636-642.

Romero, M.R., Baruzzi, A.M., Garay, F., (2012). Mathematical modeling and experimental results of a sandwich-type amperometric biosensor. Sensors and Actuators B: Chemical 162(1), 284-291.

Royer, C.A., (2005). Insights into the role of hydration in protein structure and stability obtained through hydrostatic pressure studies. Brazilian Journal of Medical and Biological Research 38, 1167-1173.

Royer, C.A., (2015). Why and How Does Pressure Unfold Proteins?, in: Akasaka, K., Matsuki, H. (Eds.), *High Pressure Bioscience: Basic Concepts, Applications and Frontiers*. Springer Netherlands, Dordrecht, pp. 59-71.

Sandborn, W.J., (2001). Rational dosing of azathioprine and 6-mercaptopurine. Gut 48(5), 591-592.

Sarath Babu, V.R., Kumar, M.A., Karanth, N.G., Thakur, M.S., (2004). Stabilization of immobilized glucose oxidase against thermal inactivation by silanization for biosensor applications. Biosensors and Bioelectronics 19(10), 1337-1341.

Sarmiento, F., Peralta, R., Blamey, J.M., (2015). Cold and Hot Extremozymes: Industrial Relevance and Current Trends. Frontiers in Bioengineering and Biotechnology 3, 1-15.

Sarrouh, B., Santos, T.M., Miyoshi, A., Dias, R., Azevedo, V., (2012). Up-to-date insight on industrial enzymes applications and global market. Journal of Bioprocessing & Biotechniques 2012, 1-10.

Sattari, Z., Pourfaizi, H., Dehghan, G., Amani, M., Moosavi-Movahedi, A.A., (2013). Thermal inactivation and conformational lock studies on glucose oxidase. Structural Chemistry 24(4), 1105-1110.

Schroer, M.A., Tolan, M., Winter, R., (2012). Exploring the thermodynamic derivatives of the structure factor of dense protein solutions. Physical Chemistry Chemical Physics 14(26), 9486-9491.

Schuabb, V., Cinar, S., Czeslik, C., (2016). Effect of interfacial properties on the activation volume of adsorbed enzymes. Colloids and Surfaces B: Biointerfaces 140, 497-504.

Senyay-Oncel, D., Kazan, A., Yesil-Celiktas, O., (2014). Processing of protease under sub- and supercritical conditions for activity and stability enhancement. Biochemical Engineering Journal 92, 83-89.

Shih, T.-Y., Pai, C.-Y., Yang, P., Chang, W.-L., Wang, N.-C., Hu, O.Y.-P., (2013). A Novel Mechanism Underlies the Hepatotoxicity of Pyrazinamide. Antimicrobial Agents and Chemotherapy 57(4), 1685-1690.

Sila, D.N., Smout, C., Satara, Y., Truong, V., Loey, A.V., Hendrickx, M., (2007). Combined thermal and high pressure effect on carrot pectinmethylesterase stability and catalytic activity. Journal of Food Engineering 78(3), 755-764.

Simpson, C., Jordaan, J., Gardiner, N.S., Whiteley, C., (2007). Isolation, purification and characterization of a novel glucose oxidase from Penicillium sp. CBS 120262 optimally active at neutral pH. Protein Expression and Purification 51(2), 260-266.

Singh, O.V., Kapur, N., Singh, R.P., (2005). Evaluation of agro-food byproducts for gluconic acid production by Aspergillus niger ORS-4.410. World Journal of Microbiology and Biotechnology 21(4), 519-524.

Sisak, C., Csanádi, Z., Rónay, E., Szaján, B., (2006). Elimination of glucose in egg white using immobilized glucose oxidase. Enzyme and Microbial Technology 39(5), 1002-1007.

Smeller, L., (2002). Pressure–temperature phase diagrams of biomolecules. Biochimica et Biophysica Acta 1595(1–2), 11-29.

Spinozzi, F., Mariani, P., Saturni, L., Carsughi, F., Bernstorff, S., Cinelli, S., Onori, G., (2007). Met-myoglobin Association in Dilute Solution during Pressure-Induced Denaturation: an Analysis at pH 4.5 by High-Pressure Small-Angle X-ray Scattering. The Journal of Physical Chemistry B 111(14), 3822-3830.

Srivastava, R., Brown, J.Q., Zhu, H., McShane, M.J., (2005). Stabilization of glucose oxidase in alginate microspheres with photoreactive diazoresin nanofilm coatings. Biotechnology and Bioengineering 91(1), 124-131.

Stepankova, V., Bidmanova, S., Koudelakova, T., Prokop, Z., Chaloupkova, R., Damborsky, J., (2013). Strategies for Stabilization of Enzymes in Organic Solvents. Acs Catalysis 3(12), 2823-2836.

Strader, M.B., Smiley, R.D., Stinnett, L.G., VerBerkmoes, N.C., Howell, E.E., (2001). Role of S65, Q67, I68, and Y69 residues in homotetrameric R67 dihydrofolate reductase. Biochemistry 40(38), 11344-11352.

Stredansky, M., Pizzariello, A., Miertus, S., Svorc, J., (2000). Selective and Sensitive Biosensor for Theophylline Based on Xanthine Oxidase Electrode. Analytical Biochemistry 285(2), 225-229.

Sulaiman, A., Soo, M.J., Yoon, M.M.L., Farid, M., Silva, F.V.M., (2015). Modeling the polyphenoloxidase inactivation kinetics in pear, apple and strawberry purees after High Pressure Processing. Journal of Food Engineering 147(0), 89-94.

Sun, M.M.C., Caillot, R., Mak, G., Robb, F.T., Clark, D.S., (2001). Mechanism of pressure-induced thermostabilization of proteins: Studies of glutamate dehydrogenases from the hyperthermophile Thermococcus litoralis. Protein Science 10(9), 1750-1757.

Sun, M.M.C., Tolliday, N., Vetriani, C., Robb, F.T., Clark, D.S., (1999). Pressure-induced thermostabilization of glutamate dehydrogenase from the hyperthermophile pyrococcus furiosus. Protein Science 8(5), 1056-1063.

Tang, L., Yang, R., Hua, X., Yu, C., Zhang, W., Zhao, W., (2014). Preparation of immobilized glucose oxidase and its application in improving breadmaking quality of commercial wheat flour. Food Chemistry 161, 1-7.

Teeter, M.M., (1984). Water structure of a hydrophobic protein at atomic resolution: Pentagon rings of water molecules in crystals of crambin. Proceedings of the National Academy of Sciences 81(19), 6014-6018.

Terefe, N., Sheean, P., Fernando, S., Versteeg, C., (2013). The stability of almond β-glucosidase during combined high pressure–thermal processing: a kinetic study. Applied Microbiology and Biotechnology 97(7), 2917-2928.

Terefe, N.S., Buckow, R., Versteeg, C., (2014). Quality-Related Enzymes in Fruit and Vegetable Products: Effects of Novel Food Processing Technologies, Part 1: High-Pressure Processing. Critical Reviews in Food Science and Nutrition 54(1), 24-63.

Terefe, N.S., Yang, Y.H., Knoerzer, K., Buckow, R., Versteeg, C., (2010). High pressure and thermal inactivation kinetics of polyphenol oxidase and peroxidase in strawberry puree. Innovative Food Science & Emerging Technologies 11(1), 52-60.

Timson, M.J., Duff, M.R., Dickey, G., Saxton, A.M., Reyes-De-Corcuera, J.I., Howell, E.E., (2013). Further Studies on the Role of Water in R67 Dihydrofolate Reductase. Biochemistry 52(12), 2118-2127.

Tomlin, B.D., Jones, S.E., Reyes-De-Corcuera, J.I., (2013). High hydrostatic pressure protection of a pectinase cocktail against thermal inactivation. Journal of Food Engineering 116(3), 674-680.

Tomlin, B.D., Jones, S.E., Teixeira, A.A., Correll, M.J., Reyes-De-Corcuera, J.I., (2014). Kinetics of viscosity reduction of pectin solutions using a pectinase formulation at high hydrostatic pressure. Journal of Food Engineering 129(0), 47-52.

Tzanov, T., Costa, S.A., Gübitz, G.M., Cavaco-Paulo, A., (2002). Hydrogen peroxide generation with immobilized glucose oxidase for textile bleaching. Journal of Biotechnology 93(1), 87-94.

USNIST, (2008). Isothermal Properties for Water US NIST Standard Reference Database 69: NIST Chemistry WebBook.

Van den Broeck, I., Ludikhuyze, L.R., Van Loey, A.M., Hendrickx, M.E., (2000). Inactivation of Orange Pectinesterase by Combined High-Pressure and -Temperature Treatments: A Kinetic Study. Journal of Agricultural and Food Chemistry 48(5), 1960-1970.

Vila-Real, H., Alfaia, A.J., Phillips, R.S., Calado, A.R., Ribeiro, M.H.L., (2010). Pressure-enhanced activity and stability of α-l-rhamnosidase and β-d-glucosidase activities expressed by naringinase. Journal of Molecular Catalysis B: Enzymatic 65(1–4), 102-109.

Wang, R., Wang, T., Zheng, Q., Hu, X., Zhang, Y., Liao, X., (2012). Effects of high hydrostatic pressure on color of spinach purée and related properties. Journal of the Science of Food and Agriculture 92(7), 1417-1423.

Weemaes, C.A., Ludikhuyze, L.R., Van den Broeck, I., Hendrickx, M.E., (1998). Kinetics of combined pressure-temperature inactivation of avocado polyphenoloxidase. Biotechnology and Bioengineering 60(3), 292-300.

Williamson, M.P., Akasaka, K., Refaee, M., (2003). The solution structure of bovine pancreatic trypsin inhibitor at high pressure. Protein Science 12(9), 1971-1979.

Wilson, R., Turner, A.P.F., (1992). Glucose oxidase: an ideal enzyme. Biosensors and Bioelectronics 7(3), 165-185.

Wilton, D.J., Kitahara, R., Akasaka, K., Pandya, M.J., Williamson, M.P., (2009). Pressure-Dependent Structure Changes in Barnase on Ligand Binding Reveal Intermediate Rate Fluctuations. Biophysical Journal 97(5), 1482-1490.

Wilton, D.J., Tunnicliffe, R.B., Kamatari, Y.O., Akasaka, K., Williamson, M.P., (2008). Pressure-induced changes in the solution structure of the GB1 domain of protein G. Proteins: Structure, Function, and Bioinformatics 71(3), 1432-1440.

Witt, S., Wohlfahrt, G., Schomburg, D., Hecht, H.J., Kalisz, H.M., (2000). Conserved arginine-516 of Penicillium amagasakiense glucose oxidase is essential for the efficient binding of beta-D-glucose. Biochemical Journal 347, 553-559.

Wohlfahrt, G., Witt, S., Hendle, J., Schomburg, D., Kalisz, H.M., Hecht, H.-J., (1999). 1.8 and 1.9 Å resolution structures of the Penicillium amagasakiense and Aspergillus niger glucose oxidases as a basis for modelling substrate complexes. Acta Crystallographica Section D: Biological Crystallography 55(5), 969-977.

Wong, C.M., Wong, K.H., Chen, X.D., (2008). Glucose oxidase: natural occurrence, function, properties and industrial applications. Applied Microbiology and Biotechnology 78(6), 927-938.

Xin, Y., Yang, H., Xia, X., Zhang, L., Zhang, Y., Cheng, C., Wang, W., (2012). Expression, purification and partial characterization of a xanthine oxidase (XOD) in Arthrobacter sp. Process Biochemistry 47(11), 1539-1544.

Yamamoto, T., Moriwaki, Y., Suda, M., Nasako, Y., Takahashi, S., Hiroishi, K., Nakano, T., Hada, T., Higashino, K., (1993). Effect of BOF-4272 on the oxidation of allopurinol and pyrazinamide in vivo. Biochemical Pharmacology 46(12), 2277-2284.

Yi, J., Yi, J., Dong, P., Liao, X., Hu, X., Zhang, Y., (2015). Effect of high-hydrostatic-pressure on molecular microstructure of mushroom (Agaricusbisporus) polyphenoloxidase. LWT - Food Science and Technology 60(2, Part 1), 890-898.

Zancan, P., Sola-Penna, M., (2005). Trehalose and glycerol stabilize and renature yeast inorganic pyrophosphatase inactivated by very high temperatures. Archives of Biochemistry and Biophysics 444(1), 52-60.

Zhang, Y., Xin, Y., Yang, H., Zhang, L., Xia, X., Tong, Y., Chen, Y., Wang, W., (2014). Thermal inactivation of xanthine oxidase from Arthrobacter M3: mechanism and the corresponding thermostabilization strategy. Bioprocess and Biosystems Engineering 37(4), 719-725.

Zhu, J., Zhu, Z., Lai, Z., Wang, R., Guo, X., Wu, X., Zhang, G., Zhang, Z., Wang, Y., Chen, Z., (2002). Planar Amperometric Glucose Sensor Based on Glucose Oxidase Immobilized by Chitosan Film on Prussian Blue Layer. Sensors 2(4), 127-136.

Zoldák, G., Zubrik, A., Musatov, A., Stupák, M., Sedlák, E., (2004). Irreversible Thermal Denaturation of Glucose Oxidase from Aspergillus niger Is the Transition to the Denatured State with Residual Structure. Journal of Biological Chemistry 279(46), 47601-47609.